Supporting Information

Argicyclamides A-C unveil enzymatic basis for guanidine bis-prenylation.

Chin-Soon Phan,[#†] Kenichi Matsuda,[#‡,^] Nandani Balloo,[†] Kei Fujita,[‡] Toshiyuki Wakimoto[*‡,^] Tatsufumi Okino[*†,§]

[†]Graduate School of Environmental Science and [§]Faculty of Environmental Earth Science, Hokkaido University, Sapporo 060-0810, Japan

[‡]Faculty of Pharmaceutical Sciences, Hokkaido University, Sapporo 060-0812, Japan

[^]Global Station for Biosurfaces and Drug Discovery, Hokkaido University, Kita 12, Nishi 6, Sapporo 060-0812, Japan

Table of Contents

Supplementary Experimental Procedures

General remarks

^{1}H and ^{13}C NMR spectra were measured on a JEOL ECA 500 (500 MHz for ^{1}H NMR), a JEOL ECX 400P (400 MHz for ^{1}H NMR), JEOL ECS 400 (400 MHz for ^{1}H NMR) or Bruker AVANCE Neo (500 MHz for ^{1}H NMR), and JEOL ECA 600 (600 MHz for ^{1}H NMR) spectrometers. Chemical shifts are denoted in δ (ppm) relative to residual solvent peaks as internal standard (DMSO-d_6, ^{1}H δ 2.50, ^{13}C δ 39.5). ESI-MS spectra were measured on a Thermo Scientific Exactive mass spectrometer or a SHIMADZU LCMS-2020 spectrometer. Optical rotations were measured on a JASCO P-1030 polarimeter. High performance liquid chromatography (HPLC) experiments were performed with a SHIMADZU HPLC system equipped with a LC-20AD intelligent pump. LC-MS experiments were performed with Agilent 1100 Series HPLC system coupled with a micrOTOF-HS mass spectrometer (Bruker Daltonics). Fragmentation of precursor ions were also performed with amaZon SL-NPC (Bruker Daltonics) using helium gas with amplitude value 1.0 V. All reagents were used as supplied unless otherwise stated. *E. coli* DH5α was used for conventional cloning procedures. Plasmids extraction was performed with GenElute^{TM} Plasmid Miniprep Kit (Sigma).

Isolation of argicyclamides A-C (1-3)

Microcystis aeruginosa NIES-88 was grown in BG-11 media,[1] with aeration (filtered air, 0.3 L/min) at 25 °C under illumination of 80 μE/m^{2}s^1 on a 12L:12D cycle. Cells were collected by continuous flow centrifugation at 10,000 rpm after incubation of 4-5 weeks. Freeze-dried cells (10.2 g from 50 L of culture in 4-5 weeks) was homogenized and extracted with MeOH (200 mL x 3). The concentrated extract was partitioned between H_2O and ethyl acetate (EtOAc), where the EtOAc layer was further partitioned between MeOH and hexane. Both H_2O (533.0 mg) and EtOAc (55.6 mg) crudes were applied to ODS (YMC-Gel, 150 μm) with aqueous MeOH elution system. The MeOH eluted fraction of both crudes contained **1-3**, thus combined fractions were purified by HPLC with C18 (Wakosil-II 5C18 AR, 20 x 250 mm, UV detection 215 nm, flow rate 4.0 mL/min) and running condition (0-12 min, 40% MeCN with 0.1% TFA; and 12-50 min, 57% MeCN with 0.1% TFA) to yield **1** (23.0 mg), **2** (2.9 mg) and **3** (2.6 mg).

Argicyclamide A (**1**): colorless amorphous solid; $[\alpha]_D^{24}$ -53.8 (*c* 0.26, MeOH); NMR (DMSO-d_6, 600 MHz) see Table S2; HRESI(+)MS *m/z* 1058.7128 $[M + H]^+$; calcd. for $C_{57}H_{92}N_{11}O_8^+$ 1058.7125.

Argicyclamide B (**2**): colorless amorphous solid; $[\alpha]_D^{24}$ -49.9 (*c* 0.20, MeOH); NMR (DMSO-d_6, 600 MHz) see Table S2; HRESI(+)MS *m/z* 990.6495 $[M + H]^+$; calcd. for $C_{52}H_{84}N_{11}O_8^+$ 990.6499.

Argicyclamide C (**3**): colorless amorphous solid; $[\alpha]_D^{24}$ -49.3 (*c* 0.19, MeOH); NMR (DMSO-d_6, 600 MHz) see Table S2; HRESI(+)MS *m/z* 922.5873 $[M + H]^+$; calcd. for $C_{47}H_{76}N_{11}O_8^+$ 922.5873.

Advanced Marfey's analysis

Hydrolysis (6 M HCl. 115 ºC, for 12 h) was carried out using 0.1 mg of **3**. The hydrolysates were evaporated *in vacuo* and freeze dried. The hydrolysates were then dissolved in 50 μL of 1 N $NaHCO_3$, subsequently 50 μL of 10 mg mL^{-1} $_L$-FDLA in acetone was added.[2] The reaction mixture was incubated at 50 ºC for 30 min. Then, the reaction was quenched by 50 μL of 2 N HCl and 300 μL of MeCN was added. The reaction mixture was analyzed by LC-MS with a gradient system (30% to 60% MeCN with 0.1% formic acid over 30 min) using a ODS-SR-3 (Develosil, 2.0 x 150 mm). While, the separation of $_L$-allo Ile and $_L$-Ile was performed with a gradient system (30% to 38% MeCN with 0.1% formic acid over 50 min). The similar approach was carried out for **1**, The authentic standards of amino acids were derivatized in a similar manner as described above. The amino acid residues in **1** (except prenylated Arg) and **3** were determined as $_L$.

Total synthesis of argicyclamide C (3)

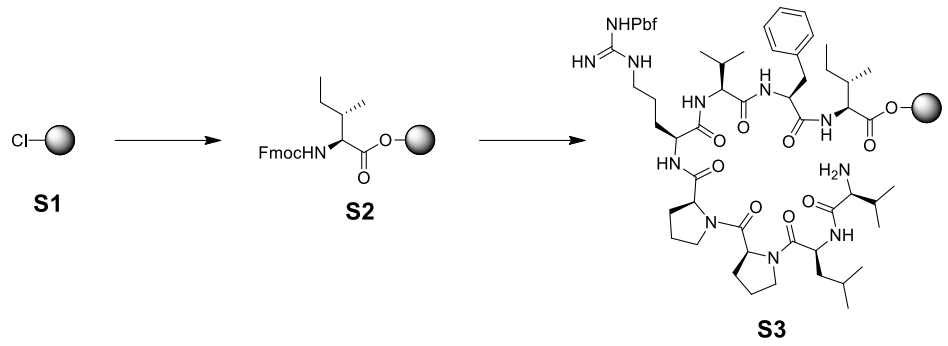

2-Chlorotrityl resin (**S1**) (48.5 mg, 0.075 mmol) in Libra tube was swollen with CH_2Cl_2 for 30 min, and then excess solvent was removed by filtration. To the resin was added a solution of Fmoc-L-Ile-OH (17.5 mg, 0.05 mmol) and *i*-Pr_2NEt (26 μL, 0.15 mmol) in CH_2Cl_2 (0.5 mL), and stirred for 1 h at 37°C. The reaction mixture was filtered, washed with DMF (× 3), CH_2Cl_2 (× 3), methanol, and Ac_2O/CH_2Cl_2 = 1:4, then dried under vacuum for 1 h to give Fmoc-L-Ile-2-chlorotrityl resin **S2**.
S2 was swelled in CH_2Cl_2 for 1 h, which was subjected to 7 cycles [Fmoc-L-Phe-OH, Fmoc-L-Val-OH, Fmoc-L-Arg(Pbf)-OH, Fmoc-L-Pro-OH, Fmoc-L-Pro-OH, Fmoc-L-Leu-OH, Fmoc-L-Val-OH] of SPPS protocol described below (Step1-4) to afford resin bound octapeptide **S3**.

Solid-phase peptide synthesis (SPPS) protocol
Step 1: Fmoc group of the solid supported peptide was removed by using 20% piperidine/DMF solution (10 min, room temperature).
Step 2: The resin in the reaction vessel was washed with DMF (× 3) and CH_2Cl_2 (× 3).
Step 3: To the solution of Fmoc-protected building blocks (4 eq) were added DIC (4 eq in NMP) and Oxyma (4 eq in DMF). After 2~3 min of pre-activation, the mixture was injected to the reaction vessel. The resulting mixture was stirred for 30 min at 37°C.
Step 4: The resin in the reaction vessel was washed with DMF (× 3) and CH_2Cl_2 (× 3). Amino acids were condensed onto the solid support by repeating Steps 1–4.

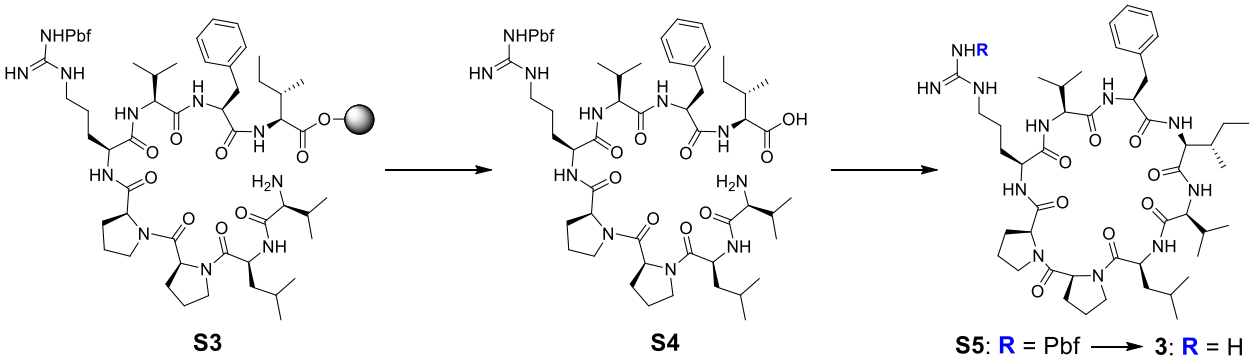

To the peptide **S3** was added $CH_2Cl_2/(CF_3)_2CHOH$ (= 70: 30) (2.0 mL), being stirred for 20 min, and the reaction product was filtered. This procedure was repeated twice. Filtrate was dried in vacuo to afford crude peptide **S4**, which was used to the next reaction without further purification. **S4** was dissolved in DMF/CH_2Cl_2 (= 10: 90) (50 mL) and to the solution were added 2,6-dimethylpyridine (28 μL, 0.2 mmol), HOAt (13.5 mg, 0.1 mmol) and PyBOP (52.0 mg, 0.1 mmol). After stirred overnight at 40 °C, the reaction mixture was extracted with EtOAc (× 3),

washed with brine, dried over $MgSO_4$, and concentrated to afford crude peptide **S5**. To **S5** residue was added TFA/phenol/anisol/ 2,2-(Ethylenedioxy)diethanethiol (= 90:5:3:2) (5.0 mL), being stirred for 10 min, and then the reaction mixture was filtered. The filtrate was diluted with Et_2O (12 mL) and was chilled (–30 °C), then centrifuged with 3,500 × *g* for 10 min at 4 °C to afford crude peptide **3**. The crude **3** was purified with reversed phase HPLC using C18 (Wakosil-II 5C18 AR, 20 × 250 mm, UV detection 215 nm, flowrate 4.0 mL/min) and running isocratic mode (40% MeCN with 0.1% TFA) to afford synthetic **3** (4.3 mg, 9.3 % for 19 steps) as colorless amorphous solid: $[\alpha]_D^{24}$ – 48.1 (*c* 0.38, MeOH); ^{1}H NMR (600 MHz, DMSO-d_6): δ 8.60 – 8.72 (br, 3H), 7.97 (br, 1H), 7.55 (t, *J* = 5.5 Hz, 1H), 7.44 (d, *J* = 9.1 Hz, 1H), 7.38 (d, *J* = 5.8 Hz, 1H), 7.28 – 7.32 (m, 4H), 7.22 – 7.25 (m, 1H), 4.48 (d, *J* = 8.0 Hz, 1H), 4.42 (m, 1H), 4.19 (t, *J* = 10.3 Hz, 1H), 4.09 (dd, *J* = 8.5, 3.9 Hz, 1H), 4.02 – 4.07 (m, 2H), 3.68 (t, *J* = 6.4 Hz, 1H), 3.30 – 3.46 (m, overlapped with solvent), 3.02 – 3.07 (m, 3H), 2.81 (dd, *J* = 13.7, 8.8 Hz, 1H), 2.22 – 2.29 (m, 3H), 2.05 – 2.10 (m, 1H), 1.89 – 1.94 (m, 1H), 1.68 – 1.87 (m, 8H), 1.65 (m, 1H), 1.49 – 1.57 (m, 3H), 1.42 – 1.47 (m, 1H), 1.15 (ddd, *J* = 12.4, 8.7, 4.4 Hz, 1H), 0.84 – 0.91 (m, 16H) 0.79 (t, *J* = 6.4 Hz, 3H), 0.64 (d, *J* = 6.4 Hz, 3H), 0.57 (t, *J* = 7.3 Hz, 3H), 0.44 – 0.50 (m, 1H). ^{13}C NMR (150 MHz, DMSO-d_6): δ 172.7, 172.4, 171.2, 171.0, 170.6, 170.4, 169.1, 156.6, 136.3, 129.1, 128.4, 126.7, 61.1, 60.3, 59.2, 57.4, 56.2, 55.6, 49.6, 46.6, 46.2, 40.5, 40.2, 36.7, 31.6, 31.0, 29.9, 28.5, 27.8, 25.4, 24.8, 24.7, 23.4, 21.8, 21.7, 19.5, 19.4, 18.5, 18.2, 15.2, 10.4. HRESI(+)MS *m/z* 922.5868 $[M + H]^+$; calcd. for $C_{47}H_{76}N_{11}O_8^+$ 922.5873.

Synthesis of cyclic peptide 6

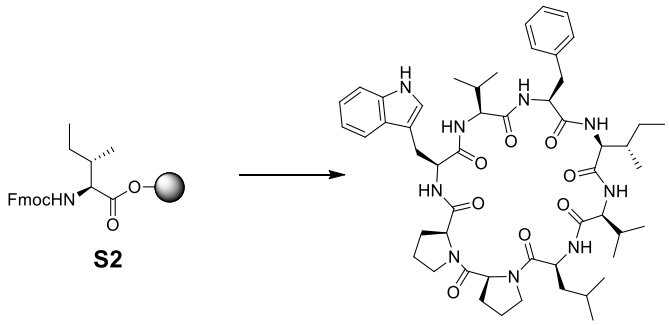

Cyclic peptide **6** was synthesized following the same procedure as **3** with the substitution of Fmoc-L-Arg(Pbf)-OH for Fmoc-L-Trp(Boc)-OH. The synthesis was initiated from Fmoc-L-Ile-2-chlorotrityl resin **S2** (0.05 mmol). The crude **6** was purified with reversed phase HPLC using C18 (Wakosil-II 5C18 AR, 20 × 250 mm, UV detection 215 nm, flowrate 4.0 mL/min) and running isocratic mode (52% MeCN with 0.1% TFA) to afford cyclic peptide **6** (4.4 mg, 9.3 % in 19 steps) as colorless amorphous solid: $[\alpha]_D^{25}$ –68.1 (*c* 0.17, MeOH). ^{1}H NMR (600 MHz, DMSO-d_6): δ 10.94 (br, 1H), 8.75 (br, 1H), 8.67 (br, 1H), 8.61 (br, 1H), 7.75 (br, 1H), 7.57 (d, *J* = 8.9 Hz, 1H), 7.52 (d, *J* = 7.9 Hz, 1H), 7.46 (d, *J* = 5.8 Hz, 1H), 7.32 (d, *J* = 7.9 Hz, 1H), 7.29 – 7.30 (m, 4H), 7.22 (m, 1H), 7.04 – 7.07 (m, 2H), 6.92 (t, *J* = 7.4 Hz, 1H), 4.44 (ddd, *J* = 9.8, 6.7, 2.9 Hz, 1H), 4.24 – 4.30 (m, 3H), 4.03 – 4.06 (m, 2H), 3.66 (t, *J* = 6.4 Hz, 1H), 3.45 – 3.56 (m, 2H), 3.46 (dt, *J* = 10.7, 7.1 Hz, 1H), 3.27 (dd, *J* = 15.0, 3.4 Hz, 1H), 3.19 (t, *J* = 12.7 Hz, 1H), 3.05 (dd, *J* = 14.3, 6.4 Hz, 1H), 2.88 – 2.93 (m, 2H), 2.80 (dd, *J* = 13.6, 9.6 Hz, 1H), 2.36 (t, *J* = 8.8 Hz, 1H), 2.19 – 2.28 (m, 2H), 1.67 – 1.94 (m, 10H), 1.61 – 1.66 (m, 1H), 0.93 – 0.96 (m, 6H), 0.86 – 0.90 (m, 14H), 0.71 – 0.76 (m, 1H), 0.64 (d, *J* = 6.4 Hz, 3H), 0.56 (t, *J* = 7.3 Hz, 3H), 0.41 – 0.46 (m, 1H), 0.07 – 0.14 (m, 1H). ^{13}C NMR (150 MHz, DMSO-d_6): δ 172.7, 172.4, 172.3, 171.3, 171.0, 170.0, 169.9, 169.0, 136.3, 136.1, 129.1, 128.3, 127.0, 126.6, 123.3, 121.1, 118.7, 117.6, 111.4, 109.7, 61.2, 59.9, 59.2, 57.4, 57.3, 56.3, 50.0, 46.6, 45.8, 40.3, 40.0, 36.7, 31.8, 30.8, 29.9, 27.6, 25.1, 24.7, 23.8,

21.6, 20.6, 19.4, 18.5, 18.3, 15.2, 10.4. HRESI(+)MS *m/z* 952.5659 $[M + H]^+$; calcd. for $C_{52}H_{74}N_9O_8^+$ 952.5655.

Synthesis of cyclic peptide 7

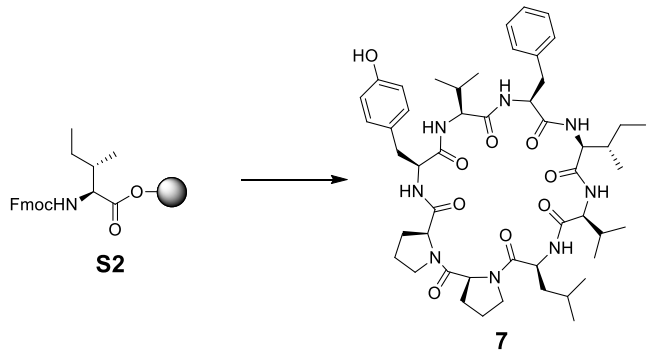

Cyclic peptide **7** was synthesized following the same procedure as **3** with the substitution of Fmoc-L-Arg(Pbf)-OH for Fmoc-L-Tyr(Boc)-OH. The synthesis was initiated from Fmoc-L-Ile-2-chlorotrityl resin **S2** (0.05 mmol). The crude **7** was purified with reversed phase HPLC using C18 (Wakosil-II 5C18 AR, 20 × 250 mm, UV detection 215 nm, flowrate 4.0 mL/min) and running isocratic mode (50% MeCN with 0.1% TFA) to afford cyclic peptide **7** (6.2 mg, 13.3 % in 19 steps) as amorphous white powder: $[\alpha]_D^{25}$ –66.0 (*c* 0.19, MeOH). ^{1}H NMR (600 MHz, DMSO-d_6): δ 9.28 (br, 1H), 8.52 – 8.76 (br, 3H), 7.93 (br, 1H), 7.41 – 7.48 (br, 1H), 7.29 – 7.30 (m, 4H), 7.23 (m, 1H), 6.92 (d, *J* = 7.7 Hz, 2H), 6.68 (d, *J* = 8.3 Hz, 2H), 4.44 (m, 1H), 4.38 (d, *J* = 7.2 Hz, 1H), 4.14 – 4.24 (m, 2H), 4.06 (m, 2H), 3.69 (br, 1H), 3.33 – 3.50 (m, overlapped with solvent), 3.18 (m, 1H), 3.04 – 3.09 (m, 2H), 2.80 – 2.95 (m, 3H), 2.22 – 2.28 (m, 2H), 2.04 – 2.08 (m, 1H), 1.80 – 1.94 (m, 5H), 1.60 – 1.69 (m, 3H), 1.54 (m, 1H), 1.19 (ddd, *J* = 12.4, 8.8, 4.4 Hz, 1H), 0.83 – 0.94 (m, 19H), 0.66 (br, 3H), 0.58 (t, *J* = 7.3 Hz, 3H), 0.45 – 0.51 (m, 1H). ^{13}C NMR (150 MHz, DMSO-d_6): δ 172.3, 170.9, 170.9, 170.9, 170.1, 169.8, 169.1, 156.1, 136.3, 129.4, 129.1, 128.2, 127.3, 126.6, 115.2, 61.0, 60.1, 59.2, 57.4, 56.3, 49.8, 46.6, 46.1, 40.4, 40.0, 36.7, 31.3, 30.7, 29.8, 29.0, 27.6, 25.0, 24.8, 23.4, 21.8, 20.8, 19.4, 19.3, 18.5, 18.2, 15.2, 10.5. HRESI(+)MS *m/z* 929.5497 $[M + H]^+$; calcd. for $C_{50}H_{73}N_8O_9^+$ 929.5495.

Synthesis of cyclic peptide 8

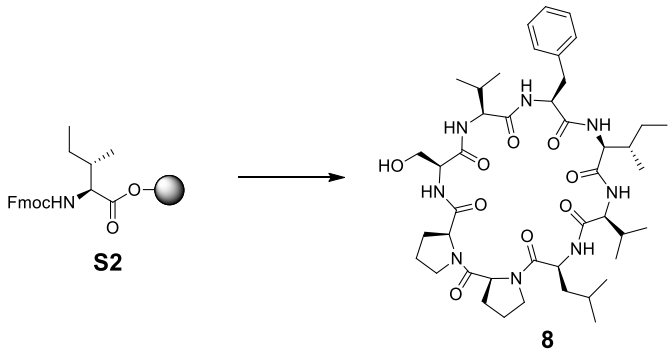

Cyclic peptide **8** was synthesized following the same procedure as **3** with the substitution of Fmoc-L-Arg(Pbf)-OH for Fmoc-L-Ser(Boc)-OH. The synthesis was initiated from Fmoc-L-Ile-2-chlorotrityl resin **S2** (0.05 mmol). The crude **8** was purified with reversed phase HPLC using C18 (Wakosil-II 5C18 AR, 20 × 250 mm, UV detection 215 nm, flowrate 4.0 mL/min)

and running isocratic mode (48% MeCN with 0.1% TFA) to afford cyclic peptide **8** (7.2 mg, 16.9 % in 19 steps) as colorless amorphous solid: $[\alpha]_D^{25}$ -61.4 (*c* 0.23, MeOH). ^{1}H NMR (600 MHz, DMSO-d_6): δ 8.40 – 8.64 (br, 3H), 7.55 (d, *J* = 8.8 Hz, 1H), 7.21 – 7.31 (m, 8H), 4.43 – 4.46 (m, 2H), 4.13 – 4.21 (m, 4H), 3.78 (m, 1H), 3.69 – 3.72 (m, 2H), 2.95 – 2.99 (m, 1H), 2.84 – 2.88 (m, 1H), 2.15 – 2.25 (m, 3H), 2.06 – 2.11 (m, 1H), 1.89 – 1.94 (m, 2H), 1.79 – 1.84 (m, 2H), 1.68 – 1.72 (m, 3H), 1.59 – 1.65 (m, 1H), 1.54 (m, 1H), 1.18 (m, 1H), 0.85 – 0.89 (m, 20H), 0.69 (br, 5H), 0.63 (br, 3H). ^{13}C NMR (150 MHz, DMSO-d_6): δ 172.6, 172.2, 171.0, 170.8, 170.4, 169.3, 168.8, 136.6, 129.0, 128.2, 126.5, 61.3, 60.7, 59.9, 58.9, 57.8, 55.9, 49.3, 46.5, 46.3, 40.4, 40.0, 36.8, 31.0, 30.8, 30.0, 29.6, 27.9, 24.6, 24.4, 23.2, 21.9, 21.6, 19.5, 19.3, 18.1, 18.0, 15.3, 10.6. HRESI(+)MS *m/z* 853.5182 $[M + H]^+$; calcd. for $C_{44}H_{69}N_8O_9^+$ 853.5182.

Synthesis of cyclic peptide 9

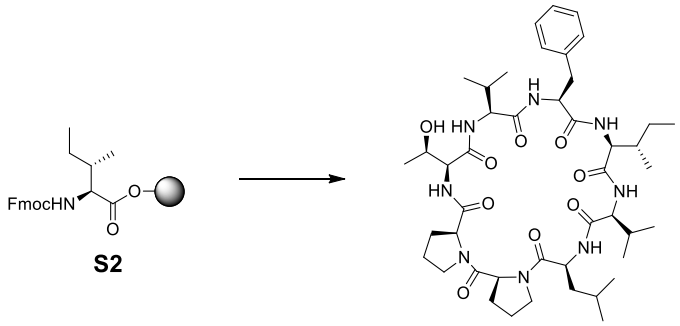

Cyclic peptide **9** was synthesized following the same procedure as **3** with the substitution of Fmoc-L-Arg(Pbf)-OH for Fmoc-L-Thr(Boc)-OH. The synthesis was initiated from Fmoc-L-Ile-2-chlorotrityl resin **S2** (0.05 mmol). The crude **9** was purified with reversed phase HPLC using C18 (Wakosil-II 5C18 AR, 20 × 250 mm, UV detection 215 nm, flowrate 4.0 mL/min) and running isocratic mode (50% MeCN with 0.1% TFA) to afford cyclic peptide **9** (4.7 mg, 10.9 % in 19 steps) as colorless amorphous solid: $[\alpha]_D^{25}$ -78.3 (*c* 0.17, MeOH). ^{1}H NMR (600 MHz, DMSO-d_6): δ 8.49 – 8.65 (br, 3H), 7.75 (br, 1H), 7.57 (d, *J* = 9.3 Hz, 1H), 7.39 (d, *J* = 7.1 Hz, 1H), 7.27 – 7.31 (m, 4H), 7.20 – 7.24 (m, 1H), 4.42 (m, 1H), 4.39 (d, *J* = 8.3 Hz, 1H), 4.12 – 4.18 (m, 2H), 4.08 (m, 1H), 3.99 (m, 1H), 3.87 (m, 1H), 3.69 (t, *J* = 6.2 Hz, 1H), 3.37 – 3.52 (m, overlapped with solvent), 3.30 (dt, *J* = 9.6, 5.8 Hz, 1H), 3.00 (dd, *J* = 13.9, 7.1 Hz, 1H), 2.95 (br, 1H), 2.81 (dd, *J* = 13.9, 8.4 Hz, 1H), 2.18 – 2.26 (m, 3H), 2.08 (m, 1H), 1.68 – 1.92 (m, 7H), 1.51 – 1.60 (m, 2H), 1.10 – 1.14 (m, 1H), 1.11 (d, *J* = 6.4 Hz, 3H), 0.83 – 0.87 (m, 15H), 0.76 (d, *J* = 6.4 Hz, 3H), 0.66 (d, *J* = 6.4 Hz, 3H), 0.59 (t, *J* = 7.3 Hz, 3H), 0.50 (m, 1H). ^{13}C NMR (150 MHz, DMSO-d_6): δ 172.9, 172.4, 172.2, 170.8, 170.5, 170.5, 169.6, 168.7, 136.5, 129.0, 128.3, 126.5, 65.8, 62.8, 60.9, 60.2, 59.1, 57.6, 55.9, 49.4, 46.4, 46.2, 40.4, 40.0, 36.5, 32.9, 31.2, 30.9 29.8, 27.7, 24.9, 24.7, 24.5, 23.3, 21.8, 21.6, 20.6, 19.5, 19.4, 18.3, 18.1, 15.2, 10.4. HRESI(+)MS *m/z* 867.5336 $[M + H]^+$; calcd. for $C_{45}H_{71}N_8O_9^+$ 867.5339.

Synthesis of cyclic peptide 10

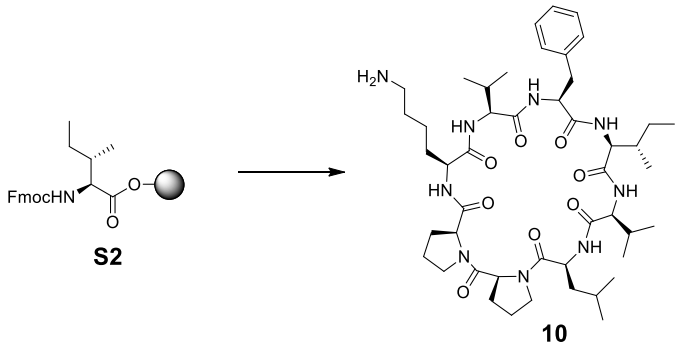

Cyclic peptide **10** was synthesized following the same procedure as **3** with the substitution of Fmoc-L-Arg(Pbf)-OH for Fmoc-L-Lys(Boc)-OH. The synthesis was initiated from Fmoc-L-Ile-2-chlorotrityl resin **S2** (0.05 mmol). The crude **10** was purified with reversed phase HPLC using C18 (Wakosil-II 5C18 AR, 20 × 250 mm, UV detection 215 nm, flowrate 4.0 mL/min) and running isocratic mode (37% MeCN with 0.1% TFA) to afford cyclic peptide **10** (6.7 mg, 15.0 % in 19 steps) as colorless amorphous solid: $[\alpha]_D^{25}$ -68.5 (*c* 0.15, MeOH). ^{1}H NMR (600 MHz, DMSO-d_6): δ 8.55 – 8.74 (br, 3H), 7.94 (br, 1H), 7.70 (br, 3H), 7.40 (br, 1H), 7.29 – 7.32 (m, 4H), 7.24 (m, 1H), 4.48 (d, *J* = 8.1 Hz, 1H), 4.41 (ddd, *J* = 10.0, 7.2, 3.8 Hz, 1H), 4.19 (t, *J* = 9.8 Hz, 1H), 4.09 (dd, *J* = 8.6, 4.1 Hz, 1H), 4.06 (m, 1H), 4.01 (m, 1H), 3.68 (t, *J* = 6.4 Hz, 1H), 3.39 – 3.46 (m, 3H), 3.31 (dt, *J* = 9.6, 6.7 Hz, 1H), 3.04 (dd, *J* = 14.3, 6.5 Hz, 1H), 2.90 – 2.97 (m, 1H), 2.81 (dd, *J* = 13.8, 9.1 Hz, 1H), 2.73 – 2.78 (m, 2H), 2.24 – 2.30 (m, 3H), 2.06 (m, 1H), 1.92 (m, 1H), 1.69 – 1.86 (m, 6H), 1.63 (m, 1H), 1.47 – 1.56 (m, 3H), 1.37 (m, 1H), 1.29 (m, 1H), 1.15 (ddd, *J* = 12.5, 8.8, 3.6 Hz, 1H), 0.84 – 0.91 (m, 19H), 0.79 (d, *J* = 6.4 Hz, 3H), 0.65 (d, *J* = 6.4 Hz, 3H), 0.58 (t, *J* = 7.3 Hz, 3H), 0.45 – 0.50 (m, 1H). ^{13}C NMR (150 MHz, DMSO-d_6): δ 172.7, 172.4, 172.3, 171.2, 170.9, 170.4, 170.3, 169.0, 136.3, 129.1, 128.3, 126.6, 61.0, 60.3, 59.2, 57.3, 56.2, 55.7, 49.6, 46.6, 46.1, 40.4, 40.0, 38.6, 36.7, 31.6, 30.8, 29.8, 27.7, 26.3, 24.8, 24.7, 24.7, 23.4, 22.7, 21.6, 19.4, 19.3, 18.4, 18.2, 15.2, 10.4. HRESI(+)MS *m/z* 894.5811 $[M + H]^+$; calcd. for $C_{47}H_{76}N_9O_8^+$ 894.5811.

Synthesis of linear peptide 11

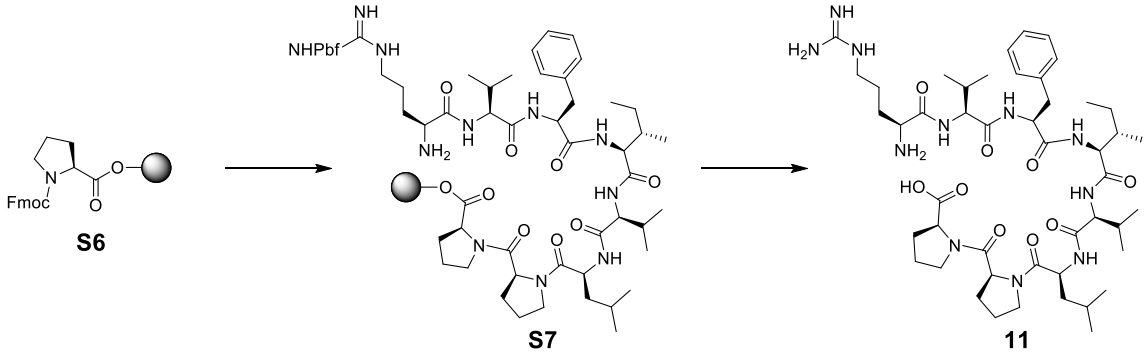

Fmoc-L-Pro-2-chlorotrityl resin **S6** was prepared following the same procedure as **S2** with the substitution of Fmoc-L-Ile-OH for Fmoc-L-Pro-OH. **S6** was swelled in CH_2Cl_2 for 1h, which was subjected to 7 cycles [Fmoc-L-Pro-OH, Fmoc-L-Leu-OH, Fmoc-L-Val-OH, Fmoc-L-Ile-OH, Fmoc-L-Phe-OH, Fmoc-L-Val-OH, Fmoc-L-Arg(Pbf)-OH] of SPPS protocol described above (Step1-4) to afford resin bound octapeptide **S7**. To **S7** was added TFA/phenol/anisol/ 2,2-(Ethylenedioxy) diethanethiol (= 90:5:3:2) (5.0 mL), being stirred for 10 min, and then the reaction mixture was filtered. The filtrate was diluted with Et_2O (12 mL) and was chilled (–30 °C),

then centrifuged with 3,500 × *g* for 10 min at 4 °C to afford crude peptide **11**. The crude **11** was purified with reversed phase HPLC using cholester (Cosmosil, 10 × 250 mm, UV detection 215 nm, flowrate 2.0 mL/min) and running isocratic mode (30% MeCN with 0.1% TFA) to afford linear peptide **11** (4.8 mg, 10.2 % in 17 steps) as colorless amorphous solid: $[\alpha]_D^{25}$ -58.3 (*c* 0.20, MeOH). ^{1}H NMR (600 MHz, DMSO-d_6): δ 8.28 (d, *J* = 7.2 Hz, 1H), 8.23 (d, *J* = 8.4 Hz, 1H), 7.99 (d, *J* = 8.9 Hz, 1H), 7.96 (d, *J* = 7.7 Hz, 1H), 7.82 (d, *J* = 8.9 Hz, 1H), 7.61 (br, 1H), 7.20 – 7.25 (m, 4H), 7.16 (t, *J* = 7.0 Hz, 1H), 4.60 (m, 1H), 4.51 – 4.56 (m, 2H), 4.23 – 4.27 (m, 2H), 4.16 – 4.20 (m, 2H), 3.79 (br, 1H), 3.61 – 3.69 (m, 2H), 3.50 (m, 1H), 3.44 (m, 1H), 3.06 (t, 6.2 Hz, 2H), 2.96 (dd, *J* = 14.1, 4.0 Hz, 1H), 2.76 (d, *J* = 7.2 Hz, 1H), 2.76 (dd, *J* = 13.9, 9.8 Hz, 1H), 2.11 – 2.15 (m, 2H), 1.96 – 2.00 (m, 1H), 1.89 – 1.93 (m , 4H), 1.81 – 1.87 (m, 2H), 1.70 – 1.77 (m, 2H), 1.58 – 1.65 (m, 3H), 1.38 – 1.48 (m, 5H), 1.06 (m, 1H), 0.87 (d, *J* = 6.4 Hz, 3H), 0.78 – 0.85 (m, 26H). ^{13}C NMR (150 MHz, DMSO-d_6): δ 173.3, 170.7, 170.6, 170.5, 170.3, 169.6, 156.8, 137.8, 129.1, 127.9, 126.1, 58.4, 57.4, 57.3, 57.2, 56.8, 53.6, 48.4, 46.6, 46.1, 40.2, 40.0, 37.2, 36.6, 31.0, 30.5, 29.0, 28.4, 27.6, 24.5, 24.3, 24.2, 24.2, 24.0, 23.2, 21.3, 19.2, 18.2, 17.7, 15.2, 10.9. HRESI(+)MS *m/z* 940.5979 $[M + H]^+$; calcd. for $C_{47}H_{78}N_{11}O_9^+$ 940.5978.

Synthesis of tripeptide 12

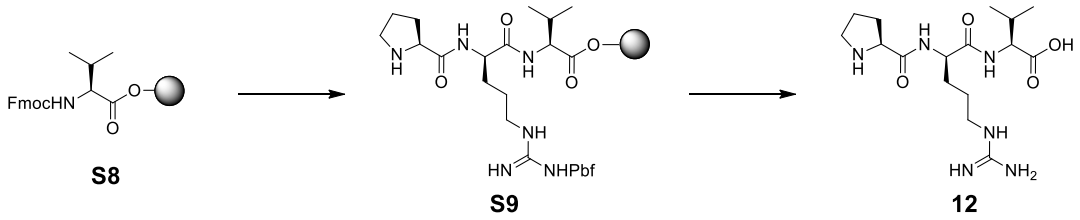

Fmoc-L-Val-2-chlorotrityl resin **S7** was prepared following the same procedure as **S2** with the substitution of Fmoc-L-Ile-OH for Fmoc-L-Val-OH. **S7** was swelled in CH_2Cl_2 for 1h, which was subjected to 2 cycles [Fmoc-L-Arg(Pbf)-OH, Fmoc-L-Pro-OH] of SPPS protocol described above (Step1-4) to afford resin bound tripeptide **S9**. To **S9** was added TFA/phenol/anisol/ 2,2-(Ethylenedioxy) diethanethiol (= 90:5:3:2) (5.0 mL), being stirred for 10 min, and then the reaction mixture was filtered. The filtrate was diluted with Et_2O (12 mL) and was chilled (–30 °C), then centrifuged with 3,500 × *g* for 10 min at 4 °C to afford crude peptide **12**. The crude **12** was purified with reversed phase HPLC (COSMOSIL MSII 20 × 250 mm) with MeCN:H_2O (=10:90) containing 0.05% TFA with flowrate at 8.0 ml/min to afford tripeptide peptide **12** (18.3 mg, 98.9 % in 8 steps) as white form: $[\alpha]_D^{25}$ -23.5 (*c* 0.15, MeOH). ^{1}H NMR (500 MHz, D_2O): δ 4.43 (d, *J* = 7.6 Hz, 1H), 4.41 (d, *J* = 6.7 Hz, 1H), 4.28 (d, *J* = 6.3 Hz, 1H), 3.38 – 3.46 (m, 2H), 3.22 (t, *J* = 6.7 Hz, 2H), 2.43 – 2.50 (m, 1H), 2.16 – 2.25 (m, 1H), 2.00 – 2.11 (m, 3H), 1.76 – 1.89 (m, 2H), 1.64 – 1.71 (m, 2H), 0.97 (d, *J* = 6.7 Hz, 6H). ^{13}C NMR (125 MHz, D_2O): δ 175.0, 173.4, 169.5, 156.8, 59.5, 58.5, 53.7, 46.6, 40.5, 29.9, 28.1, 24.3, 23.7, 18.3, 17.2. HRESI(+)MS *m/z* 371.2401 $[M + H]^+$; calcd. for $C_{16}H_{31}N_6O_4^+$ 371.2402.

Synthesis of pentadecapeptide 13

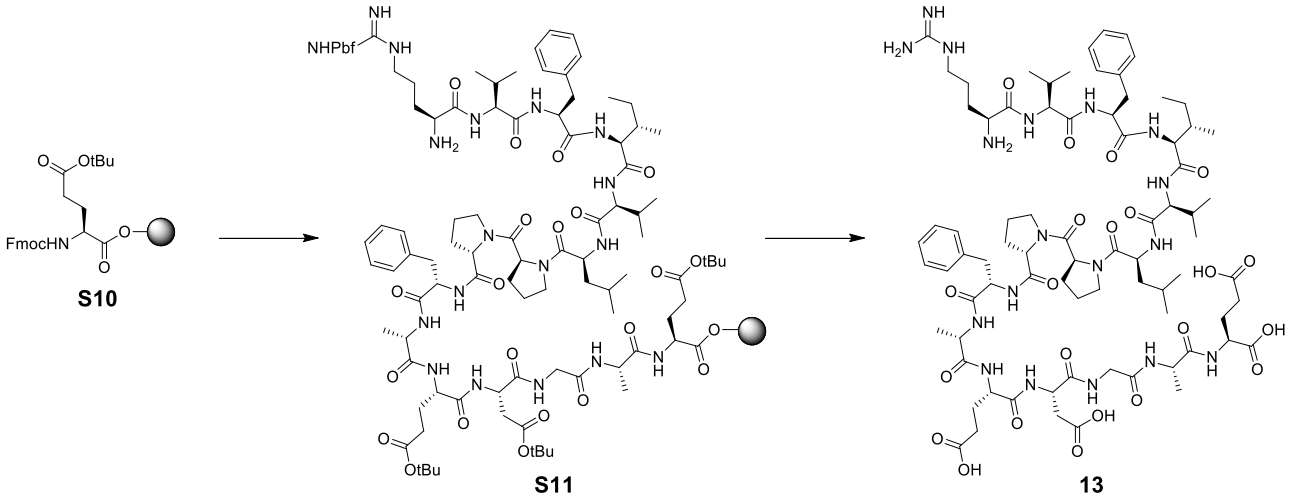

Fmoc-L-Glu(OtBu)-2-chlorotrityl resin **S10** was prepared following the same procedure as **S2** with the substitution of Fmoc-L-Ile-OH for Fmoc-L-Glu(OtBu)-OH. **S10** was swelled in CH_2Cl_2 for 1h, which was subjected to 14 cycles [Fmoc-L-Ala-OH, Fmoc-Gly-OH, Fmoc-L-Asp(OtBu)-OH, Fmoc-L-Glu(OtBu)-OH, Fmoc-L-Ala-OH, Fmoc-L-Phe-OH, Fmoc-L-Pro-OH, Fmoc-L-Pro-OH, Fmoc-L-Leu-OH, Fmoc-L-Val-OH, Fmoc-L-Ile-OH, Fmoc-L-Phe-OH, Fmoc-L-Val-OH, Fmoc-L-Arg(Pbf)-OH] of SPPS protocol described above (Step1-4) to afford resin bound pentadecapeptide **S11**. To **S11** was added TFA/phenol/anisol/ 2,2-(Ethylenedioxy) diethanethiol (= 90:5:3:2) (5.0 mL), being stirred for 10 min, and then the reaction mixture was filtered. The filtrate was diluted with Et_2O (12 mL) and was chilled (–30 °C), then centrifuged with 3,500 × *g* for 10 min at 4 °C to afford crude peptide **13**. The crude **13** was purified with reversed phase HPLC (COSMOSIL MSII 20 × 250 mm) with MeCN:H_2O (=13:27) containing 0.05% TFA with flowrate at 8.0 ml/min to afford linear peptide **13** (31.2 mg, 38% in 31 steps) as a white foam: $[\alpha]_D^{25}$ –29.87 (c 2.60, DMSO); ^{1}H-NMR (500 MHz, DMSO-d_6) δ 8.30 (d, *J* = 8.0 Hz, 1H), 8.15 (s, 4H), 8.09 (d, *J* = 5.7 Hz, 1H), 8.05-8.01 (m, 2H), 7.95 (s, 4H), 7.77 (s, 3H), 7.70 (d, *J* = 6.3 Hz, 1H), 7.28-7.12 (m, 16H), 4.58 (s, 1H), 4.46 (s, 2H), 4.38 (s, 1H), 4.27-4.14 (m, 8H), 3.84 (s, 1H), 3.70-3.53 (m, 4H), 3.36-3.50 (m, 2H), 3.01 (s, 3H), 2.92 (d, *J* = 11.5 Hz, 1H), 2.80 (d, *J* = 10.3 Hz, 1H), 2.74-2.65 (m, 2H), 2.52-2.60 (m, 1H), 2.46 (s, 1H), 2.19-2.32 (m, 4H), 2.02-2.12 (m, 2H), 1.85-2.02 (m, 5H), 1.67-1.85 (m, 6H), 1.59 (s, 2H), 1.38 (s, 4H), 1.17 (d, *J* = 5.2 Hz, 6H), 1.02 (s, 1H), 0.62-0.92 (m, 30H); ^{13}C-NMR (125 MHz, DMSO-d_6) δ 175.5, 175.3, 174.6, 173.8, 173.8, 173.3, 173.0, 172.6, 172.4, 172.3, 172.3, 172.2, 172.1, 171.8, 171.8, 171.3, 169.7, 169.6, 158.5, 139.3, 130.8, 130.6, 129.5, 127.7, 61.0, 59.1, 59.0, 58.9, 58.4, 55.2, 55.2, 53.5, 53.2, 52.7, 51.2, 50.0, 49.9, 49.4, 48.1, 43.8, 41.6, 41.4, 41.2, 41.0, 40.8, 38.9, 38.4, 38.3, 38.2, 37.5, 32.4, 32.3, 32.1, 32.0, 31.6, 31.5, 30.1, 29.3, 28.7, 27.8, 26.0, 25.9, 25.8, 25.6, 25.5, 24.7, 22.8, 22.7, 20.7, 19.7, 19.3, 16.7, 12.4; HRMS (ESI) calcd for $C_{78}H_{120}N_{18}O_{22}^{2+}$ $[M+2H]^{2+}$ 830.4407, found 830.4416.

Cytotoxicity assay

P388 mouse leukemia cells were cultured in DMEM media (Wako Chemicals), supplemented with 10% g/mL of penicillin/streptomycin (Invitrogen) and 10% FBS (MP Biomedicals) at 37 °C under a 5% CO_2 atmosphere.[3] Each well of 96-well microplate contained 99 μL of 1 × 10^5 cells/mL, with or without 1 μL of compounds (final concentrations: 100, 10, 1, 0.1 and 0.01 μM). After the plates were incubated for 48 h, 10 μL of 2-(2-methoxy-4-nitrophenyl)-3-(4-nitrophenyl)-5-(2,4-disulfophenyl)-2H-tetrazolium, WST-8 (Dojindo Laboratories) was added to each well, and the plate was incubated for another 3 h under

the same conditions. Measurement was taken with the infinite M200 microplate reader (Tecan) at absorbance of 450 nm. Triplicate were carried out. The positive control, doxorubicin has IC_{50} value of 1.08 μM against P388.

MCF-7 human breast cancer cells were cultured in RPMI-1640 medium (Wako Chemicals), supplemented with 10% FBS (BioWest) at 37 °C under a 5% CO_2 atmosphere.[4] Each well of 96-well microplate contained 99 μL of 1×10^4 cells/mL, with or without 1 μL of compounds (final concentrations: 100, 10 and 1 μM). After the plates were incubated for 72 h, the medium from each well was removed and replaced with 100 μL of 3-(4,5-dimethylthiazol-2-yl)-2,5-diphenyl-2H-tetrazolium bromide, MTT in RPMI-1640 with 10% FBS (0.5 mg/mL), and the plate was incubated for another 3 h under same condition. Then, MTT solution from each well was removed and replaced with DMSO, and the plate was incubated for another 10 min under same condition. Measurement was taken with the Multiskan JX microplate reader (Thermo Laysystems) at absorbance of 570 nm. Triplicate were carried out. The positive control, cisplatin has IC_{50} value of 9.18 μM against MCF-7.

Antimicrobial assay

The minimum inhibitory concentration (MIC) assays were performed by the microdilution method against *Bacillus subtilis* (ATCC 6051), *Pseudomonas aeruginosa* (ATCC 10145), *Staphylococcus aureus* (ATCC 12600), and methicillin resistant *Staphylococcus aureus* (ATCC 43300).[5] Serial two-fold dilutions were carried out on 96-well microplates with pure compounds (final concentration 100, 50, 25, 12.5, 6.25, 3.12 and 1.56 μM) were added to 100 μl Mueller Hinton broth with a bacteria inoculum (1.0×10^4 CFU per well). The 96-well microplates were incubated for 24 h at 35 °C. Measurement was taken with Multiskan JX microplate reader (Thermo Labsystems) at absorbance of 630 nm. The absorbance values and no visual growth of bacteria were recorded as the endpoint MIC. Triplicate were carried out. The positive controls, vancomycin has MIC value of 6.48 – 12.95 μM against methicillin-resistant *S. aureus*, nalidixic acid has MIC value of 2.5 – 5.0 μM against *P. aeruginosa*, oxacillin has MIC value of 3.90 – 7.79 μM and 7.79 – 15.59 μM against *S. aureus* and *B. subtilis*, respectively.

DNA extraction and genome sequencing *M. aeruginosa* NIES-88

M. aeruginosa NIES-88 was grown in BG-11 media,[1] with aeration (filtered air, 0.3 L/min) at 25 °C under illumination of 80 $\mu E/m^2s^1$ on a 12L:12D cycle. Cells were collected by continuous flow centrifugation at 10,000 rpm after incubation of 4-5 weeks. High molecular weight DNA was extracted by first crushing the frozen cells with mortar and pester, then dissolved the powder with CTAB buffer (3% CTAB, 1.4 M NaCl, 0.2% β-mercaptoethanol, 20 mM EDTA, 100 mM Tris pH 8, RNase A) and incubated at 50 °C for 30 min. Later, 750 μL $CHCl_3$ was added, gently inverted and centrifuged at 15,000 rpm for 5 min. The resulted upper layer was gently transferred into a centrifuged tube contain 200 μL isopropanol. The appearance of white string (precipitated DNA) became visible after gently rotation of the tube, this precipitated DNA was collected for genomic sequencing. Extracted DNA was quantified by a Qubit v3.0 fluorometer (Life Technologies, Thermo Fisher Scientific, Inc.).

Genome was sequenced by DNBSEQ for short-reads and Oxford nanopore GridION X5 for long-reads. For short-reads, library preparation was done using 400 ng of DNA by MGIEasy FS PCR-Free DNA Library Prep Set (MGI), following the standard protocol. DNA was fragmented enzymatically to be approximately 400 bp. As a result of sequence (150 bp x 2) and quality filtering ($Q > 30$), 87.2×coverage was obtained (genome size of *M. aeruginosa* NIES-88 was roughly estimated to be 10 Mb). For long-reads, 1000 ng of DNA was treated with Short Read Eliminator XS (Circulomics) to remove fragments shorter than 10 kb. Resultant 600 ng of DNA was subjected to library preparation Ligation Sequencing Kit (SQK-LSK 109), following the 1D genomic DNA by ligation protocol. The library was applied to MinION flowcell (FLO MIN106 R9.41revD) operated by MinKNOW (20.06.9) software, then processed by Guppy basecaller (4.0.11) with high accuracy

mode.[6] As a result, 77.4×coverage data (Q > 10) was obtained (genome size was roughly estimated to be 10 Mb).

The reads were subjected to hybrid *de novo* assembly using Unicycler (v0.4.8),[7] resulting a one circular chromosome (accession number: AP024565) and two circular plasmids (accession numbers: AP024566, AP024567). Possibility of mis-assembly was accessed by SV-Quest (1.0), which detected no possible chimeric assembly.[8] The assembles were polished by pilon (1.23) iteratively until no corrections were made.[9] The statistics of final *de novo* assembly is summarized in Table 4. The assembly was annotated using DFAST (version 1.2.13) (Table 5).[10] Gene prediction was accomplished by Prodigal:2.6.3.[11]

Bioinformatic analysis of the newly assembled *M. aeruginosa* NIES-88 genome

Identification of *agcE*, genes coding for precursor peptides of argicyclamide. Genome sequence of *M. aeruginosa* NIES-88 was searched by tBLASTn in BioEdit software (version 7.0.5.3) using the sequence of argicyclamide (RVFIVLPP) as a query. The expectation value was set at E = 100. Default values were used for other parameters. This identified two distantly encoded genes, *agcE1* (MAN88_05370) (Figure S11) and *agcE2* (MAN88_22110) (Figure S12). Both genes encode identical protein that belong to TIGR04446 family (product name: anacyclamide/piricyclamide family prenylated cyclic peptide). While no genes related to cyanobactin biosynthesis was found around *agcE1* gene, *agcF* (MAN88_22130) that shows similarity to cyanobactin prenyltransferase such as KgpF (41.38%) was found in the vicinity region of *agcE2* gene (Figure S12).

Cyanobactin proteases in *M. aeruginosa* NIES-88. As no cyanobactin proteases are encoded in the vicinity regions of *agcE*s, we hypothesized that AgcEs are processed by proteases that are encoded in remote genetic locus. To identify the candidate protease genes, we first annotated genome of *M. aeruginosa* NIES-88 by using DFAST.[10] This revealed duplicated kawaguchipeptin biosynthetic gene clusters (*kgp*) MAN88_12770–12820 (*kgp1*; 1358843–1365740 bp, Figure S13) and MAN88_48390–48430 (*kgp2*; 4956413–4961787 bp, Figure S14) in *M. aeruginosa* NIES-88. This duplication was not detected in the previous genome sequence study, probably because of the fragmented assembly.[12] *kgp1* and *kgp2* are near identical at nucleotide sequence level, except for two genetic regions. One difference is found in upper half of *kgpA*. In *kgp2*, *kgpA2* (MAN88_48430) apparently encodes full-length of PatA family protease, whereas in *kgp1*, *N*-terminal region (approx. 100 aa) of KgpA1 (MAN88_12820) is truncated (Figure S15). The removed region encodes catalytic triad that is generally required for protease activity,[13] thus KgpA1 is predicted to be an inactivated enzyme. The other difference between *kgp1* and *kgp2* locates in *kgpC* gene, where *kgpC* in region 2 is disrupted by the insertion of 195 bp fragment. As C family protein is dispensable for cyanobactin production *in vitro* and also in *E. coli*-based heterologous system,[14] the effect of this insertion for cyanobactin production is unclear. We additionally observed two nucleotide substitutions between *kgpG1* and *kgpG2*, but these don't alter amino acid sequence of encoded protein. *kgpB*, *kgpE*, and *kgpF* are identical between *kgp1* and *kgp2* at nucleotide sequence level. Comparison of cyanobactin related genetic regions and their positions in chromosome are summarized in Figure S16 and Figure S17, respectively.

To search other proteins that belongs to Peptidase S8A, PatG family, we searched the profile (IPR023830) against *M. aeruginosa* NIES-88 proteome, using HMMER (3.3.2).[15] This generated eleven proteins including KgpA1, KgpA2, KgpG1, and KgpG2. Each protein was further analyzed by InterProScan (v85.0)[16] for functional annotation. As a result, while KgpA1, KgpA2, KgpG1, and KgpG2 showed lowest e-values with IPR023830, other seven proteins exhibited lowest e-value with other protein families (IPR017295, 34204, 36852, or 000415), suggesting that these are unlikely to be involved in cyanobactin biosynthesis. These results are summarized in Table S6. Based on this observation, we hypothesized that argicyclamide precursor peptides (AgcE1 and E2) are processed by proteases involved in kawaguchipeptin biosynthesis. This hypothesis is supported by *E.*

coli-based heterologous expression of *agcE*, *kgpA2* and *kgpG*, which resulted in production of argicyclamide C (Figure 3c in main text). We further accessed enzymatic activity of KgpG *in vitro*, using AgcE-core-follower peptide (RVFIVLPPFAEDGAE; core peptide is underlined) as a substrate. This also resulted in production argicyclamide C (Figure S19), showing that KgpG is capable of processing AgcE-core-follower peptide.

Data availability

The sequence was deposited in the public database under the following accession numbers; AP024565, AP024566 and AP024567 (Bioproject number: PRJDB11480).

Plasmids construction

Oligonucleotides and plasmids used in this study were listed in Table S7 and S8, respectively. The DNA fragments encoding AgcE, AgcF, KgpA2, and KgpG were amplified with the designed primers from genomic DNA of *Microcystis aeruginosa* NIES-88 by KOD One® PCR Master Mix (TOYOBO). DNA fragments coding for AgcE and KgpG were inserted into the BamHI and KpnI sites of multi-cloning site (MCS) of pUC19 to yields AgcE-pUC19 and KgpG-pUC19, while AgcF was inserted into MCS of pUC19 using BamHI and EcoRI to generate AgcF-pUC19, and KgpA2 was inserted into the BamHI and HindIII sites of pUC19 to afford KgpA2-pUC19. After sequences were validated, DNA fragments coding for AgcE was transferred to pCold-II using the sites of NdeI and KpnI to yield AgcE-pCold-II. DNA fragment coding for KgpA2 was transferred to pRSFDuet-1 to obtain KgpA2-pRSFDuet-1. DNA fragment of KgpG was cleaved by NdeI and KpnI and cloned to both pRSFDuet-1 and KgpA2-pRSFDuet-1 to generate KgpG-pRSFDuet-1 and KgpA2G-pRSFDuet-1. The insert fragment of AgcF was inserted into the NdeI and EcoRI sites of pCold-II to acquire AgcF-pCold-II. To construct the expression plasmid of AgcF(E49A) mutant, mutated DNA fragment was amplified by KOD One® PCR Master Mix with a set of primers AgcF(E49A)-F/R using AgcF-pUC19 as a template. The fragment was treated with DpnI (TaKaRa) and was introduced into *E. coli* DH5α. Plasmids were extracted and sequence was validated. The mutated fragment was transferred to NdeI and EcoRI sites of pCold-II to yield AgcF(E49A)-pCold-II.

LC-MS analysis of *E. coli* transformants

Each plasmid was introduced into *Escherichia coli* BL21 (DE3) to generate *E. coli* AgcE, *E. coli* AgcE-KgpA2, *E. coli* AgcE-KgpG and *E. coli* AgcE-KgpA2G (Table S9). A single colony of each strain was inoculated into 10 mL of 2xYT media (1.6% Bacto tryptone, 1.0% Bacto yeast extract, 0.5% NaCl) and cultured at 37 °C overnight. The media containing 50 μg/mL kanamycin and 200 μg/mL ampicillin for *E. coli* AgcE-KgpA2, *E. coli* AgcE-KgpG and *E. coli* AgcE-KgpA2G, while for *E. coli* AgcE contained 200 μg/mL ampicillin. The overnight culture broth of 1% was transferred to 20 mL of M9 media comprised of 20 mL from M9 salt (6 g Na_2HPO_4, 3 g KH_2PO_4, 0.5 g NaCl, 1 g NH_4Cl in 500 mL), 40 μL of 1 M $MgSO_4$, 224 μL of 2 M glucose, 40 μL of 1 M $CaCl_2$ and 4 μL of 1% thiamine, subsequently cultured at 37 °C for 6-8 h to obtain OD_{600} of 0.5. The expression of each gene was induced by adding Isopropyl β-D-1-thiogalactopyranoside (IPTG) at a final concentration of 0.1 mM, and cells were cultured at 16 °C for 48 h. The culture broth was centrifuged at 10,000 rpm for 5 min and the resultant supernatant was partitioned with EtOAc. The concentrated EtOAc was analyzed by LC-MS (Agilent 1100 Series HPLC system coupled with a Bruker Daltonics micrOTOF-HS mass spectrometer using ESI source with positive mode). Samples were loaded onto reversed-phased column (Develosil C_{18} ODS-SR-3, 2.0 x 150 mm). Column was eluted with gradient mode (30-65% for mobile phase B in 0-15 min and, 65% for mobile phase B in 15-21 min) with flowrate at 0.2 mL/min. H_2O with 0.1% formic acid and MeCN with 0.1% formic acid were used as mobile phase A and B, respectively. Column elutes were monitored with UV absorption at 210-400 nm.

Preparation of recombinant proteins

For preparation of recombinant AgcF, AgcF-pCold II was introduced into *E. coli* BL21 (DE3) harboring chaperon expressing plasmid pGro7. A single colony was inoculated into 2xYT media containing 200 μg/mL ampicillin and 30 μg/mL chloramphenicol and grown for overnight at 37 °C. The overnight culture broth of 1% was transferred to 200 mL of 2xYT media containing 200 μg/mL ampicillin and 30 μg/mL chloramphenicol and 4 mg/mL of L-arabinose, then cultured at 37 °C for 3 h. The expression of AgcF gene was induced by adding IPTG at a final concentration of 0.1 mM, and cells were cultured at 16 °C overnight. Cells were harvested by centrifugation (3,500 × *g* for 10 min) and were disrupted by ultrasonic homogenizer. After removing debris by centrifugation (17,000 × *g* for 10 min), the fraction containing soluble protein was subjected to Ni-NTA affinity column (Merck Millipore) that was equilibrated by washing buffer (20 mM Tris-HCl pH 8.0, 150 mM NaCl, 20 mM imidazole). The column was washed with washing buffer and eluted with 500 mM imidazole washing buffer. Column eluted was concentrated by Amicon Ultra 0.5 mL filter (Merck Millipore). The concentration of protein solution was measured by Bio-Rad protein assay kit.

For preparation of recombinant KgpG, KgpG-pRSFDuet-1 was introduced to *E. coli* BL21 (DE3). The recombinant KgpG was expressed and purified following same procedure as AgcF, except 200 μg/mL ampicillin was replaced by 50 μg/mL kanamycin.

***in vitro assay* of KgpG**

50 μL of reaction mixture containing 20% DMSO, and 10 mM MES (pH 7.0), 100 μM **13**, 4.0 μM KgpG was prepared and incubated at 25 °C for 16 h. Reaction was quenched by adding equal volume of MeOH and then centrifuged at 20,000 × *g* for 10 min. A 5 μL of resultant supernatants were loaded onto COSMOSIL 2.5C_{18}-MS-II 2.0 × 100 mm (nacalai tesque) then eluted with gradient method (2–98% in 10 min for mobile phase B) using H_2O with 0.1% formic acid and acetonitrile with 0.1% formic acid as mobile phases A and B, respectively. Column elutes were analyzed by LCMS-2020 (Shimadzu) coupled with SPD-M20A (Shimadzu).

***in vitro* assay of AgcF**

For prenylation of cyclic peptide **3**, 50 μL of reaction mixtures containing 50 mM HEPES (pH 8.0), 200 μM substrate peptide (**3**, **6**-**12**), 2 mM isoprenyl donor (DMAPP, GPP, FPP), 2 mM dithiothreitol, 500 mM NaCl, 50 mM $MgCl_2$ were prepared. Reactions were initiated by adding 5 μM recombinant AgcF and reaction mixtures were incubated at 37 °C. Reactions were quenched by adding equal volume of MeOH at each time points, then centrifuged at 20,000 × *g* for 10 min. A 5 μL of resultant supernatants were loaded onto COSMOSIL 3C_{18}-MS-II 2.0 × 150 mm (nacalai tesque) then eluted with gradient method (2-98% in 5 min for mobile phase B) using H_2O with 0.1% formic acid and acetonitrile with 0.1% formic acid as mobile phases A and B, respectively. Column elutes were monitored by UV absorption at 200 nm. In addition, 20 μL samples were analyzed by LC-MS (Agilent 1100 Series HPLC system coupled with a Bruker Daltonics micrOTOF-HS mass spectrometer equipped with Develosil C18 ODS-SR-3 (2.0 × 150 mm) column. Samples were eluted by gradient mode (30-65% in 15 min of MeCN 0.1% formic acid; 65% in 21 min of MeCN 0.1% formic acid).

To evaluate the effect of pH on AgcF activity, AgcF was incubated with 50 μL of reaction mixtures containing 50 mM phosphate buffer (pH 6.0), 50 mM phosphate buffer (pH 7.0), 50 mM HEPES (pH 8.0), or 50 mM Tris-HCl buffer (pH 9.0). Reaction mixtures also contain 200 μM cyclic peptide **3**, 2 mM DMAPP, 2 mM dithiothreitol, 500 mM NaCl, 50 mM $MgCl_2$ and 5 μM AgcF. Reaction mixtures were incubated at 37 °C, then reactions were quenched at following time points: 0, 10, 30, 60, 120 min, by adding an equal volume of MeOH. A 5 μL of resultant supernatants were loaded onto COSMOSIL 3C_{18}-MS-II 2.0 × 150 mm then eluted with gradient method (2-98% in 5 min for mobile phase B) using H_2O with 0.1% formic acid and acetonitrile with 0.1% formic acid as mobile phases A and B, respectively. Column elutes were monitored by UV

absorption at 200 nm. Relative abundance was evaluated based on area values of peaks corresponding to **1**-**3**. Extinction coefficient (200 nm) of **1**-**3** were assumed to be equal.

To evaluate the effect of temperature on AgcF activity, 50 μL of reaction mixture containing 50 mM HEPES (pH 8.0), 200 μM cyclic peptide **3**, 2 mM DMAPP, 2 mM dithiothreitol, 500 mM NaCl, 50 mM $MgCl_2$ and 5 μM AgcF were incubated at 16 °C, 30 °C, or 37 °C. Reactions were quenched at following time points: 0, 10, 30, 60, 120 min, by adding an equal volume of MeOH. A 5 μL of resultant supernatants were loaded onto COSMOSIL 3C_{18}-MS-II 2.0 × 150 mm then eluted with gradient method (2-98% in 5 min for mobile phase B) using H_2O with 0.1% formic acid and acetonitrile with 0.1% formic acid as mobile phases A and B, respectively. Column elutes were monitored by UV absorption at 200 nm. Relative abundance was evaluated based on area values of peaks corresponding to **1**-**3**. Extinction coefficient (200 nm) of **1**-**3** were assumed to be equal.

Computational model of AgcF

The model of AgcF was generated by SWISS-MODEL web tool,[17] using PagF structure (5TU6) as a template. Amino acid sequence identity between PagF and AgcF is 42%. Structures were compared on Maestro software (Schrödinger).

Table S1. ^{13}C (150 MHz) and ^{1}H (600 MHz) NMR data for (**1**) in CD_3OD.

Position	**^{13}C**	**^{1}H**
Arg		
1	174.1	
2	57.2	4.23, m
3	30.2	1.96, m
4	26.7	1.72, m
		1.65, m
5	41.9	3.24, m
6	156.0	
NH		8.10, d, 7.4
Prenyl		
1	40.7	3.82, d, 6.7
2	119.8	5.22, td, 6.8, 1.3
3	138.6	
4	18.1	1.71, m
5	25.8	1.76, m
Val(1)		
1	174.3	
2	59.8	4.23, m
3	32.7	1.82, m
4	19.1	0.91, d, 6.5
5	20.2	1.00, d, 6.5
NH		7.82, d, 9.6
Phe		
1	175.1	
2	58.4	4.09, dd, 9.6, 6.1
3	38.1	3.12, dd, 14.1, 6.1
		2.95, dd, 14.1, 9.7
4	137.0	
5,5’	130.2	7.28, d, 7.2
6,6’	129.9	7.33, t, 7.2
7	128.2	7.24, t, 7.2
NH		8.74 brs
Ile		
1	175.2	
2	66.5	2.99, brd, 10.8
3	34.7	2.34, m
4	26.5	0.83, m
		0.49, m
5	10.9	0.65, t, 7.2
6	15.7	0.73, d, 6.9
Val(2)		
1	174.1	
2	63.5	3.78, d, 7.1
3	31.8	1.93, m
4	19.3	0.98, d, 6.5
5	20.1	0.99, d, 6.5
NH		8.92, d, 5.7
Leu		
1	171.3	

2	51.7	4.66, m
3	42.1	1.87, m
		1.24, ddd, 12.6, 8.8, 3.7
4	26.5	1.60, m
5	22.2	0.97, d, 6.5
6	24.1	0.92, d, 6.5
NH		7.65, d, 7.2
Pro(1)		
1	173.3/173.4	
2	61.1	4.24, m
3	29.4	2.28, m
		1.83, m
4	26.2	2.06, m
		1.92, m
5	48.5	3.56, m
		3.52, m
Pro(2)		
1	173.3/173.4	
2	62.4	4.55, d, 8.0
3	32.5	2.37, m
		2.21, m
4	23.0	1.99, m
		1.70, m
5	47.8	3.56, m

Table S2. ^{13}C (150 NMR) and ^{1}H (600 MHz) NMR data for (**1-3**) in DMSO-d_6.

Position	**1**		**2**		**3**	
	^{13}C	**^{1}H**	**^{13}C**	**^{1}H**	**^{13}C**	**^{1}H**
Arg						
1	171.1		171.1		171.1	
2	55.5	4.05, m	55.5	4.05, m	55.5	4.04, m
3	28.5	1.83, m	28.5	1.83, m	28.5	1.81, m
		1.79, m		1.79, m		1.78, m
4	25.3	1.56, m	25.4	1.56, m	25.4	1.55, m
		1.47, m		1.46, m		1.44, m
5	40.5	3.11, m	40.4	3.08, m	40.2	3.05, m
						2.87, m
6	153.9		155.4		156.6	
NH		7.96, brs		7.97, brs		7.97, brs
N^{δ}H		7.37, m		7.41, m		7.60, t, 5.5
N^{ω}H		7.42, m		7.37, m		
Prenyl						
1	39.3	3.75, t, 5.5	38.9	3.71, t, 6.9		
2	119.5	5.15, td, 6.4, 1.3	119.2	5.16, td, 6.5, 1.3		
3	135.4		136.0			
4	17.8	1.63, s	17.8	1.63, s		
5	25.3	1.69, s	25.3	1.70, s		
Val(1)						
1	172.4		172.4		172.4	
2	57.4	4.20, d, 10.1	57.4	4.20, d, 9.6	57.4	4.20, d, 10.2
3	31.6	1.64, m	31.5	1.65, m	31.5	1.65, m
4	18.5	0.80, d, 6.4	18.5	0.79, d, 6.4	18.5	0.79, d, 6.4
5	19.3	0.91, d, 6.4	19.4	0.90, d, 6.4	19.4	0.90, d, 6.4
NH		7.43, m		7.44, m		7.44, d, 9.1
Phe						
1	172.7		172.7		172.7	
2	56.2	4.06, m	56.2	4.06, m	56.2	4.06, m
3	36.7	3.05, dd, 14.2, 6.4	36.7	3.04, dd, 14.1, 6.5	36.7	3.04, m
		2.81, dd, 14.2, 8.7		2.82, dd, 14.1, 8.6		2.81, dd, 13.7, 8.8
4	136.3		136.3		136.3	
5,5’	128.3	7.30, m	128.3	7.30, m	128.3	7.29, m
6,6’	129.1	7.31, m	129.1	7.30, m	129.1	7.30, m
7	126.6	7.24, m	126.6	7.24, m	126.6	7.23, m
NH		8.73, brs		8.73, brs		8.72, brs
Ile						
1	172.3		172.4		172.3	
2	64.2	2.92, m	64.3	2.92, m	64.3	2.91, m
3	32.7	2.26, m	32.8	2.27, m	32.7	2.26, m
4	24.7	0.78, m	24.7	0.78, m	24.7	0.77, m
		0.47, m		0.47, m		0.47, m
5	10.4	0.57, t, 7.3	10.4	0.57, t, 7.3	10.4	0.57, t, 7.3
6	15.2	0.65, t, 6.4	15.2	0.65, t, 6.4	15.2	0.65, d, 6.4
NH		8.61, brs		8.61, brs		8.61, brs

Val(2)						
1	170.9		171.0		171.0	
2	61.0	3.68, t, 6.4	61.0	3.68, t, 6.2	61.0	3.68, t, 6.3
3	29.9	1.82, m	29.9	1.83, m	29.9	1.82, m
4	18.2	0.85, d, 6.4	18.2	0.85, d, 6.4	18.2	0.84, d, 6.4
5	19.4	0.87, d, 6.4	19.5	0.87, d, 6.4	19.5	0.87, d, 6.4
NH		8.64, brs		8.64, brs		8.64, brs
Leu						
1	169.0		169.0		169.0	
2	49.6	4.41, m	49.6	4.41, m	49.6	4.42, m
3	40.4	1.73, m 1.16, ddd, 12.4, 8.7, 4.4	40.4	1.74, m 1.16, ddd, 12.4, 8.7, 4.4	40.4	1.73, m 1.16, ddd, 12.4, 8.7, 4.4
4	24.7	1.52, m	24.7	1.53, m	24.7	1.52, m
5	21.7	0.88, d, 6.4	21.7	0.88, d, 6.4	21.7	0.88, d, 6.4
6	23.3	0.84, d, 6.4	23.3	0.84, d, 6.4	23.4	0.84, d, 6.4
NH		7.39, m		7.38, m		7.38, d, 5.8
Pro(1)						
1	170.2		170.3		170.3	
2	59.2	4.10, dd, 8.7, 4.1	59.2	4.10, dd, 8.6, 4.1	59.2	4.09, dd, 8.5, 3.9
3	27.7	2.27, m 1.70, m	27.7	2.27, m 1.71, m	27.7	2.26, m 1.70, m
4	24.7	1.92, m 1.81, m	24.8	1.92, m 1.82, m	24.7	1.91, m 1.81, m
5	46.6	3.44, m 3.31, dt, 9.6, 6.4	46.6	3.44, m 3.31, dt, 9.6, 6.2	46.6	3.44, m 3.31, dt, 9.6, 6.3
Pro(2)						
1	170.4		170.5		170.5	
2	60.3	4.49, d, 8.3	60.3	4.48, d, 7.9	60.3	4.48, d, 8.0
3	30.8	2.24, m 2.08, m	30.9	2.24, m 2.08, m	31.0	2.23, m 2.07, m
4	21.6	1.84, m 1.50, m	21.6	1.85, m 1.52, m	21.6	1.84, m 1.52, m
5	46.1	3.40, m	46.2	3.40, m	46.2	3.40, m

Table S3. The cytotoxicity (IC_{50}, μM) and antibacterial activities (MIC, μM) of **1**-**3**.

	IC_{50}, μM		**MIC, μM**			
	P388	**MCF-7**	***S. aureus***	**Methicillin resistant *S. aureus***	***B. subtilis***	***P. aeruginosa***
1	43.9	>100	3.12 – 6.25	3.12 – 6.25	3.12 – 6.25	>100
2	63.9	>100	50 - 100	50 - 100	50 – 100	>100
3	24.0	>100	>100	>100	>100	>100

Table S4. *De novo* assembly statistics

name	Length (bp)	Circular/Linear	GC (%)	average read depth	Accession number
chromosome	5,478,552	Circular	42.5	97.0149	AP024565
plasmid1	19,436	Circular	46.2	241.5548	AP024566
plasmid2	3,117	Circular	40.9	407.4963	AP024567

Table S5. Statistics of DFAST analysis

Total Sequence Length (bp):	5501105
Number of Sequences:	3
Longest Sequences (bp):	5478552
N50 (bp):	5478552
Gap Ratio (%):	0
GCcontent (%):	42.6
Number of CDSs:	5340
Average Protein Length:	277.8
Coding Ratio (%):	80.9
Number of rRNAs:	4
Number of tRNAs:	43
Number of CRISPRs:	3

Table S6. Hmmsearch and InterProScan of possible cyanobactin peptidases

Locus	length	e-value[1)]	Interproscan	e-value[2)]	Description[3)]
MAN88_48430 (**KgpA2**)	657	0	IPR023830	0	Peptidase S8A, PatG
MAN88_12770 (**KgpG1**)	672	0	IPR034056 /IPR023830	0	PatG/PatA-like domain/Peptidase S8A, PatG
MAN88_48390 (**KgpG2**)	672	0	IPR034056 /IPR023830	0	PatG/PatA-like domain/Peptidase S8A, PatG
MAN88_12820 **(KgpA1**)	572	4.10E-303	IPR023830	2.30E-250	Peptidase S8A, PatG
MAN88_19930	592	2.00E-33	IPR017295	0	Peptidase S8A, subtilisin-related, cyanobacteria-1
MAN88_50540	1024	5.30E-26	IPR034204	1.32E-138	Subtilisin SUB1-like catalytic domain
MAN88_49390	1024	8.30E-26	IPR034204	6.97E-140	Subtilisin SUB1-like catalytic domain
MAN88_52830	1202	7.00E-25	IPR034204	9.67E-133	Subtilisin SUB1-like catalytic domain
MAN88_49380	1421	1.10E-23	IPR034204	1.29E-127	Subtilisin SUB1-like catalytic domain
MAN88_24010	527	3.00E-05	IPR036852	6.28E-27	Peptidase S8/S53 domain superfamily
MAN88_09490	504	5.80E-02	IPR000415	0	Nitroreductase-like

[1)] Result of hmmsearch with the profile of IPR023830.
[2)] Result of InterProScan of each protein.
[3)] Description for InterPro accessions.

Table S7. Primers used in this study

Primer	**Sequence (restriction enzyme sites are underlined)**	Restriction enzymes
AgcE-F*	ggcggatcccatatg**gcaagctggagccacccgcagttcgaaaagatcgat**aaaaacaaaactttacttccc	BamHI/NdeI
AgcE-R	cggggtaccttactcagctccatcttcag	KpnI
AgcF-F	cgcggatcccatatgttgaaaagcaacaaaaag	BamHI/NdeI
AgcF-R	ccggaattcctagagcagataatatagattgagattc	EcoRI
KgpA2-F	ggcggatccgaatagtttatttttggaagtccc	BamHI
KgpA2-R	gggaagcttttagtaaggtgcagaccattgtt	HindIII
KgpG-F**	ggcggatcccatatgggcagcagc**catcaccatcatcaccac**agcccggatataattgatatacc	BamHI/NdeI
KgpG-R	cggggtaccttagttgggagaatcccac	KpnI
AgcF(E49A)-F	aaaattgtgtcctcgcatcttcctgtaaaat	-
AgcF(E49A)-R	attttacaggaagatgcgaggacacaatttt	-

*; strep-tag sequence was described in bold letter.
**; His6-tag sequence was described in bold letter.

Table S8. Plasmids constructed in this study

Vectors/Plasmids	**Description**
AgcE-pCold-II	Plasmid for expression of AgcE
AgcF-pCold-II	Plasmid for expression of AgcF
KgpA2-pRSFDuet-1	Plasmid for expression of KgpA2
KgpG-pRSFDuet-1	Plasmid for expression of KgpG
KgpA2G-pRSFDuet-1	Plasmid for expression of KgpA2 and KgpG
AgcF(E49A)-pCold-II	Plasmid for expression of AgcF(E49A)

Table S9. Strains used in this study

Stains	**Description of Strains**
E. coli AgcE	*E. coli* BL21 (DE3) harboring AgcE-pCold-II
E. coli AgcF/pGro7	*E. coli* BL21 (DE3) harboring AgcF-pCold-II and pGro7 (chaperone plasmid)
E. coli AgcE-KgpA2	*E. coli* BL21 (DE3) harboring AgcE-pCold-II and KgpA2-pRSFDuet-1
E. coli AgcE-KgpG	*E. coli* BL21 (DE3) harboring AgcE-pCold-II and KgpG-pRSFDuet-1
E. coli AgcE-KgpA2G	*E. coli* BL21 (DE3) harboring AgcE-pCold-II and KgpA2G-pRSFDuet-1
E. coli AgcF(E49A)/pGro7	*E. coli* BL21 (DE3) harboring AgcF(E49A)-pCold-II and pGro7 (chaperone plasmid)
E. coli KgpG	*E. coli* BL21 (DE3) harboring KgpG-pRSFDuet-1

Table S10. Substrate specificity of AgcF

isoprenyl acceptor	structure	isoprenyl donor	relative activity (%)
3	cyc(RVFIVLPP)	DMAPP	100
3	cyc(RVFIVLPP)	GPP	N.D.*
3	cyc(RVFIVLPP)	FPP	0
6	cyc(**W**VFIVLPP)	DMAPP	0
7	cyc(**Y**VFIVLPP)	DMAPP	0
8	cyc(**S**VFIVLPP)	DMAPP	0
9	cyc(**T**VFIVLPP)	DMAPP	0
10	cyc(**K**VFIVLPP)	DMAPP	0
11	*seco*-(RVFIVLPP)	DMAPP	0
12	*seco*-(PRV)	DMAPP	0

N.D.*: not determined. Low yield of geranylated product precluded accurate estimation.

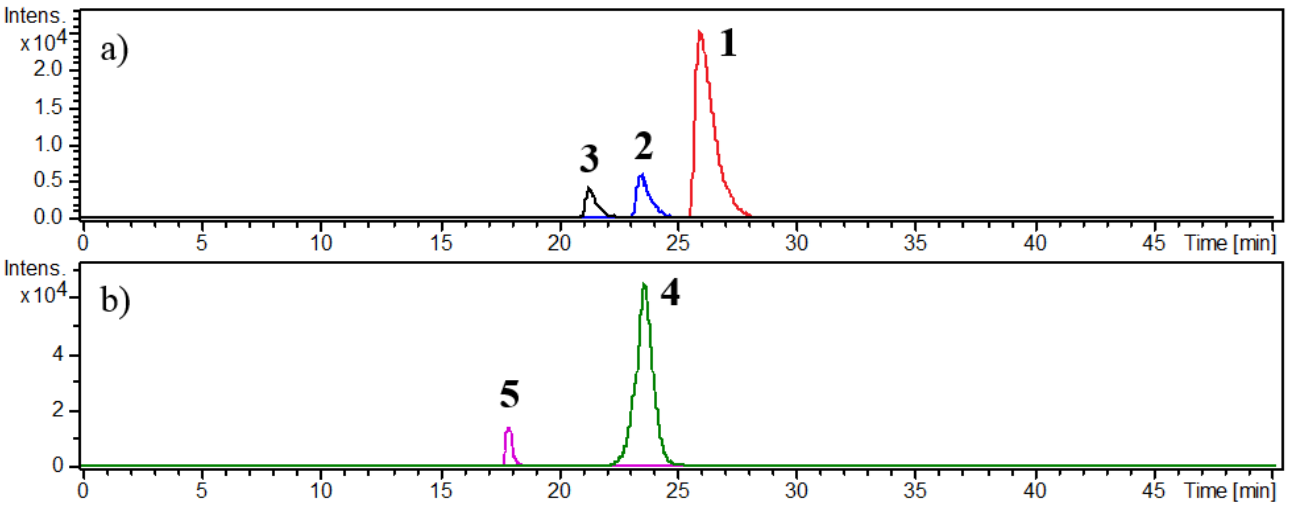

Figure S1. (a) LC-MS profile of argicyclamides A-C (**1-3**) from EtOAc fraction with ESI(+) extracted ion chromatographs (EICs) of *m/z* 1058.5000 for **1** (red), 990.5000 for **2** (blue), and 922.5000 for **3** (black) are overlaid. (b) LC-MS profile of kawaguchipeptins A and B (**4** and **5**) from H_2O fraction with ESI(-) EICs of *m/z* 1419.5000 for **4** (green), and 1283.5000 for **5** (purple) are overlaid.

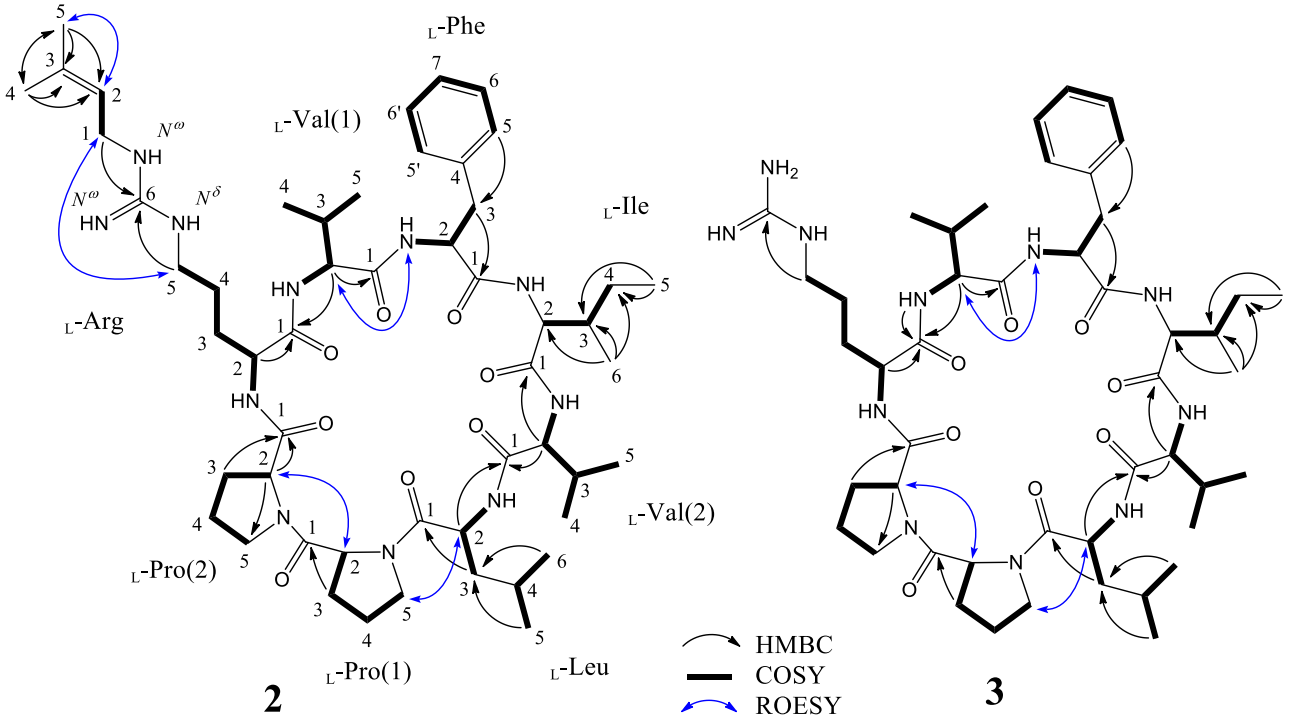

Figure S2. 2D NMR correlations of **2** and **3** in DMSO-d_6

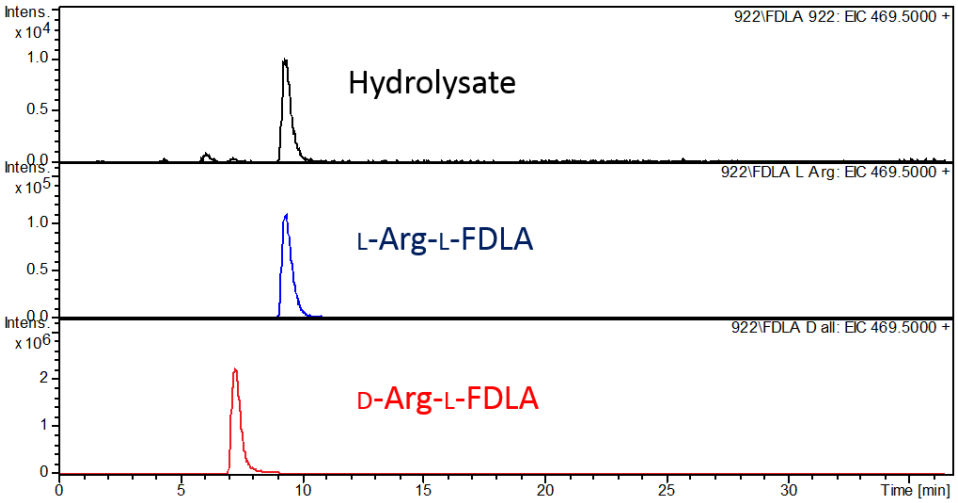

Figure S3A. LC-MS chromatogram of Marfey's analysis of hydrolysate **3** and standards L-Arg and D-Arg

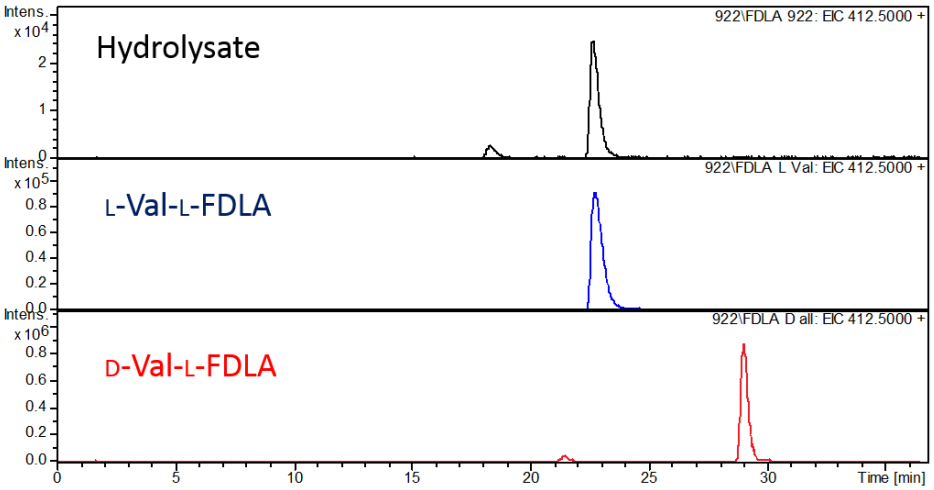

Figure S3B. LC-MS chromatogram of Marfey's analysis of hydrolysate **3** and standards L-Val and D-Val

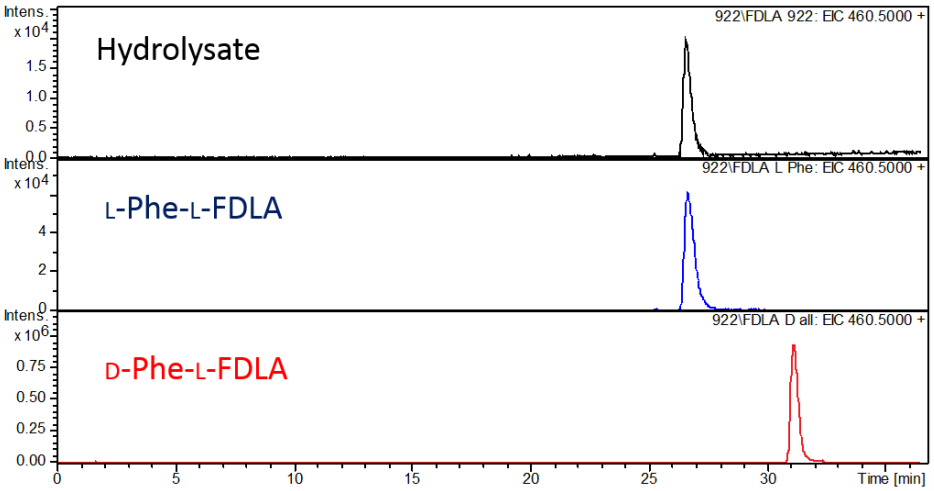

Figure S3C. LC-MS chromatogram of Marfey's analysis of hydrolysate **3** and standards L-Phe and D-Phe

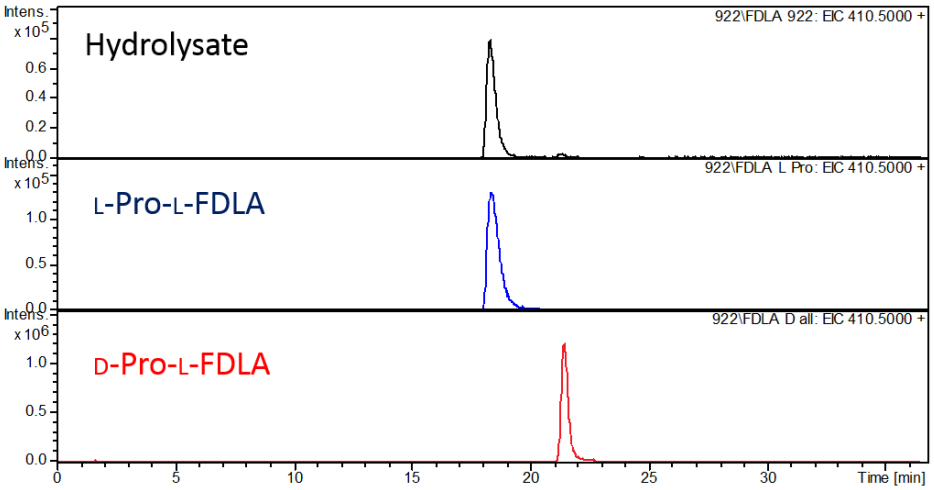

Figure S3D. LC-MS chromatogram of Marfey's analysis of hydrolysate **3** and standards L-Pro and D-Pro

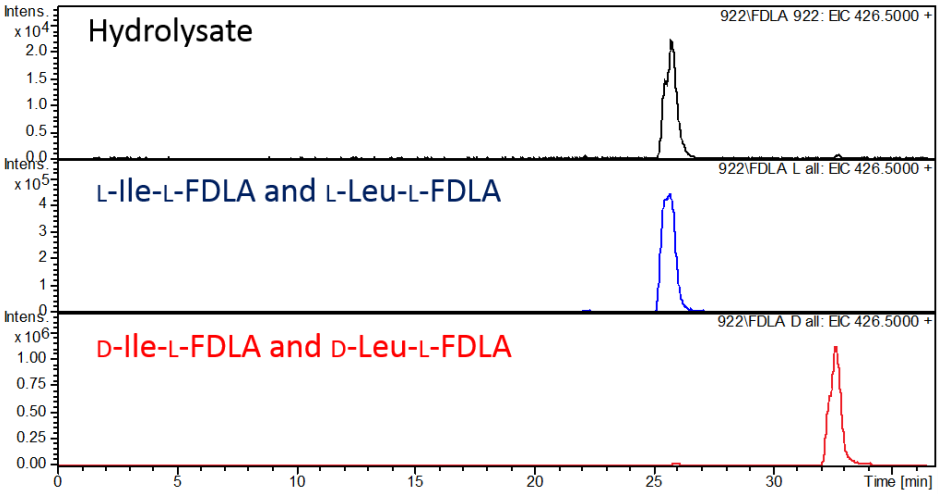

Figure S3E. LC-MS chromatogram of Marfey's analysis of hydrolysate **3** and standards L-Ile, L-Leu, D-Ile and D-Leu

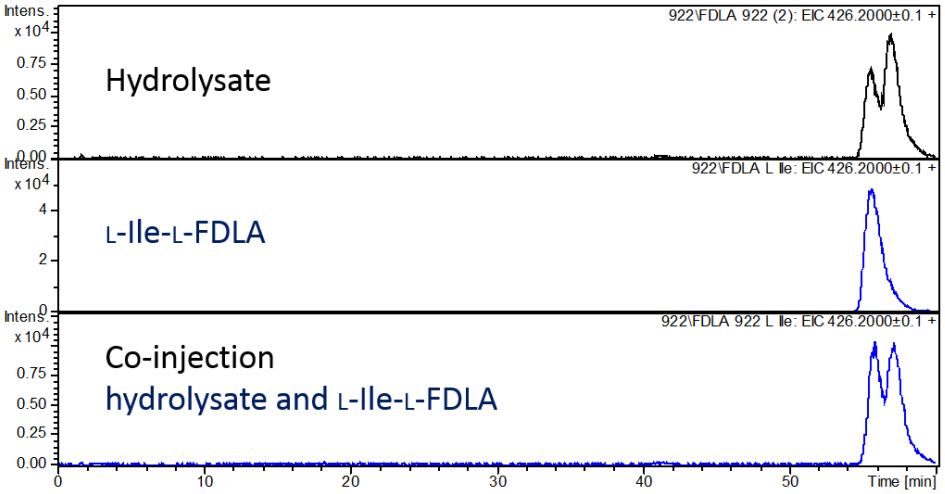

Figure S3F. LC-MS chromatogram of Marfey's analysis of hydrolysate **3** and standard L-Ile

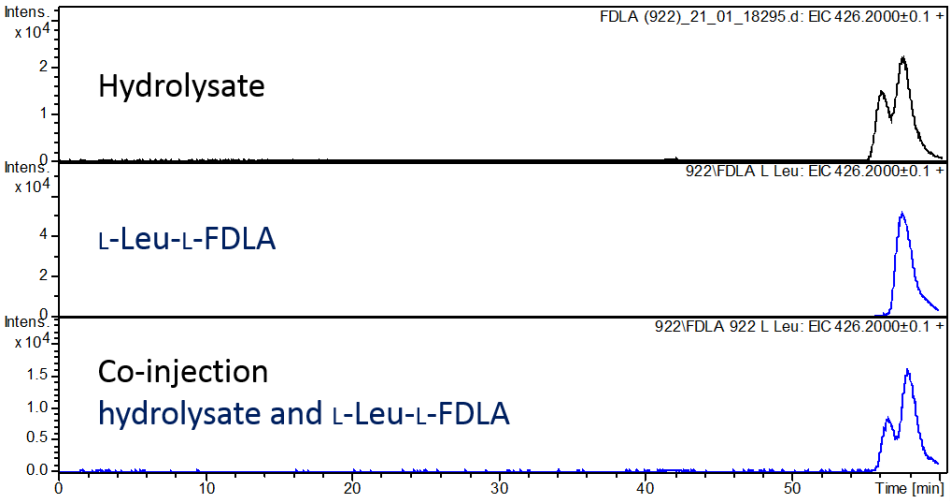

Figure S3G. LC-MS chromatogram of Marfey's analysis of hydrolysate **3** and standard L-Leu

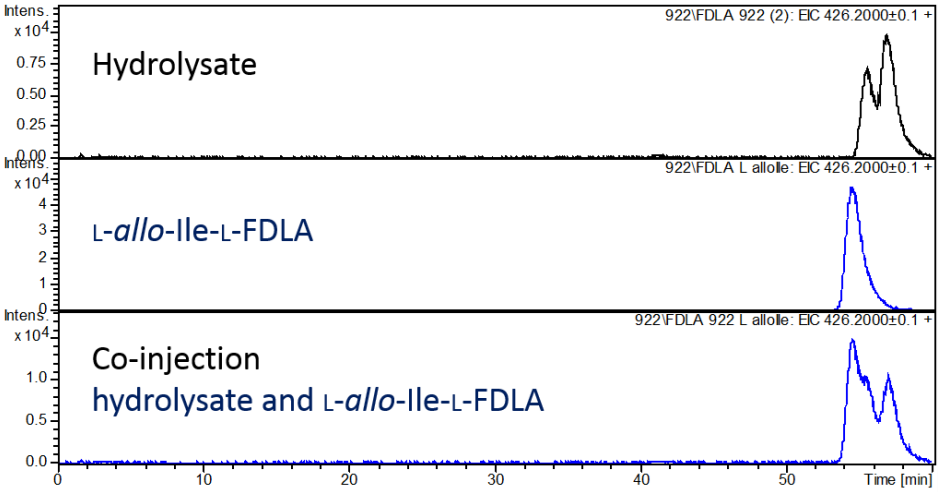

Figure S3H. LC-MS chromatogram of Marfey's analysis of hydrolysate **3** and standard L-*allo*-Ile

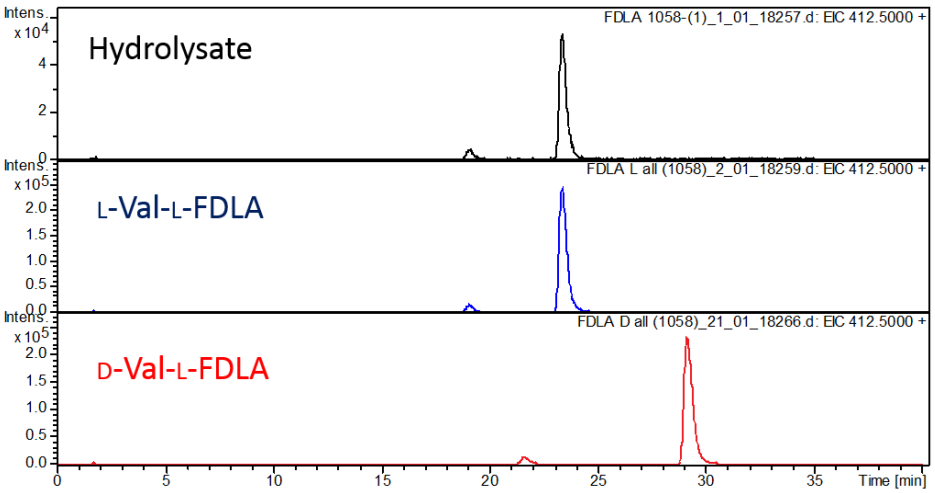

Figure S3I. LC-MS chromatogram of Marfey's analysis of hydrolysate **1** and standards L-Val and D-Val

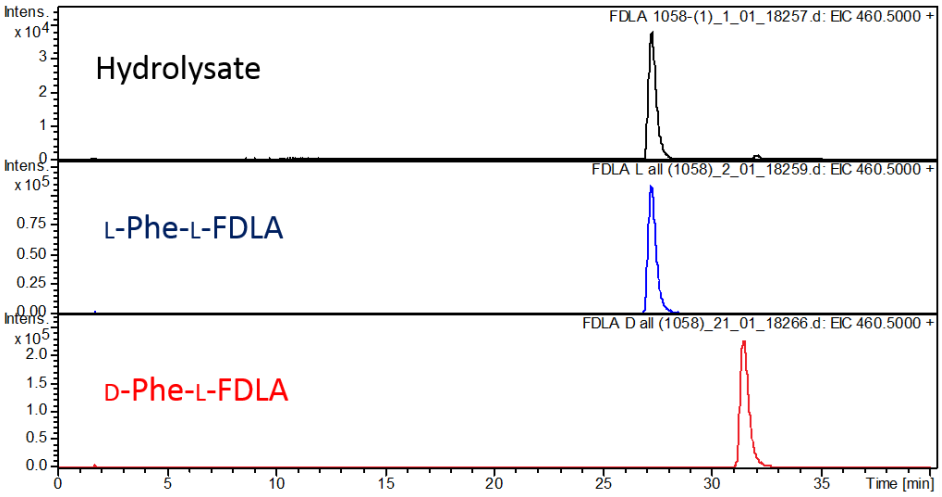

Figure S3J. LC-MS chromatogram of Marfey's analysis of hydrolysate **1** and standards L-Phe and D-Phe

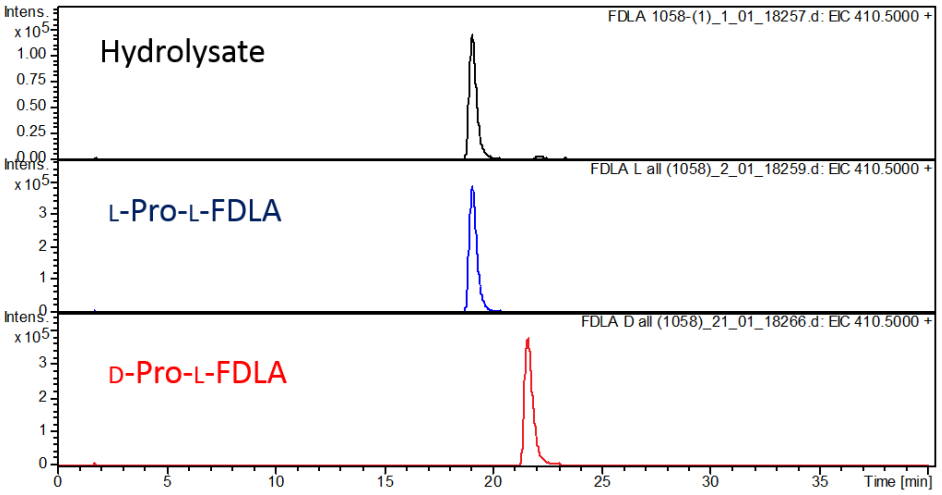

Figure S3K. LC-MS chromatogram of Marfey's analysis of hydrolysate **1** and standards L-Pro and D-Pro

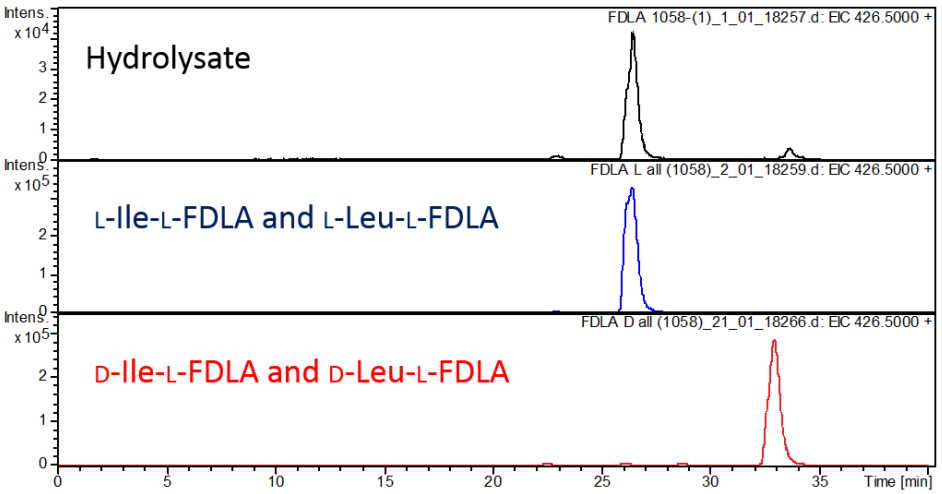

Figure S3L. LC-MS chromatogram of Marfey's analysis of hydrolysate **1** and standards L-Ile, L-Leu, D-Ile and D-Leu

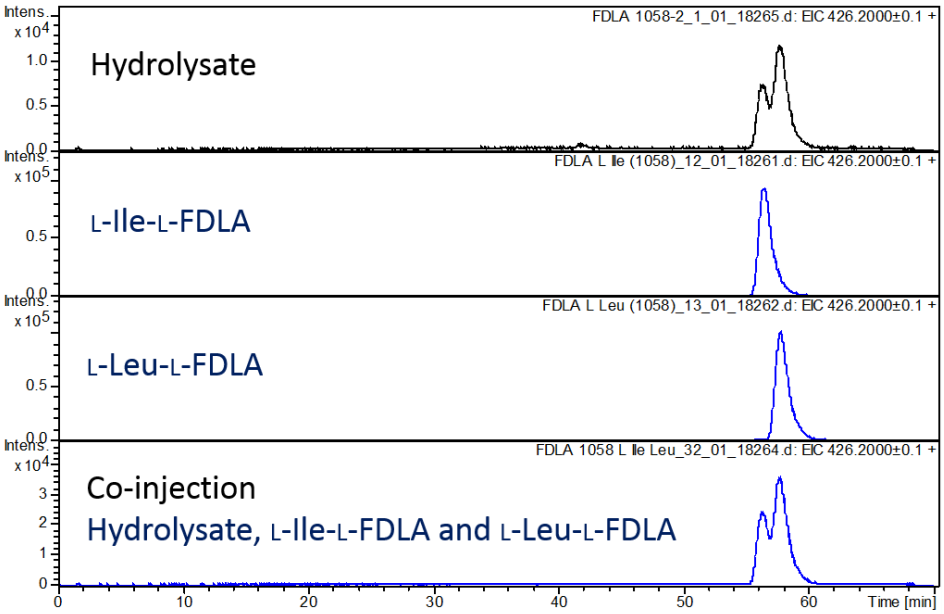

Figure S3M. LC-MS chromatogram of Marfey's analysis of hydrolysate **1** and standards L-Ile and L-Leu

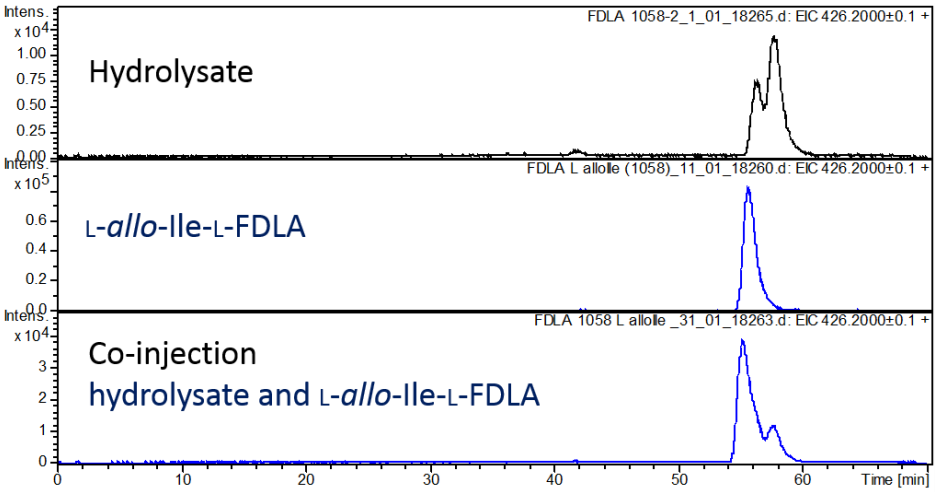

Figure S3N. LC-MS chromatogram of Marfey's analysis of hydrolysate **1** and standard L-*allo*-Ile

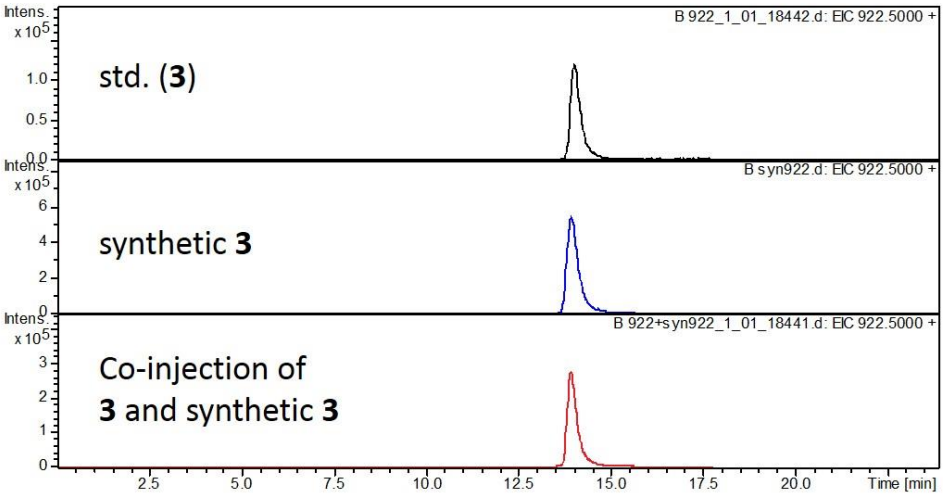

Figure S4. LC-MS comparison of natural and synthetic **3**

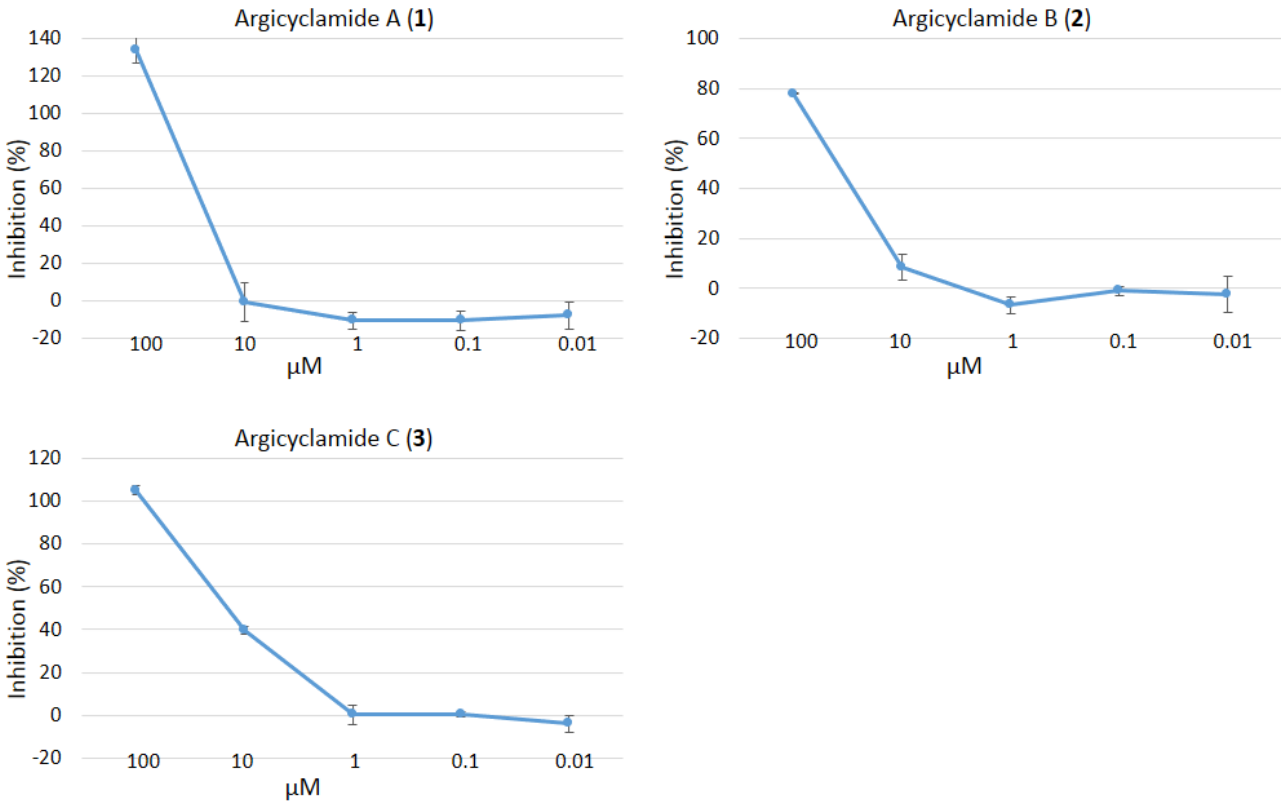

Figure S5. Cytotoxicity of **1-3** against P388 mouse leukemia cells.

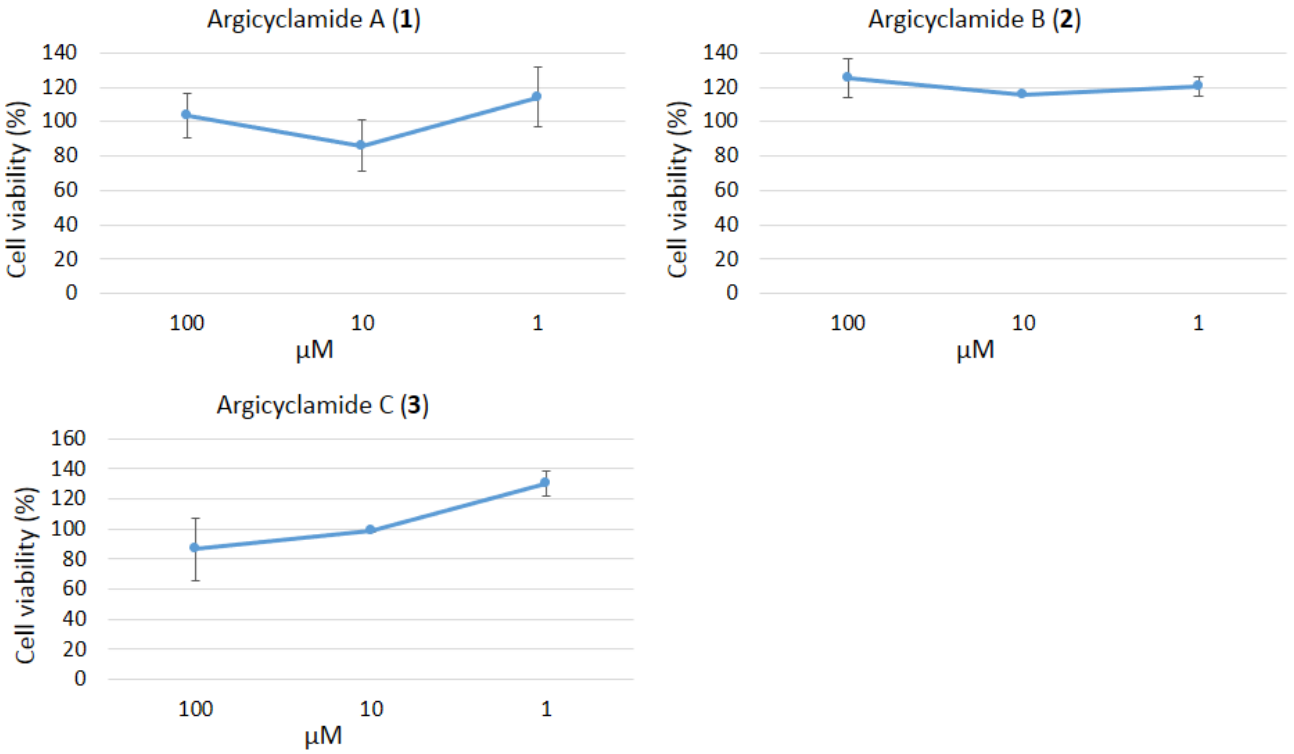

Figure S6. Cytotoxicity of **1-3** against MCF-7 human breast cancer cells.

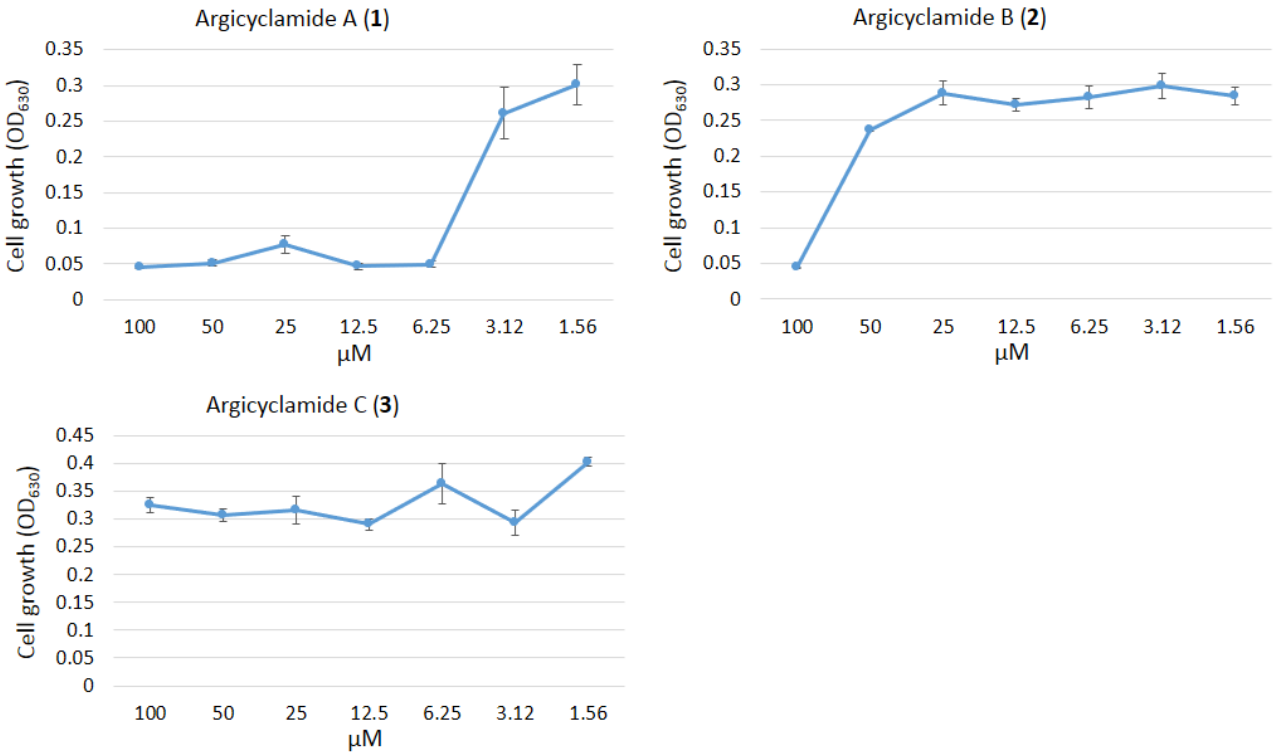

Figure S7 Antibacterial activity of **1**-**3** against *Staphylococcus aureus* (ATCC 12600).

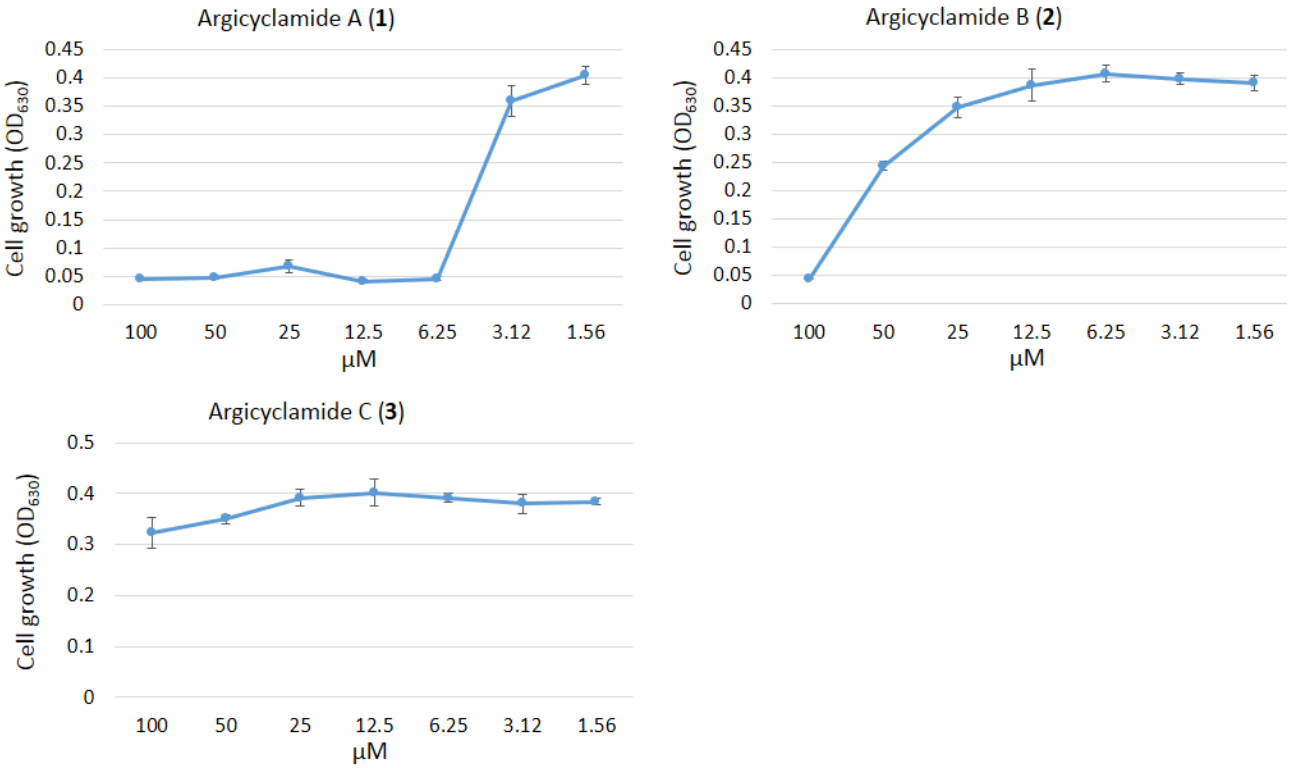

Figure S8. Antibacterial activity of **1**-**3** against methicillin-resistant *Staphylococcus aureus* (ATCC 43300).

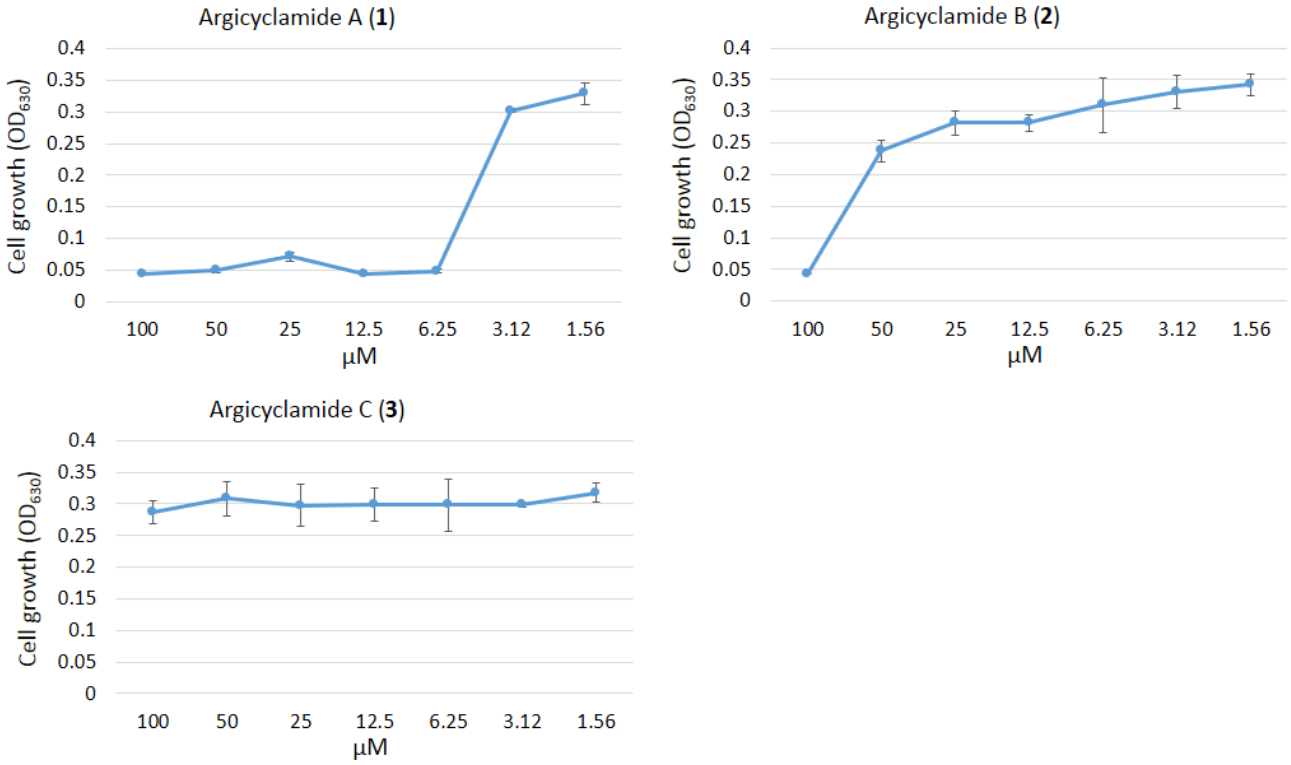

Figure S9. Antibacterial activity of **1-3** against *Bacillus subtilis* (ATCC 6051).

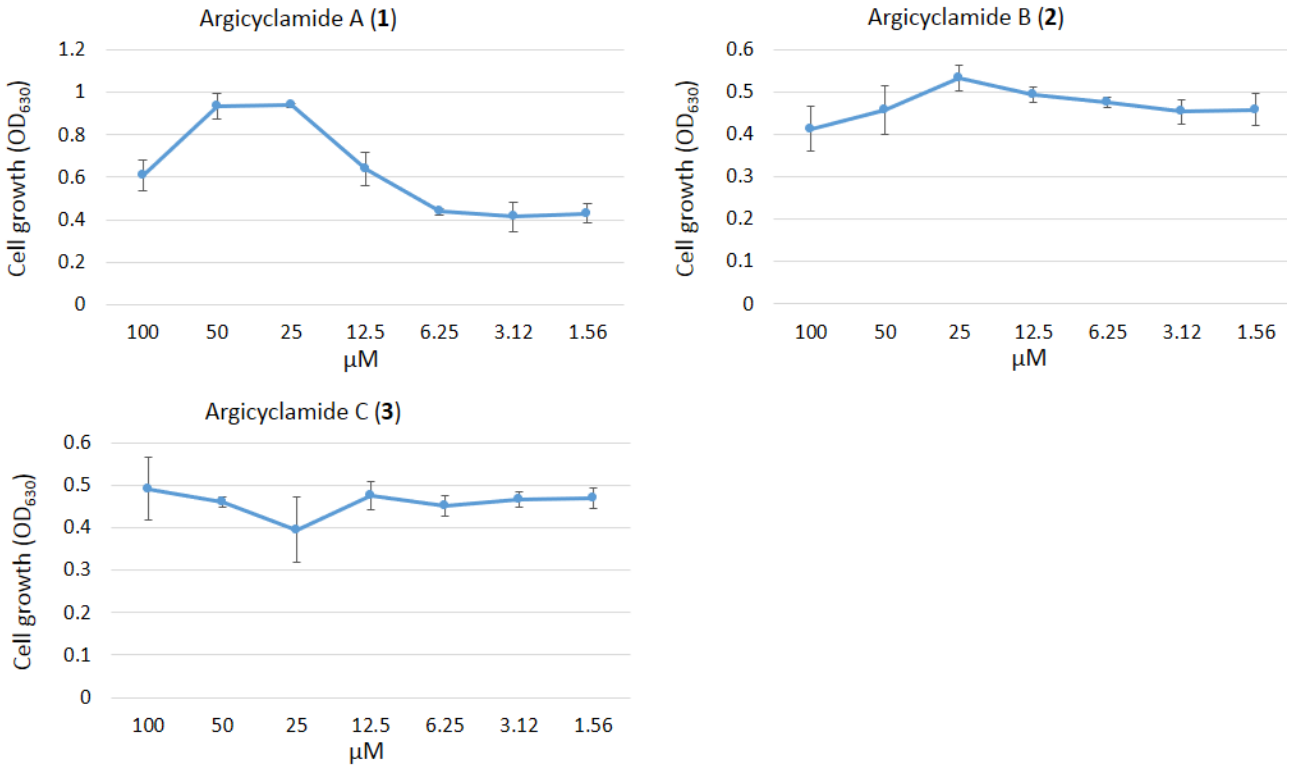

Figure S10. Antibacterial activity of **1-3** against *Pseudomonas aeruginosa* (ATCC 10145).

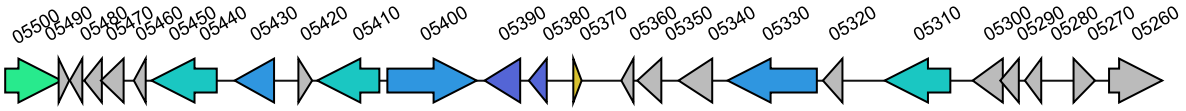

Locus	position	product	note
05260	complement(522525..523511)	IS30 family transposase	WP_011142006.1 IS30 family transposase
05270	complement(523771..524175)	hypothetical protein	
05280	524772..525071	hypothetical protein	
05290	525184..525534	hypothetical protein	
05300	525489..526040	hypothetical protein	WP_011969941.1 IS630 family transposase
05310	526460..527674	ISL3 family transposase ISMac21	WP_011022377.1 ISL3 family transposase ISMac21
05320	528463..528819	hypothetical protein	
05330	528935..530593	IS4 family transposase	WP_011142246.1 IS4 family transposase
05340	530882..531499	hypothetical protein	WP_010933391.1 DNA methylase
05350	531817..532269	hypothetical protein	
05360	532338..532565	hypothetical protein	TIGR01552; phd_fam: prevent-host-death family protein
05370	complement(533301..533450)	AgcE1	TIGR04446; pren_cyc_PirE: prenylated cyclic peptide, anacyclamide/piricyclamide family
05380	533947..534276	hypothetical protein	
05390	534440..535099	hypothetical protein	WP_010947421.1 IS630 family transposase
05400	complement(535248..536906)	IS4 family transposase	WP_011142246.1 IS4 family transposase
05410	537052..538206	ISL3 family transposase	WP_010932205.1 ISL3 family transposase
05420	complement(538297..538560)	hypothetical protein	WP_011673997.1 transposase
05430	539010..539738	hypothetical protein	WP_011142246.1 IS4 family transposase
05440	540071..541285	ISL3 family transposase ISMac21	WP_011022377.1 ISL3 family transposase ISMac21
05450	541396..541614	hypothetical protein	
05460	541801..542217	hypothetical protein	
05470	542205..542534	hypothetical protein	
05480	542564..542797	hypothetical protein	

Figure S11. Genetic region surrounding *agcE1* (MAN88_05370). No genes related to cyanobactin biosynthesis is encoded around *agcE1* gene.

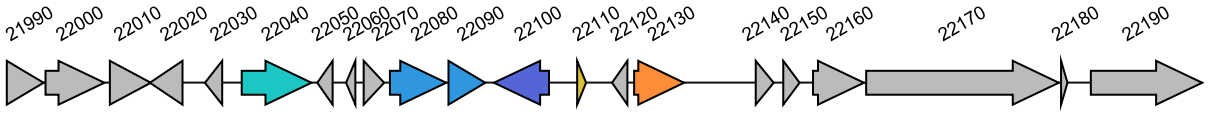

Locus	position	product	note
21990	2270250..2270885	phosphoheptose isomerase 2	gmhA2
22000	2270923..2271948	dehydrogenase	hddA
22010	2272040..2272756	D-mannose-1-phosphate guanyltransferase	TIGR03992; Arch_glmU: UDP-N-acetylglucosamine diphosphorylase/glucosamine-1-phosphate N-acetyltransferase
22020	complement(2272734..2273303)	hypothetical protein	
22030	complement(2273697..2273993)	hypothetical protein	
22040	2274335..2275549	ISL3 family transposase ISMac21	WP_011022377.1 ISL3 family transposase ISMac21
22050	complement(2275972..2276118)	hypothetical protein	
22060	complement(2276147..2276308)	hypothetical protein	WP_011143213.1 transposase
22070	2276456..2276809	hypothetical protein	
22080	2276911..2277885	hypothetical protein	WP_011142246.1 IS4 family transposase
22090	2277931..2278569	hypothetical protein	WP_011142246.1 IS4 family transposase
22100	complement(2278718..2279674)	hypothetical protein	WP_010947421.1 IS630 family transposase
22110	2280171..2280320	AgcE2	TIGR04446; pren_cyc_PirE: prenylated cyclic peptide, anacyclamide/piricyclamide family
22120	complement(2280908..2281123)	hypothetical protein	
22130	2281154..2282026	AgcF	preny_LynF_TruF: peptide O-prenyltransferase, LynF/TruF/PatF family
22140	2283276..2283581	hypothetical protein	TIGR03798; ocin_TIGR03798: nif11-like leader peptide domain
22150	2283750..2284034	hypothetical protein	TIGR03798; ocin_TIGR03798: nif11-like leader peptide domain
22160	2284270..2285154	hypothetical protein	TIGR:TIGR01575; rimI: ribosomal-protein-alanine acetyltransferase
22170	2285195..2288542	hypothetical protein	TIGR:TIGR03897; lanti_2_LanM: type 2 lantibiotic biosynthesis protein LanM
22180	2288578..2288691	hypothetical protein	
22190	2289099..2291033	hypothetical protein	TIGR:TIGR01844; type_I_sec_TolC: type I secretion outer membrane protein, TolC family

Figure S12. Genetic region surrounding *agcE2* (MAN88_22110). *agcF* (MAN88_22130) that exhibits similarity to cyanobactin prenyltransferase is colored in orange. No other cyanobactin biosynthetic enzymes such as PatA/G family proteases are encoded in neighboring region of *agcE2*.

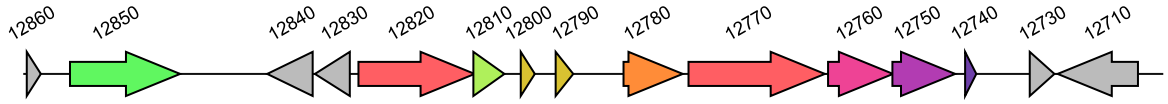

Locus	position	product	note
12710	1352918..1354195	hypothetical protein	TIGR03937; PgaC_IcaA: poly-beta-1,6 N-acetyl-D-glucosamine synthase
12720	1354222..1355406	glycosyl transferase	TIGR04182: glycosyltransferase, TIGR04182 family
12730	complement(1355450..1355815)	hypothetical protein	WP_011057900.1 hypothetical protein
12740	complement(1356108..1356305)	hypothetical protein	WP_011056077.1 transposase
12750	complement(1356919..1357842)	hypothetical protein	
12760	complement(1357839..1358798)	hypothetical protein	WP_003978028.1 hypothetical protein
12770	complement(1358843..1360861)	KgpG1	TIGR03895; protease_PatA: cyanobactin maturation protease, PatA/PatG family
12780	complement(1360948..1361820)	KgpF1	TIGR04445; preny_LynF_TruF: peptide O-prenyltransferase, LynF/TruF/PatF family
12790	complement(1362563..1362826)	KgpE1	
12800	complement(1363329..1363487)	KgpC1	
12810	complement(1363576..1364040)	KgpB1	TIGR04220; patB_acyB_mcaB: cyanobactin biosynthesis protein, PatB/AcyB/McaB family
12820	complement(1364022..1365740)	KgpA1	TIGR03895; protease_PatA: cyanobactin maturation protease, PatA/PatG family
12830	1365864..1366376	hypothetical protein	
12840	1366412..1367086	hypothetical protein	WP_011119850.1 transposase
12850	complement(1368375..1369997)	hypothetical protein	
12860	complement(1370430..1370639)	hypothetical protein	

Figure S13. Genes encoded in *kgp1* (MAN88_12770–12820) and its vicinity region.

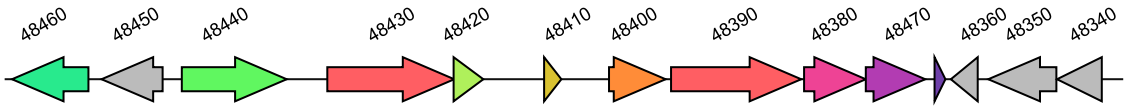

Locus	position	product	note
48340	4951141..4952439	O-acetylhomoserine (thiol)-lyase	cysD
48350	4952455..4953507	homoserine O-acetyltransferase	metX
48360	4953677..4954087	hypothetical protein	TIGR00675; dcm: DNA (cytosine-5-)-methyltransferase
48370	complement(4954489..4955412)	hypothetical protein	
48380	complement(4955409..4956368)	hypothetical protein	WP_003978028.1 hypothetical protein
48390	complement(4956413..4958431)	KgpG2	TIGR03895; protease_PatA: cyanobactin maturation protease, PatA/PatG family
48400	complement(4958518..4959390)	KgpF2	TIGR04445; preny_LynF_TruF: peptide O-prenyltransferase
48410	complement(4960133..4960396)	KgpE2	
48420	complement(4961341..4961805)	KgpB2	TIGR04220; patB_acyB_mcaB: cyanobactin biosynthesis protein, PatB/AcyB/McaB family
48430	complement(4961787..4963760)	KgpA2	TIGR03895; protease_PatA: cyanobactin maturation protease, PatA/PatG family
48440	complement(4964391..4966013)	hypothetical protein	
48450	4966315..4967265	cytosine-specific methyltransferase	TIGR00675; dcm: DNA (cytosine-5-)-methyltransferase
48460	4967464..4968651	transposase	WP_011056077.1 transposase

Figure S14. Genes encoded in *kgp2* (MAN88_48390–48430) and its vicinity region.

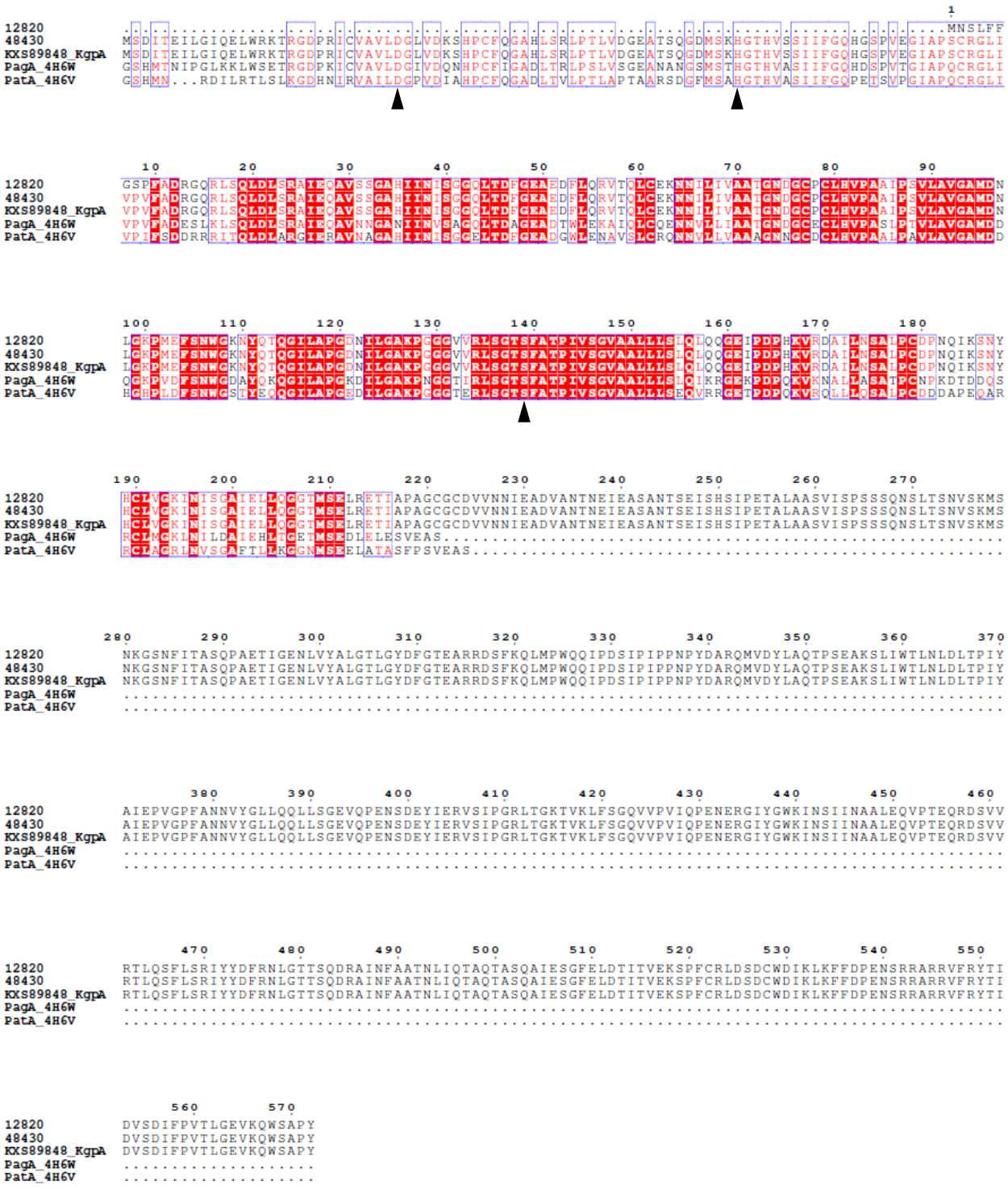

Figure S15. Amino acid sequence comparison of KgpAs in *M. aeruginosa* NIES-88. KgpA1 (MAN88_12820) and KgpA2 (MAN88_48430) were compared with KgpA sequence in public database (OA58_19035) and protease domains of PatA (PDB: 4H6V) and PagA (PDB: 4H6W) that are involved in patellamide and prenylagaramide biosyntheses, respectively. Catalytic triad are highlighted by black arrows. KgpA1 (MAN88_12820) lacks *N*-terminal region (approx. 100 aa) that contains two catalytic residues, suggesting that enzymatic activity of KgpA1 is abolished.

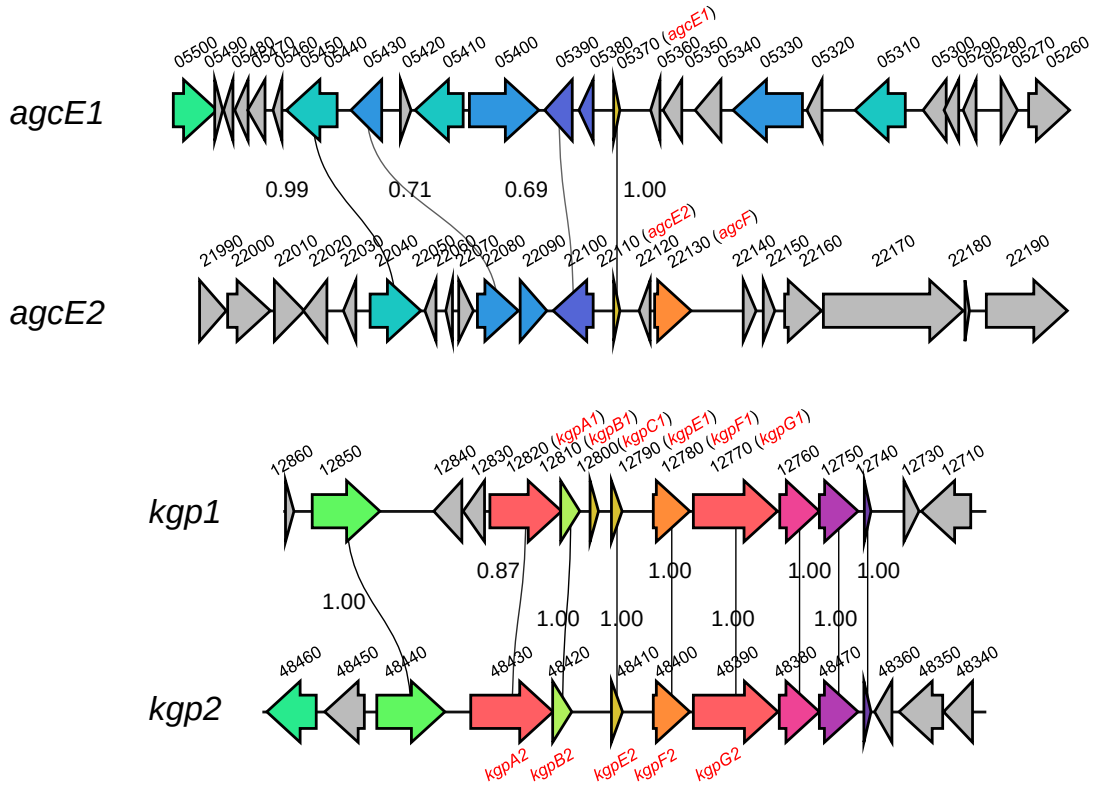

Figure S16. Comparison of cyanobactin related genetic regions in *M. aeruginosa* NIES-88. Genes are labeled with their locus numbers. Homologous genes are depicted in same color. Homologous genes are connected with lines. Sequence identities (1.00 means identical) are labeled upon each line. Figure was generated by clinker.[18]

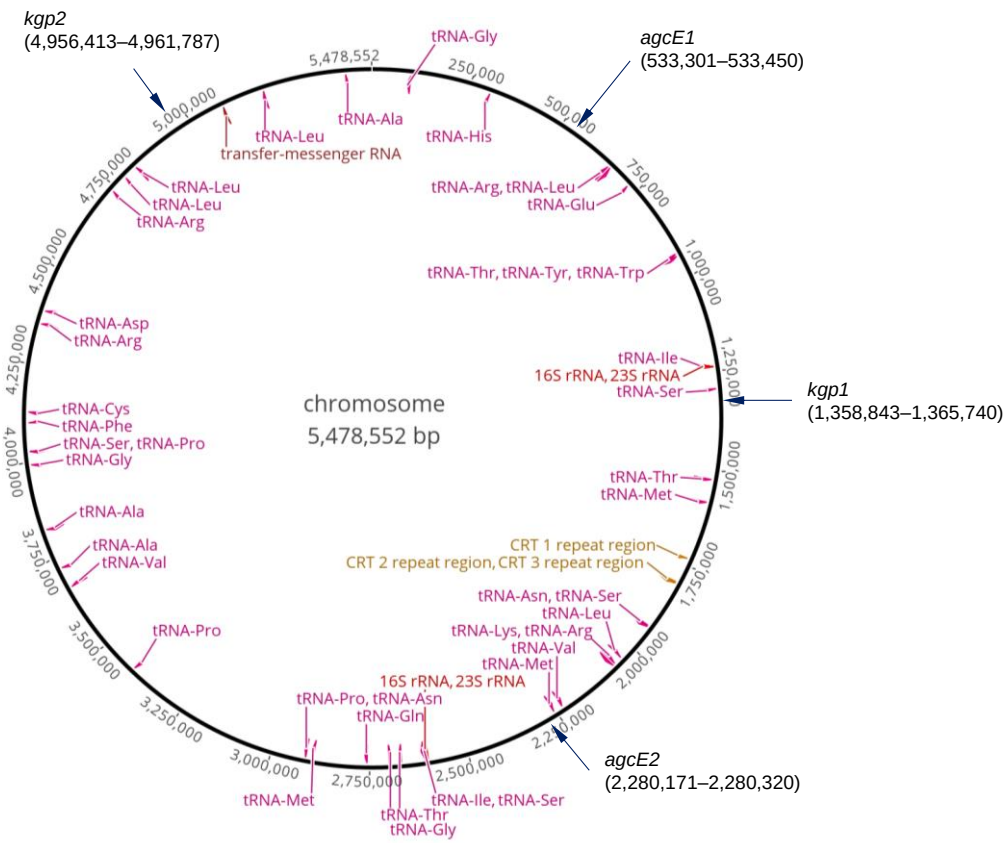

Figure S17. Positions of cyanobactin-related genes in the chromosome of *M. aeruginosa* NIES-88.

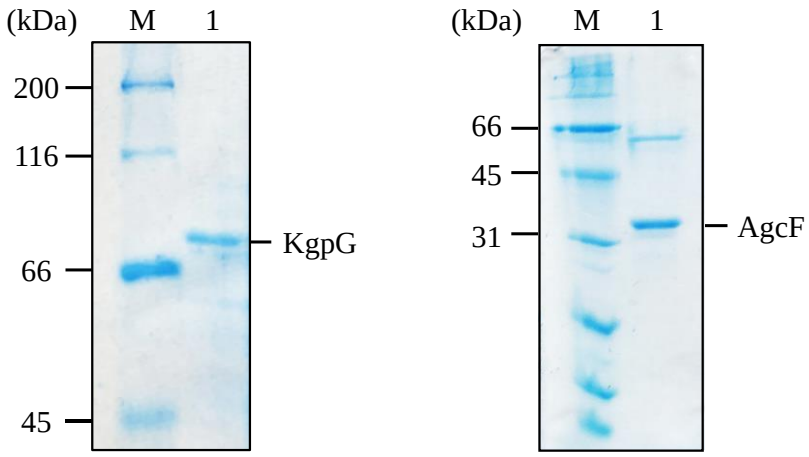

Figure S18. SDS-PAGE for recombinant KgpG (left) and AgcF (right). Left) KgpG M: molecular weight marker, 1: KgpG eluted from Ni-NTA column. Theoretical molecular weight of recombinant KgpG is 74 kDa. Right) M: molecular weight marker, 1: AgcF eluted from Ni-NTA column. Theoretical molecular weight of recombinant AgcF is 35 kDa.

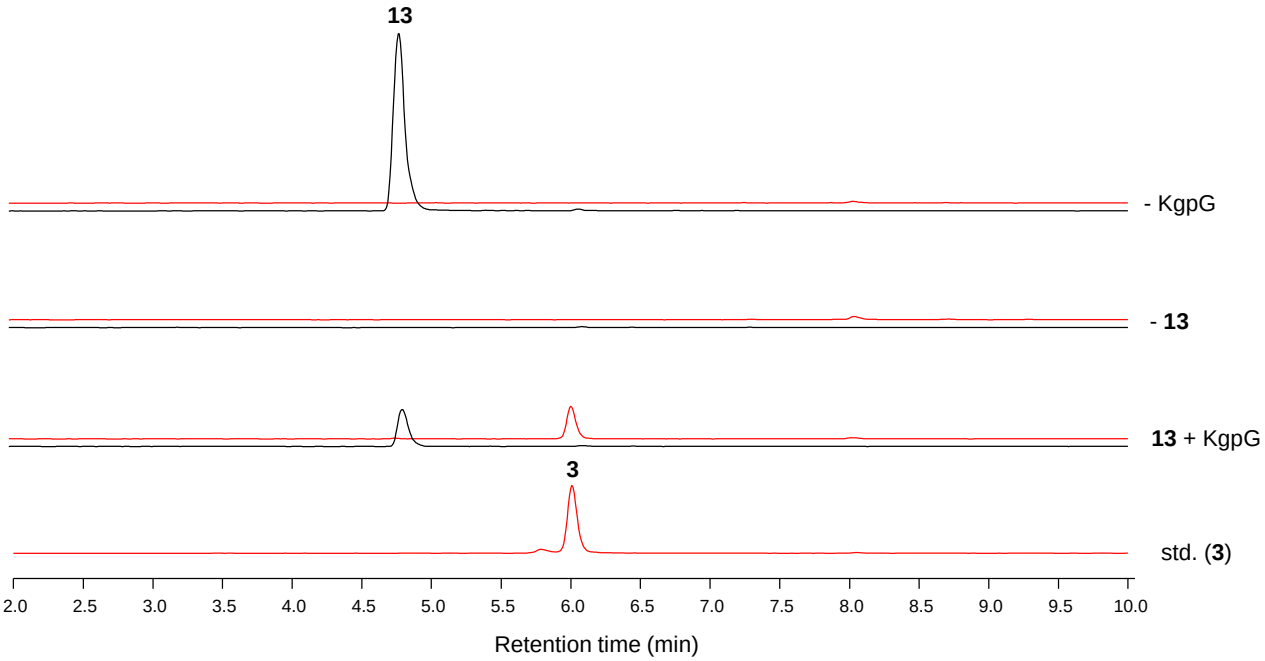

Figure S19. LC-MS analysis of KgpG reaction mixture. Extracted ion chromatographs (EICs) at *m/z* 830.0 for pentadecapeptide (**13**) and *m/z* 922.0 for argicyclamide C (**3**) are depicted as black, and red lines, respectively. **3** is accumulated in KgpG-dependent manner, showing that KgpG is capable of cyclizing **13** *in vitro*.

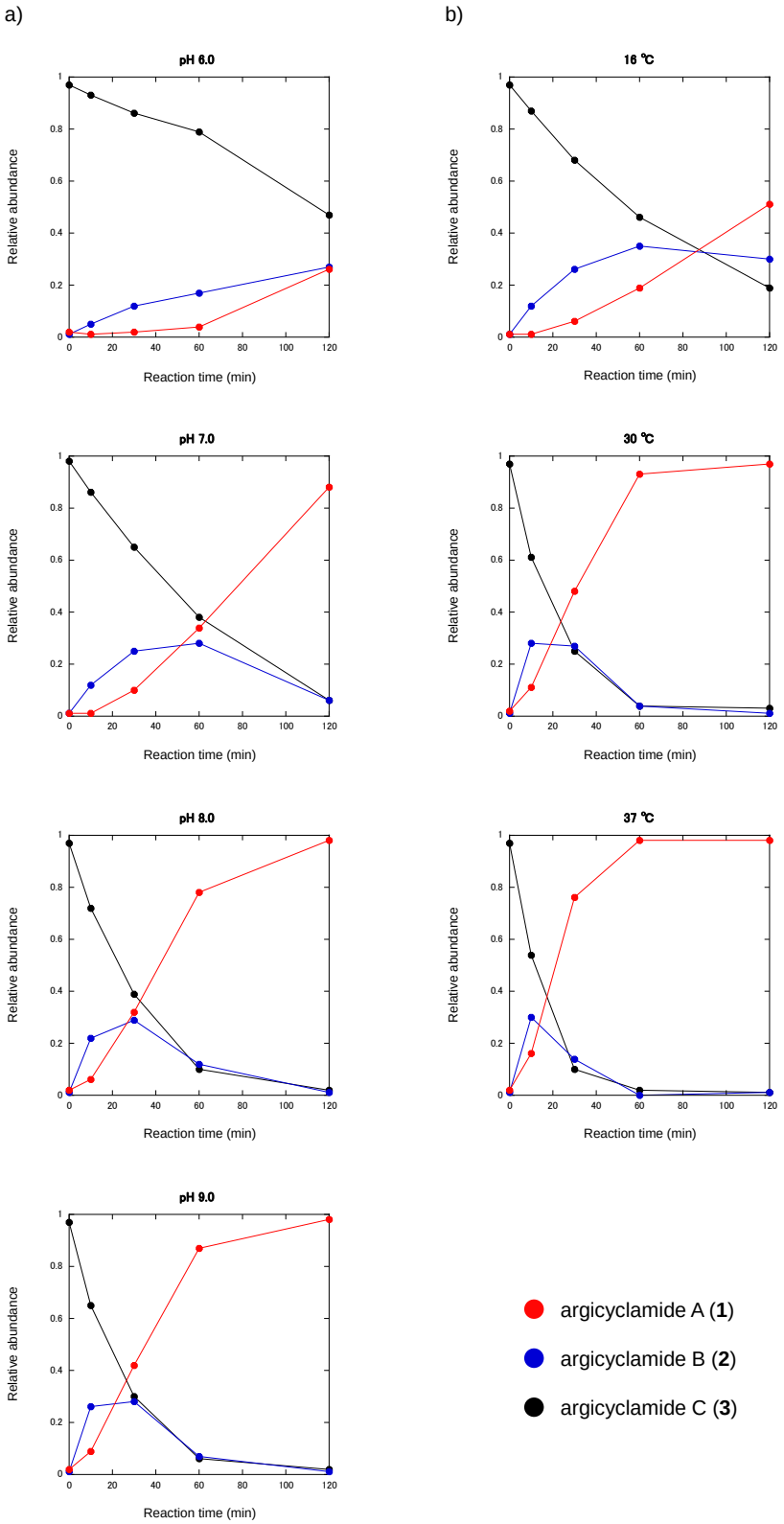

Figure S20. Effect of pH and temperature on AgcF activity. Relative abundance of **1**-**3** in different reaction conditions at each reaction time are shown in red, blue and black lines, respectively. a) Effect of pH on AgcF activity was evaluated by reaction mixtures containing 50 mM of phosphate buffer (pH 6.0), 50 mM phosphate buffer (pH 7.0), 50mM HEPES buffer (pH 8.0) or Tris buffer (pH 9.0). Mixtures were incubated at 37 °C. The highest enzymatic activity was observed at pH 9.0. b) Effect of temperature on AgcF activity was evaluated by incubating reaction mixtures at 16 °C, 30 °C, or 37 °C. All reaction contains 50 mM HEPES buffer (pH8.0). The highest enzymatic activity was exerted at 37 °C.

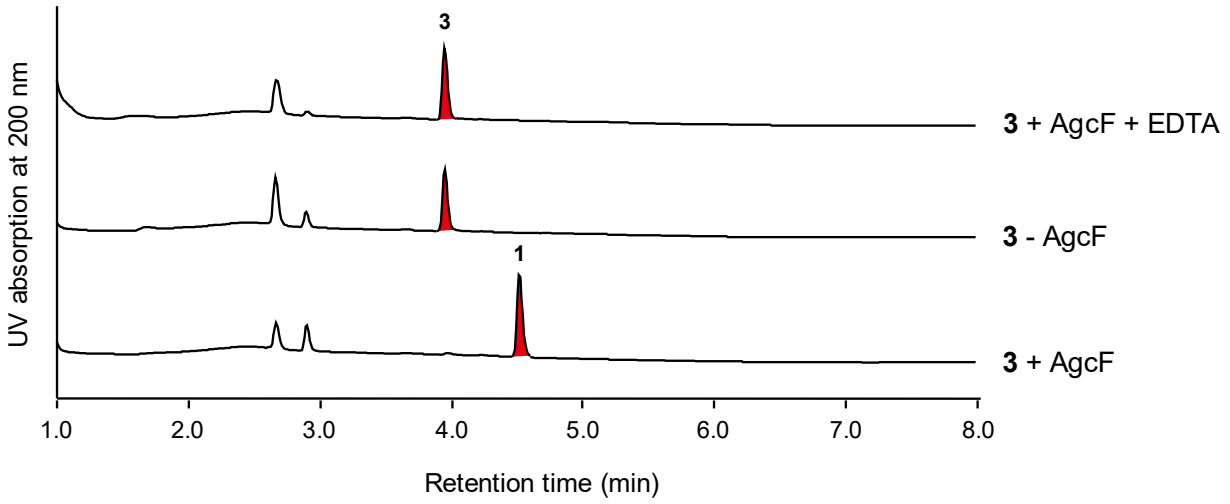

Figure S21. Mg^{2+} dependency of AgcF. Prenylation activity of AgcF was abolished by addition of 10 mM EDTA. Reaction mixtures were analyzed by UPLC-MS monitoring UV absorption at 200 nm.

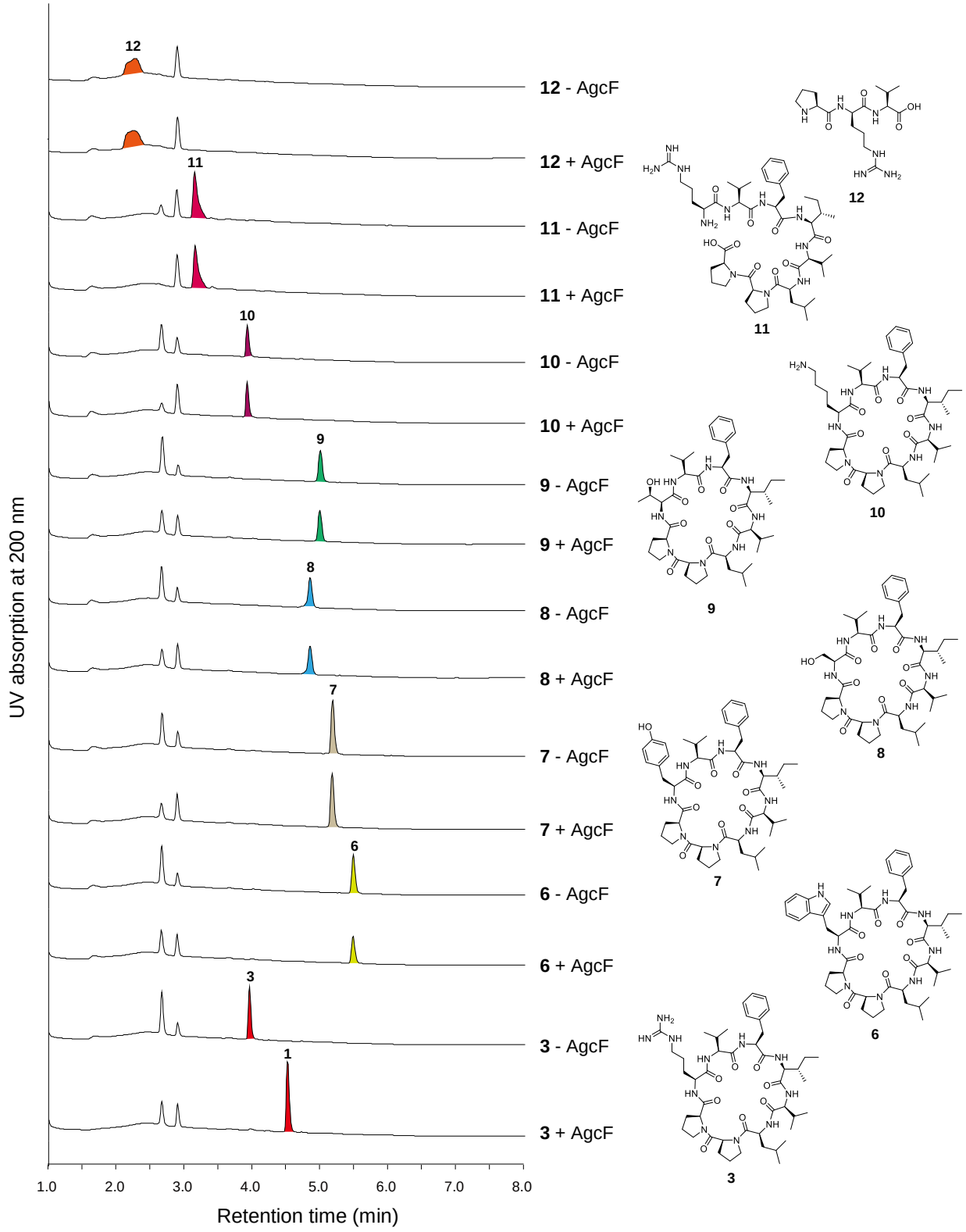

Figure S22. AgcF specifically prenylates argicyclamide C (**3**). Substrate specificity of AgcF on prenyl acceptor was accessed by using **6**-**12**, synthetic analogs of **3**. Structure of peptidyl substrates are shown in right side of each chromatogram. Reaction mixtures were analyzed by UPLC-MS monitoring UV absorption at 200 nm. AgcF catalyzed bis-prenylation of **3** to yield **1**, while it showed no activity against **3** analogs including R1W (**6**), R1Y (**7**), R1S (**8**), R1T (**9**), and R1K (**10**). This result shows that AgcF is guanidine-specific prenyltransferase. AgcF was incapable of prenylating linear peptide (**11**) and PRV tripeptide (**12**), showing that AgcF is specific for cyclic peptide.

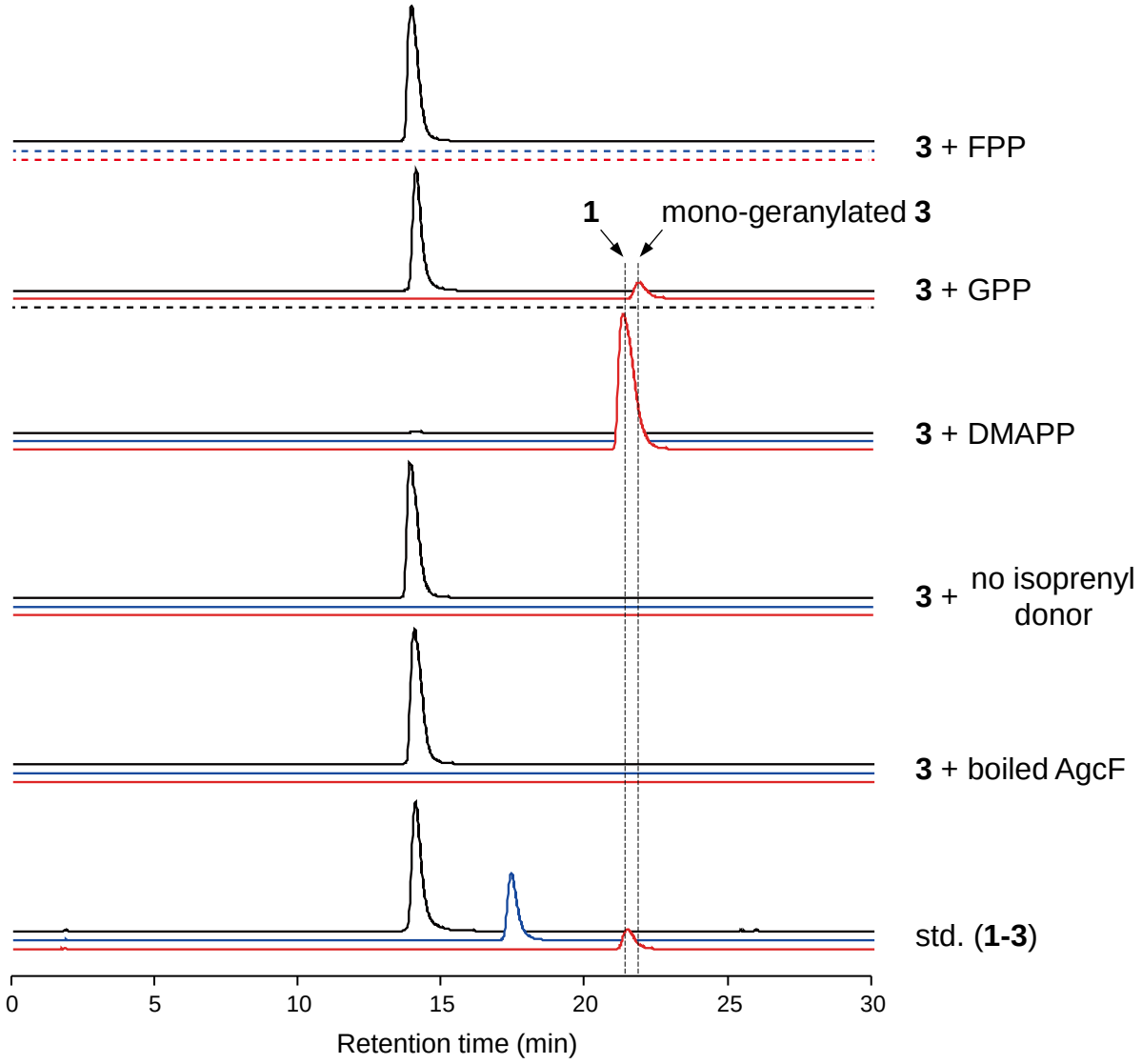

Figure S23. Specificity of AgcF on isoprenyl donor. Reaction mixtures were analyzed by LC-MS. EICs of *m/z* 922.5000 (black) for **3**, *m/z* 990.5000 (blue) for **2**, 1058.5000 (red) for **1** and geranylated **3** (*m/z* 1058.7123 $[M + H]^+$; calcd. for $C_{57}H_{92}N_{11}O_8^+$ 1058.7125), *m/z* 1194.5000 (dashed black line) for bis-geranylated **3**, *m/z* 1126.5000 (dashed blue line) for mono-farnesylated **3**, *m/z* 1330.5000 (dashed red line) for bis-farnesylated **3** were shown. **3** was mono-geranylated by AgcF after 24h of incubation at 37 °C.

a)

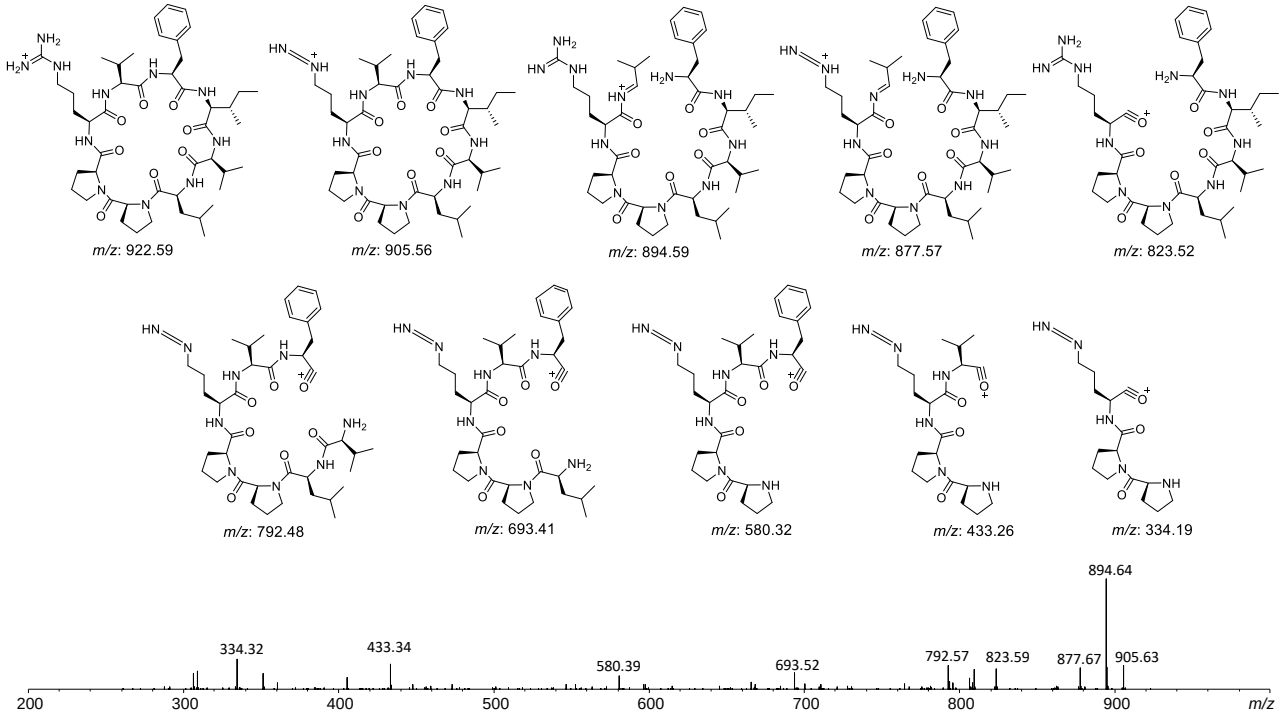

b)

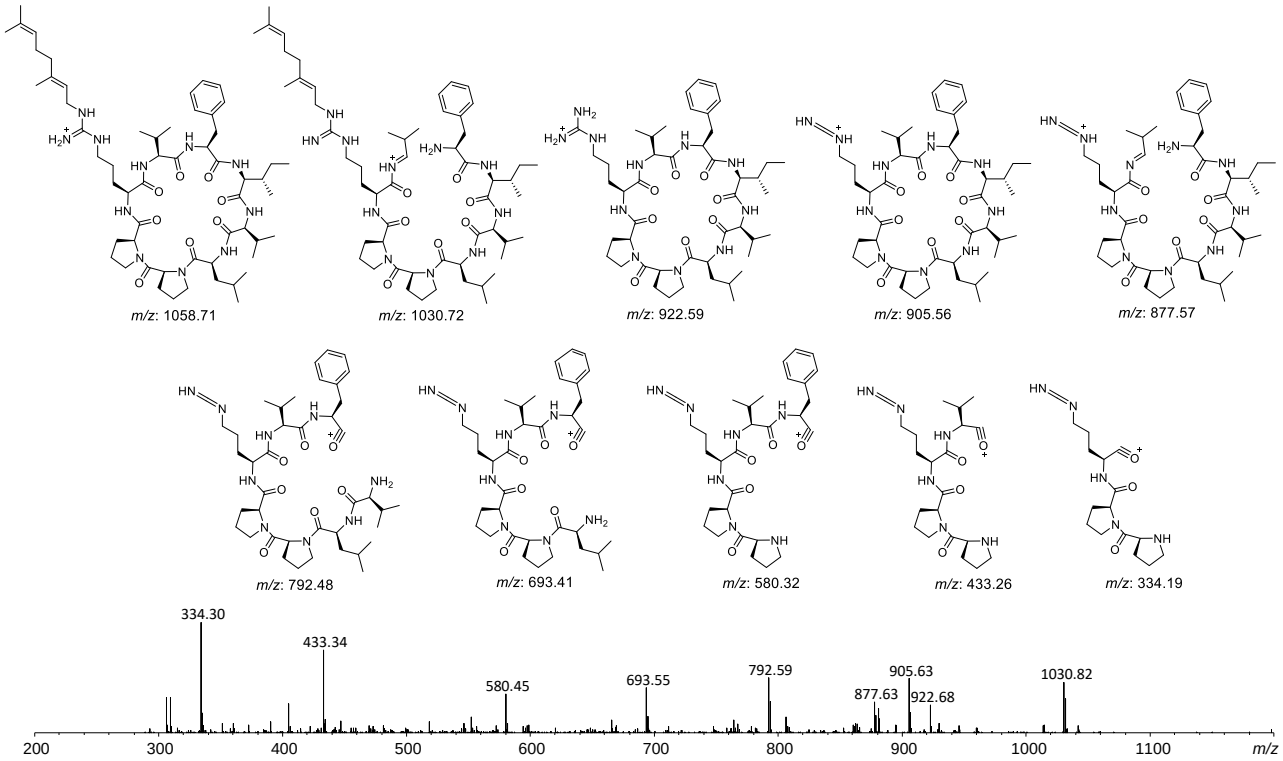

Figure S24. MS2 spectra of (a) argicyclamide C (**3**), and (b) geranylated **3**.

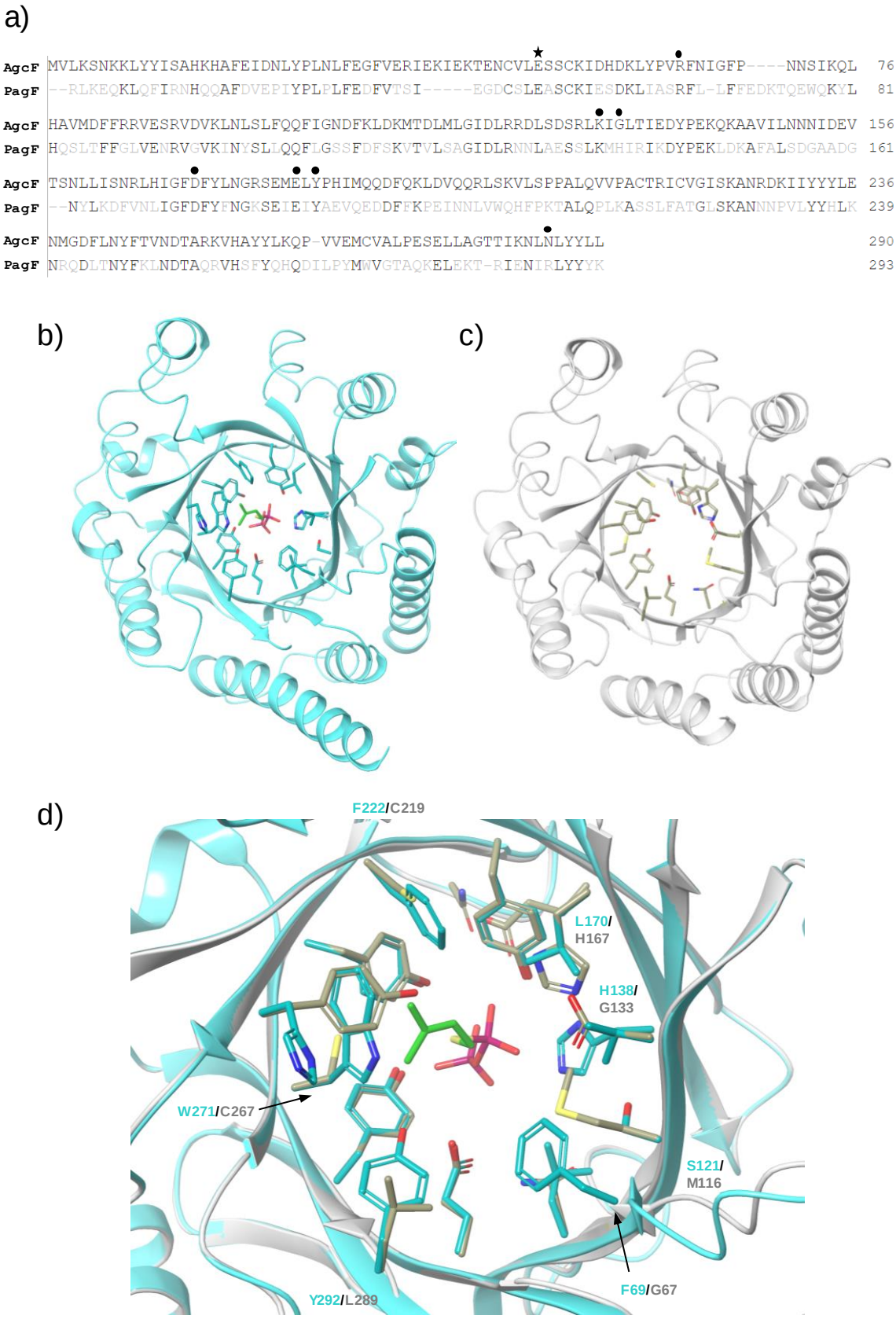

Figure S25. Structural comparison of AgcF and PagF. (a) Primary sequence alignment of AgcF and PagF. The proposed catalytic residue Glu51 (in PagF) is highlighted by star. Residues involved in binding of Mg ion and diphosphate group are highlighted by dot. The proposed catalytic residue

Glu49 and diphosphate recognizing residues are well conserved between AgcF and PagF. (b) Structure of PagF (PDB ID: 5TU6). DMSPP and the residues at the active site entrance are represented as thick tube. (c) Computational modeling of AgcF. The model was generated by SWISS-MODEL web tool,[17] using PagF structure (5TU6) as a template. Corresponding residues are represented as thick tube. (d) Superposition of PagF active sites (cyan) and that of AgcF model (gray). Several residues with bulky side chain in PagF are substituted to smaller residues in AgcF; for example, F69, H138, W271, and Y292 in PagF are substituted to G67, G133, C267, and L289 in AgcF, respectively. These substitutions in AgcF should enlarge its active site entrance, facilitating the accommodation of bulky mono-prenylated Arg residue for second round prenylation.

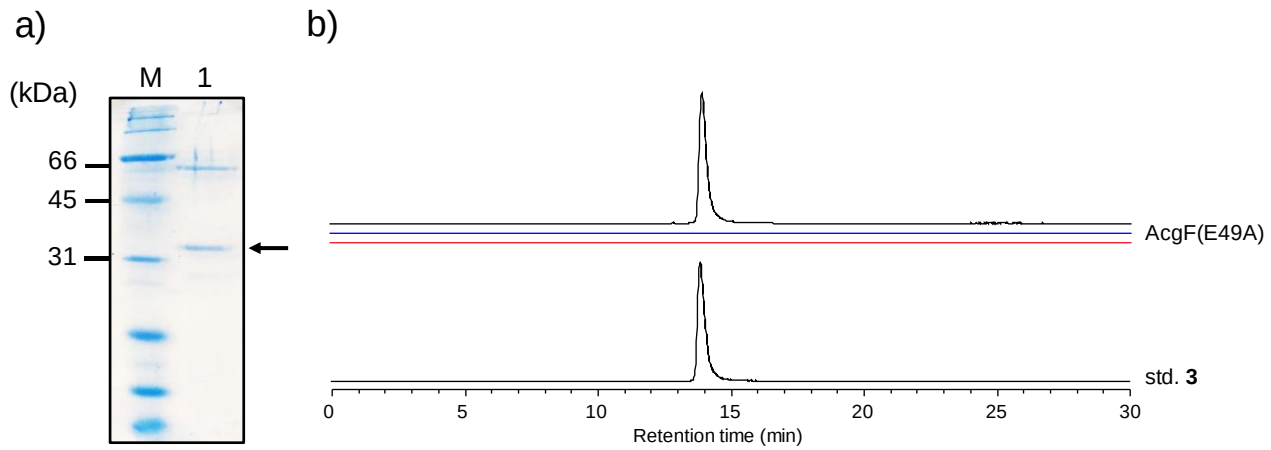

Figure S26. *in vitro* analysis of AgcF(E49A) mutant. (a) SDS-PAGE for AgcF(E49A) mutant (Theoretical molecular weight: 35 kDa). The recombinant protein is shown by an arrow. M: molecular weight marker, 1: AgcF eluted from Ni-NTA column. (b) LC -MS analysis of reaction mixture containing AgcF(E49A) mutant. EICs of *m/z* 922.5000 for **3** (black line), 990.5000 for **2** (blue line) and 1058.5000 for **1** (red line) are depicted. E49A mutation resulted in loss of prenylation activity of AgcF.

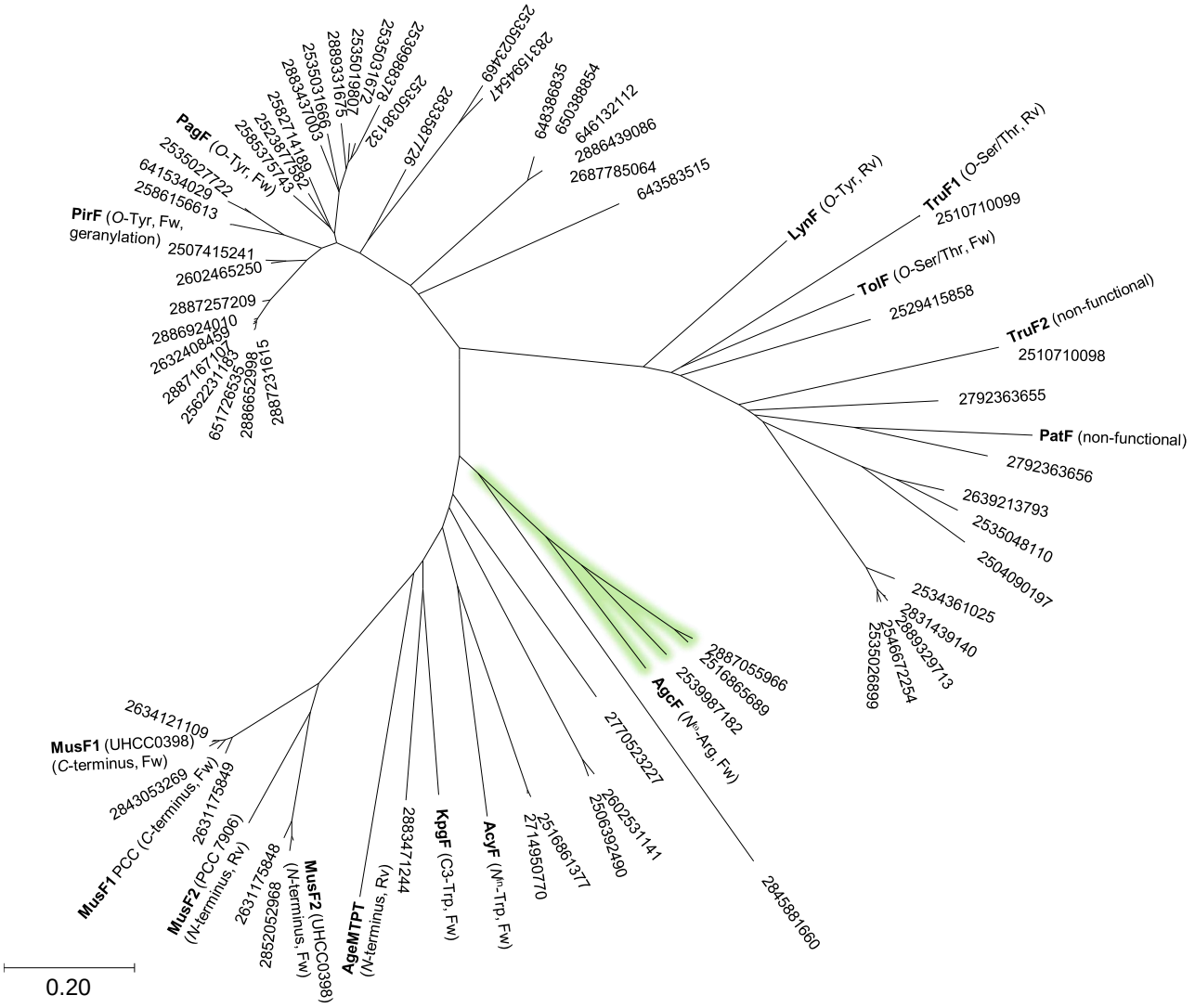

Figure S27. Phylogenetic analysis of cyanobactin PTases. Amino acid sequences were retrieved from JGI database[19] and NCBI database. Tree was constructed by Neighbor-Joining method using MEGA X.[20] JGI gene id of each PTase homologs are described. PTases with biochemical characterization are indicated by bold letters, and their gene ids are listed in the legend of Figure S28. Prenylation sites and orientations (Fw: forward prenylation, Rv: reverse prenylation) of these PTases are also described. The PTase domain of AgeMTPT (aeruginosamide pathway) was used for constructing the tree. AgeMTPT is a di-domain protein with *N*-terminal methyltransferase and *C*-termianl PTases domain. The tree suggests that cyanobactin PTases forms clades according to their chemo-selectivity. Similar trend was also observed in sequence similarity network analysis of cyanobactin PTases.[14,21] The phylogenetic analysis indicates that AgcF forms a small clade highlighted in green together with some homologs derived from *Microcystis aeruginosa* PCC 9443 (JGI gene id: 2539987182), *Aphanizomenon* sp. UHCC 0183 (JGI gene id: 2887055966) and *Dolichospermum circinale* AWQC310F (JGI gene id: 2516865689). The vicinity regions of these homologous genes are depicted in Figure S29.

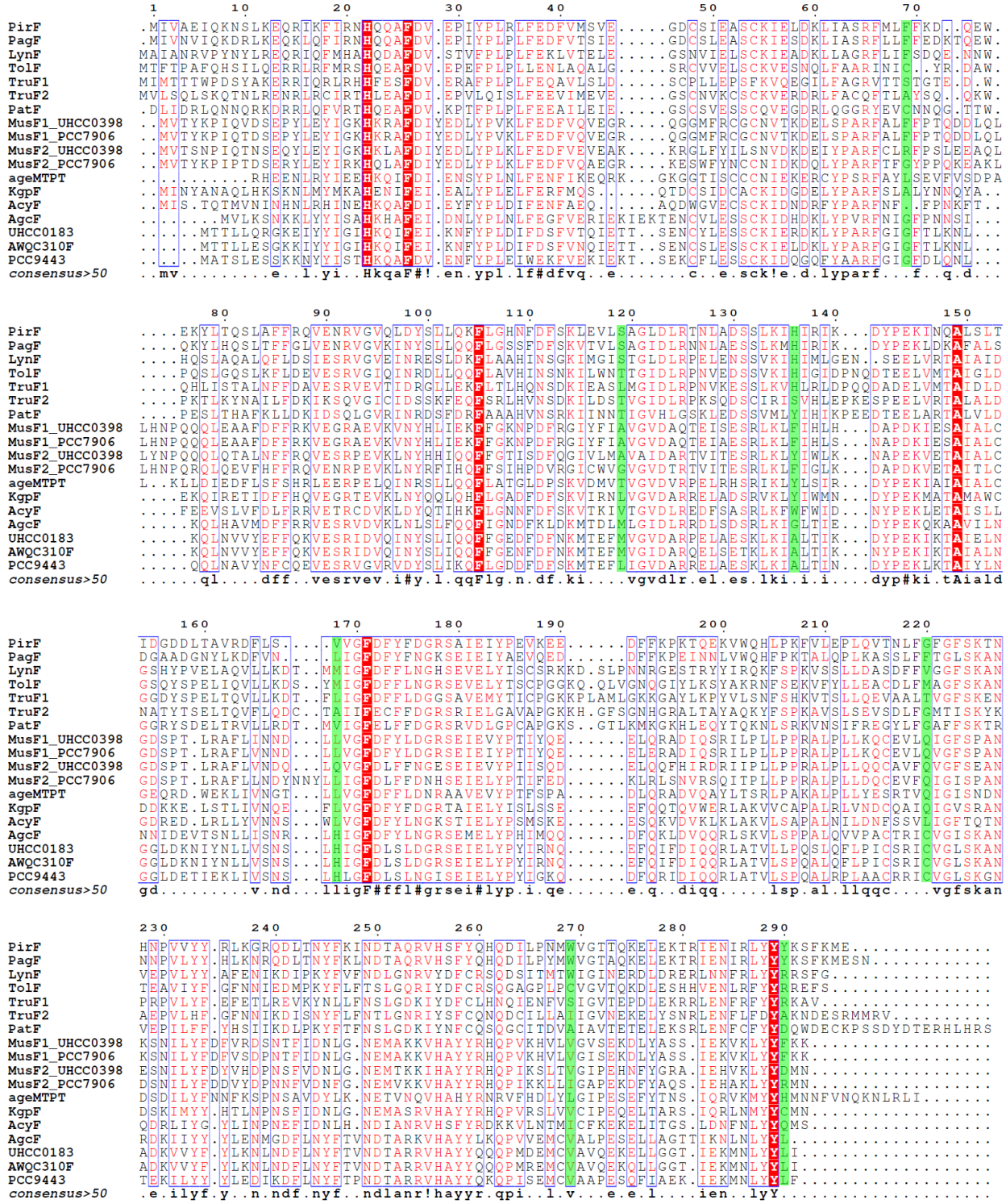

Figure S28. Multiple alignment of cyanobactin PTases. Positions of the residues at the substrate entrance site in PagF (PDB ID: 5TU6) are colored in green. Following sequences are used to construct this alignment; AgcF: PTase in argicyclamide biosynthesis (GenBank id: BCU11649); UHCC0183: the AgcF homolog in *Aphanizomenon* sp. UHCC 0183 (JGI gene id: 2887055966); AWQC310F: the AgcF homolog in *Dolichospermum circinale* AWQC310F (JGI gene id: 2516865689); PCC9443: *Microcystis aeruginosa* PCC 9443 (JGI gene id: 2539987182); AcyF: PTase in anacyclamide biosynthesis (GenBank id: AZB51087); KgpF: PTase in kawaguchipeptin biosynthesis (GenBank id: KXS89935); ageMTPT; PTase in aeruginosamide biosynthesis

(GenBank id: CCH92966); MusF1_UHCC0398: PTase in muscoride B biosynthesis (GenBank id: QGA72595); MusF1_PCC7906: PTase in muscoride A biosynthesis (GenBank id: QGA72590); MusF2_UHCC0398: PTase in muscoride B biosynthesis (GenBank id: QGA72594); MusF2_PCC7906: PTase in muscoride A biosynthesis (GenBank id: QGA72591); PirF: PTase in piricyclamide biosynthesis (GenBank id: AFK79989); PagF: PTase in prenylagaramide biosynthesis (GenBank id: AED99429); TruF1: PTase in trunkamide biosynthesis (GenBank id: ACA04492); LynF: PTase in aestuaramide biosynthesis (GenBank id: EAW34319); TruF2: PTase in trunkamide biosynthesis (GenBank id: ACA04493); PatF: PTase in patellamide biosynthesis (PDB id: 4BG2). TolF: PTase in tolypamide biosynthesis (GenBank id: EKF00815)

a) *Microcystis aeruginosa* PCC 9443, Scaffold ID: 2537631176 (7724 bp)

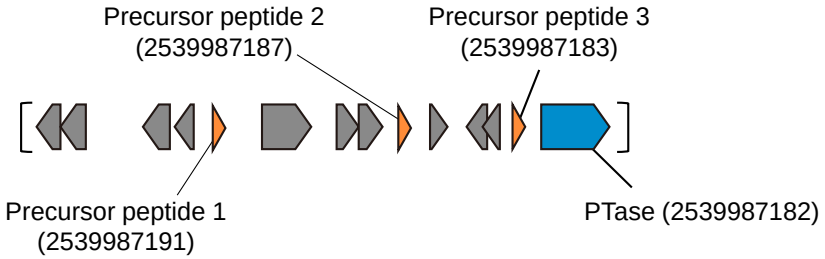

Aphanizomenon sp. UHCC 0183, Scaffold ID: 2887050839 (177534 bp)

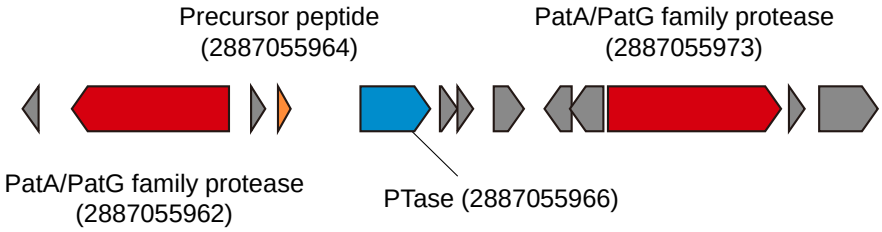

Dolichospermum circinale AWQC310F, Scaffold ID: 2516665518 (85182 bp)

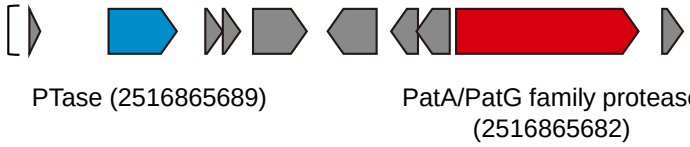

protease *precursor peptide* *prenyltransferase (PTase)* *other*

b)

```
                                                    RSII                RSIII
AgcE            MKNKTLLPQLTTPVERQHQAAASSESGANSLSASRVFIVLP---PFAEDGAE
PCC9443_2       MKTKKLTPRNDPPVQRENTATVSRDGNAIRPTAYDLER-----LPFAGDDAE
PCC9443_3       MKTKKLTPRNAAPVQRENTATVSRDGNAIAPLNAALPRSYNGFDPFAGDDAE
PCC9443_1       MKTKKLTPRNAAPVQRENTATVSRDGNAIASHIFIFLLT-----PFAGDDAE
UHCC 0183       MTKKNIRPQQVAPVERETISTAKDQSGQVQAQLSLRYPGMEY--PFAGDDAE
                *..*.: *:  .**:*:  ::.. :..                 *** *.**
```

Figure S29. Homologous gene clusters possibly encode biosynthetic pathways of bis-prenylated Arg-containing cyanobactins. (a) The vicinity regions of *agcF* homologs (JGI gene id: 2539987182, 2887055966, 2516865689) are depicted. Genes coding for precursor peptides, PTases, PatA/G family proteases, and others are colored in orange, blue, rad, and gray, respectively. In *M. aeruginosa* PCC 9443, AgcF homolog gene (2539987182) and multiple precursor peptides are encoded in short contig (< 8 kb), thus PatA/G protease genes are not visible. In *D. circinale* AWQC310F, gene coding for precursor peptide is not visible, since AgcF homolog gene (2516865689) locates near the end of contig. (b) Primary sequence alignment of precursor peptides

found in neighboring regions of *agcF* and its close homologs. RSII and RSIII are colored in gray. Although RSII in PCC 9443 and UHCC 0183 precursors are not predictable, presence of Arg residues (highlighted in red letter) near RSIII strongly suggest that these are the precursors of Arg-containing cyanobactins, which maybe be bis-prenylated by AgcF homologs encoded in neighboring regions.

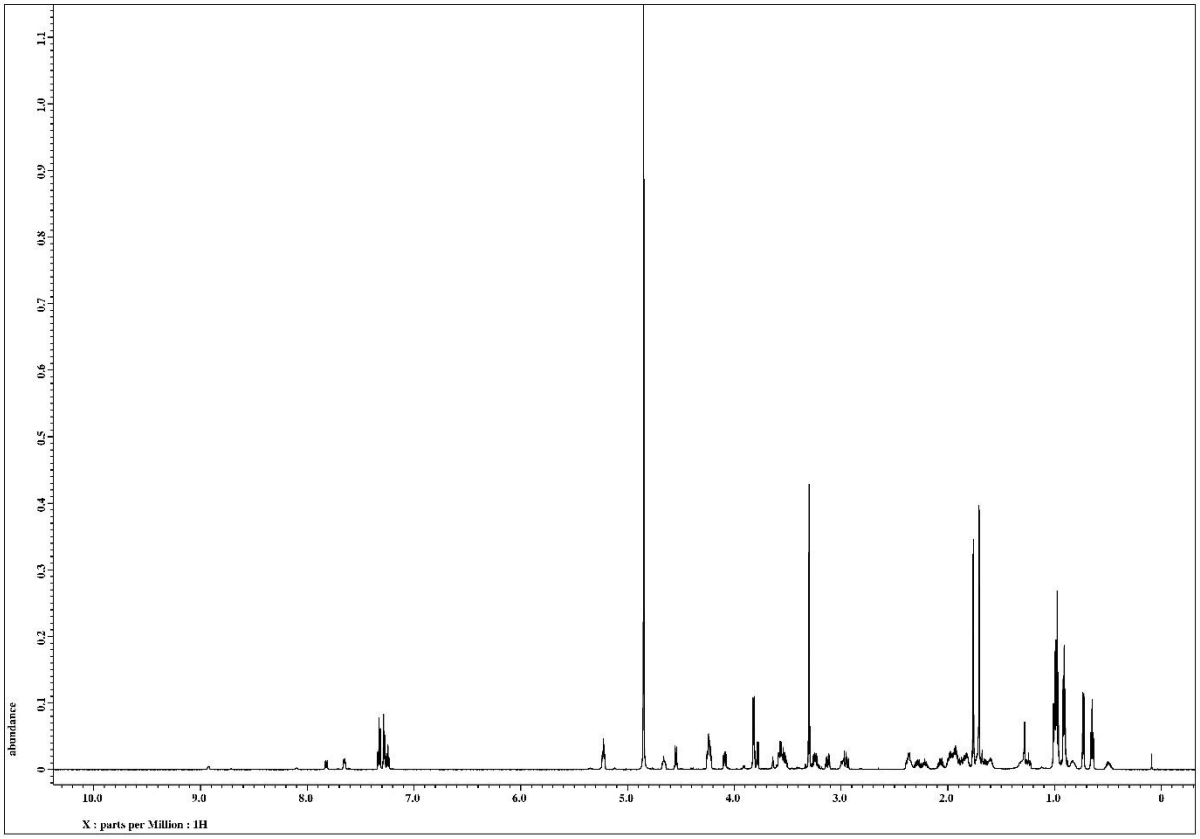

Figure S30. ^{1}H NMR (600 MHz) spectrum of **1** in CD_3OD

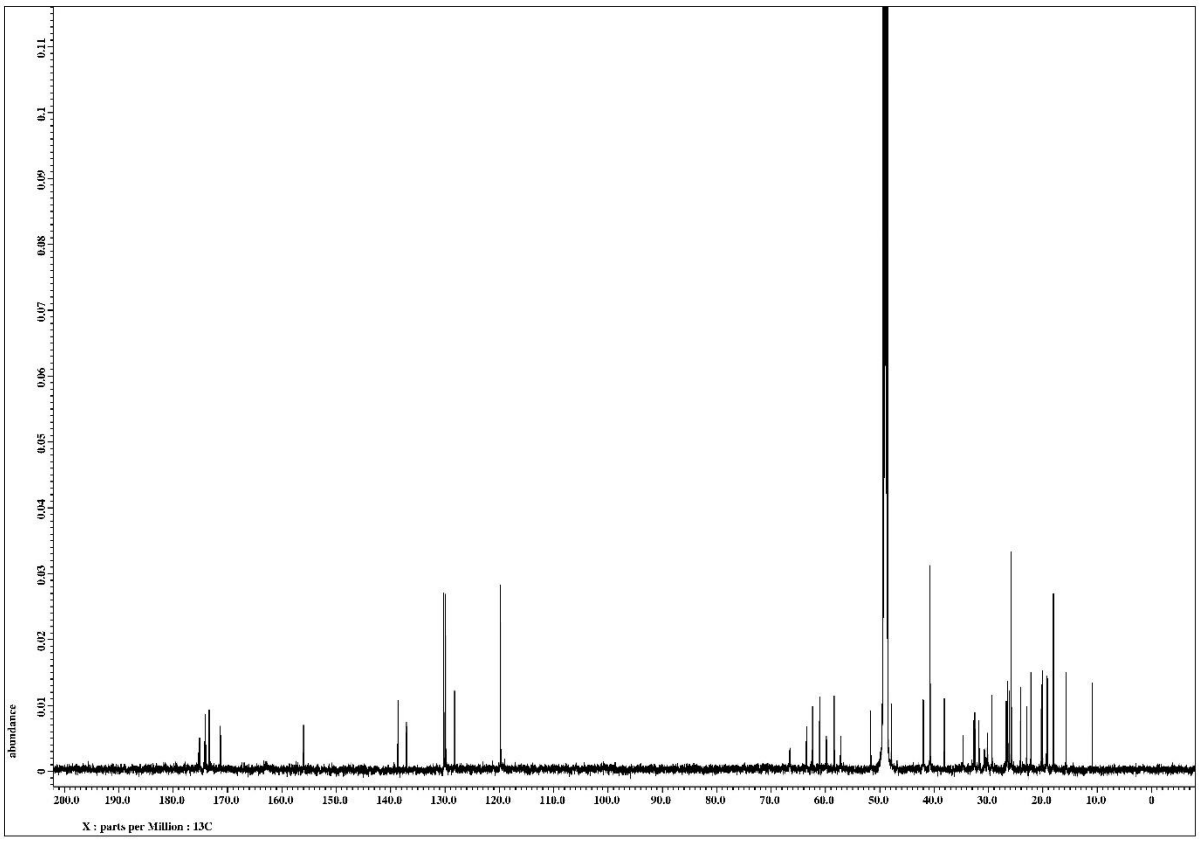

Figure S31. ^{13}C NMR (150 MHz) spectrum of **1** in CD_3OD

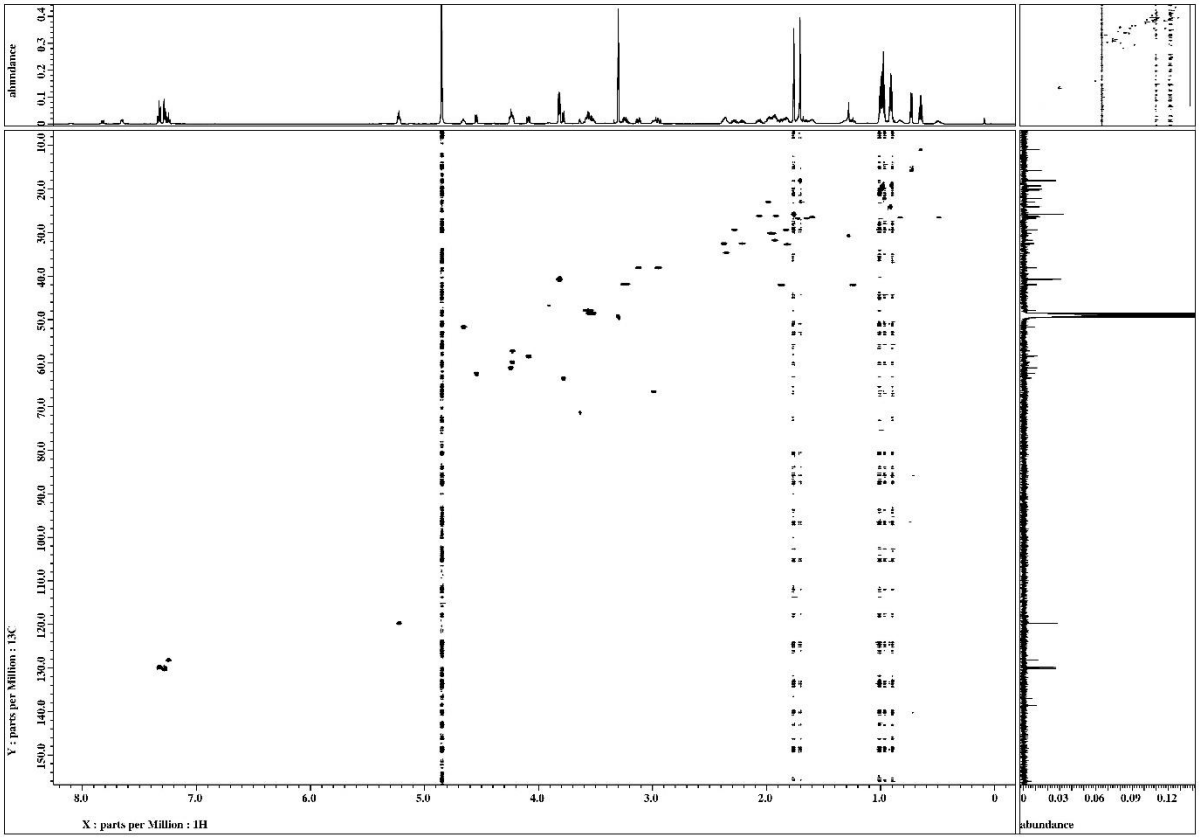

Figure S32. HSQC spectrum of **1** in CD_3OD

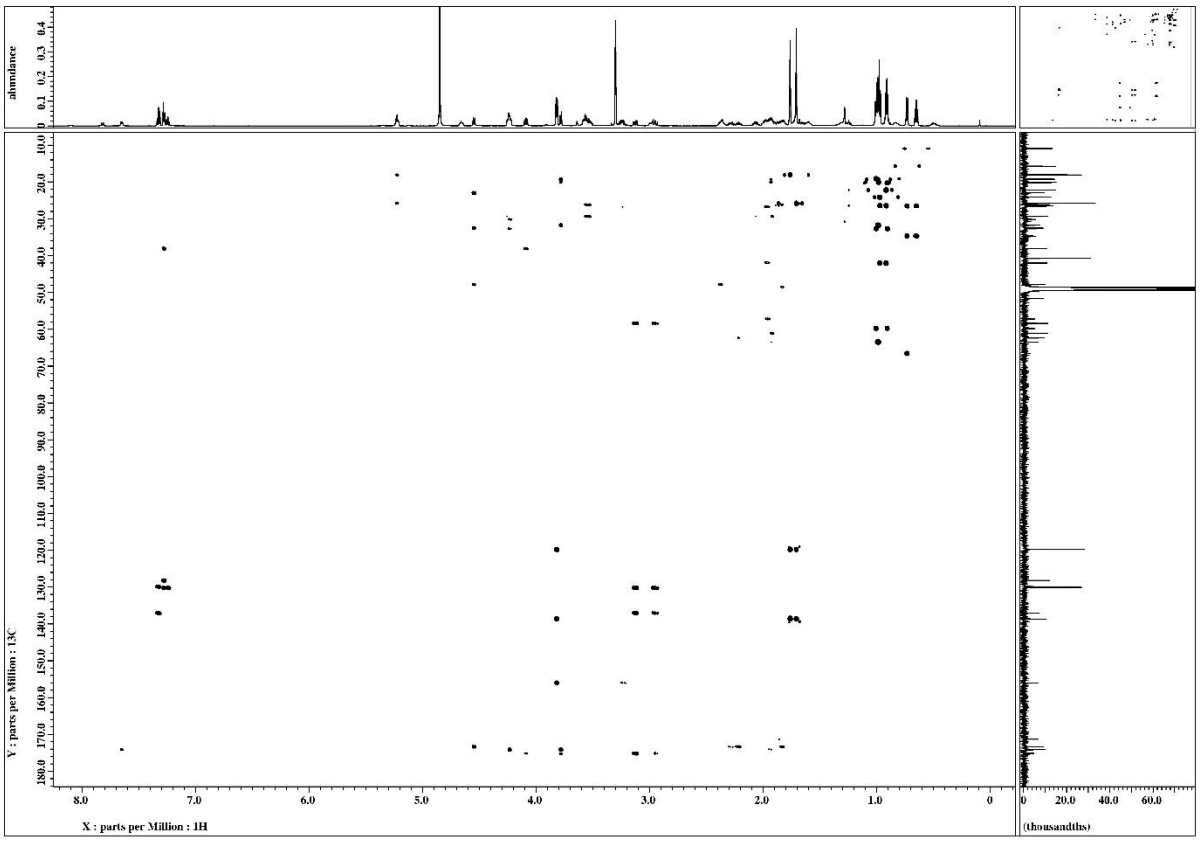

Figure S33. HMBC spectrum of **1** in CD_3OD

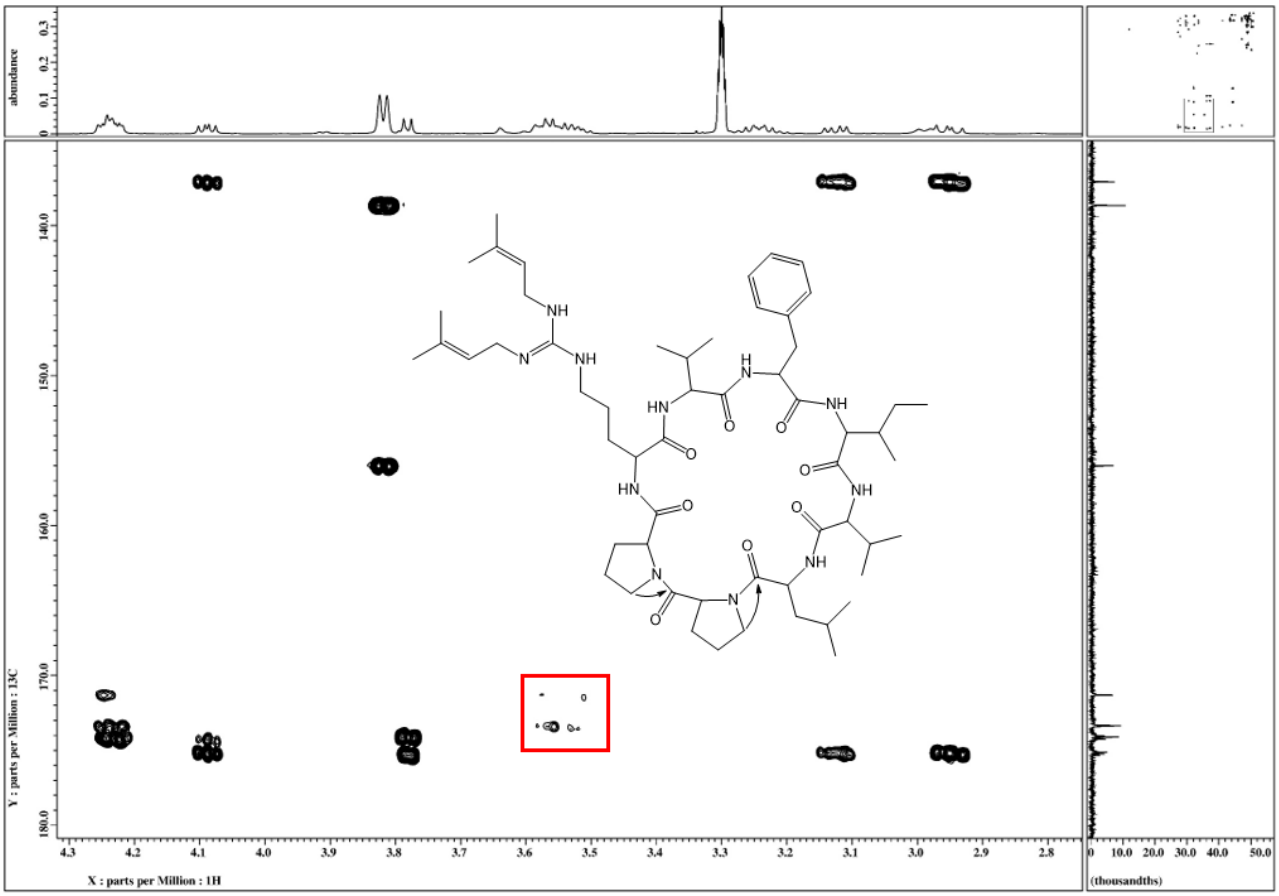

Figure S34. HMBC ($^{n}J_{CH}$ = 4 Hz) spectrum of **1** in CD_3OD

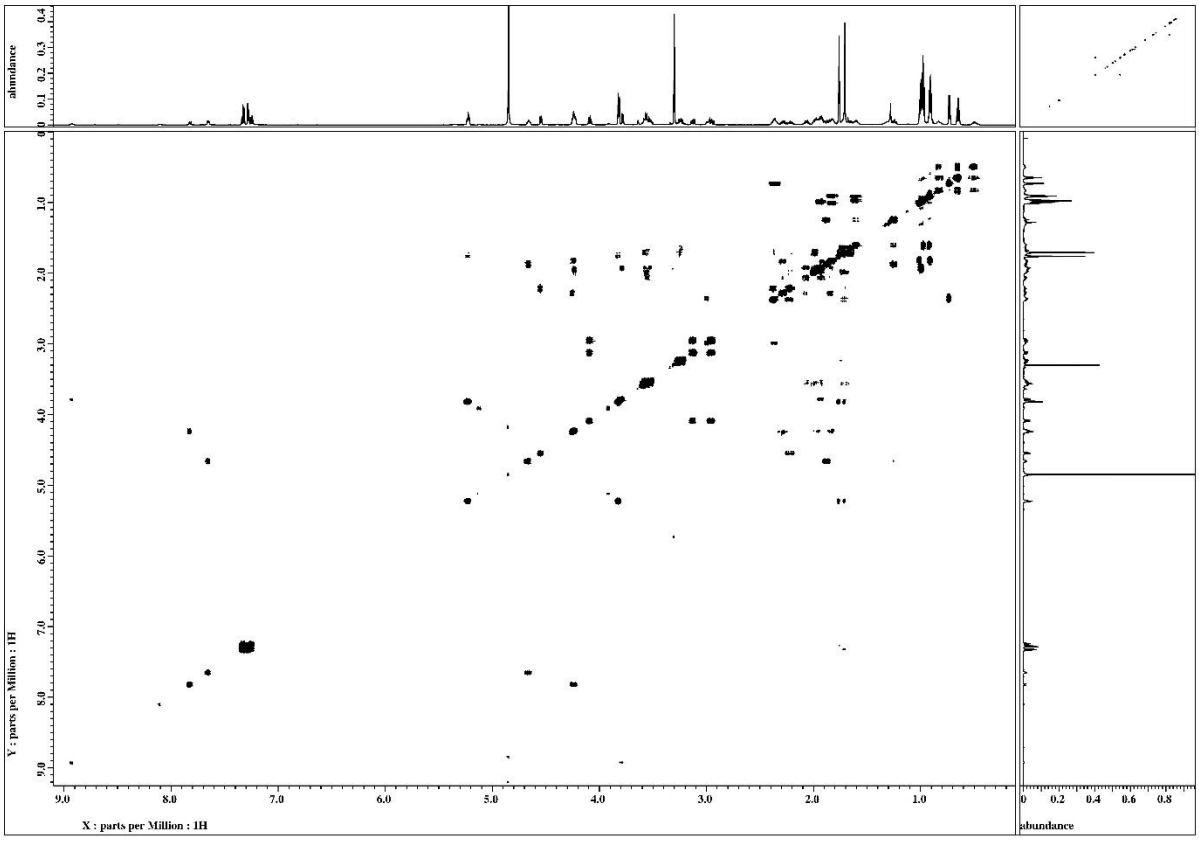

Figure S35. ^{1}H-^{1}H DQF COSY spectrum of **1** in CD_3OD

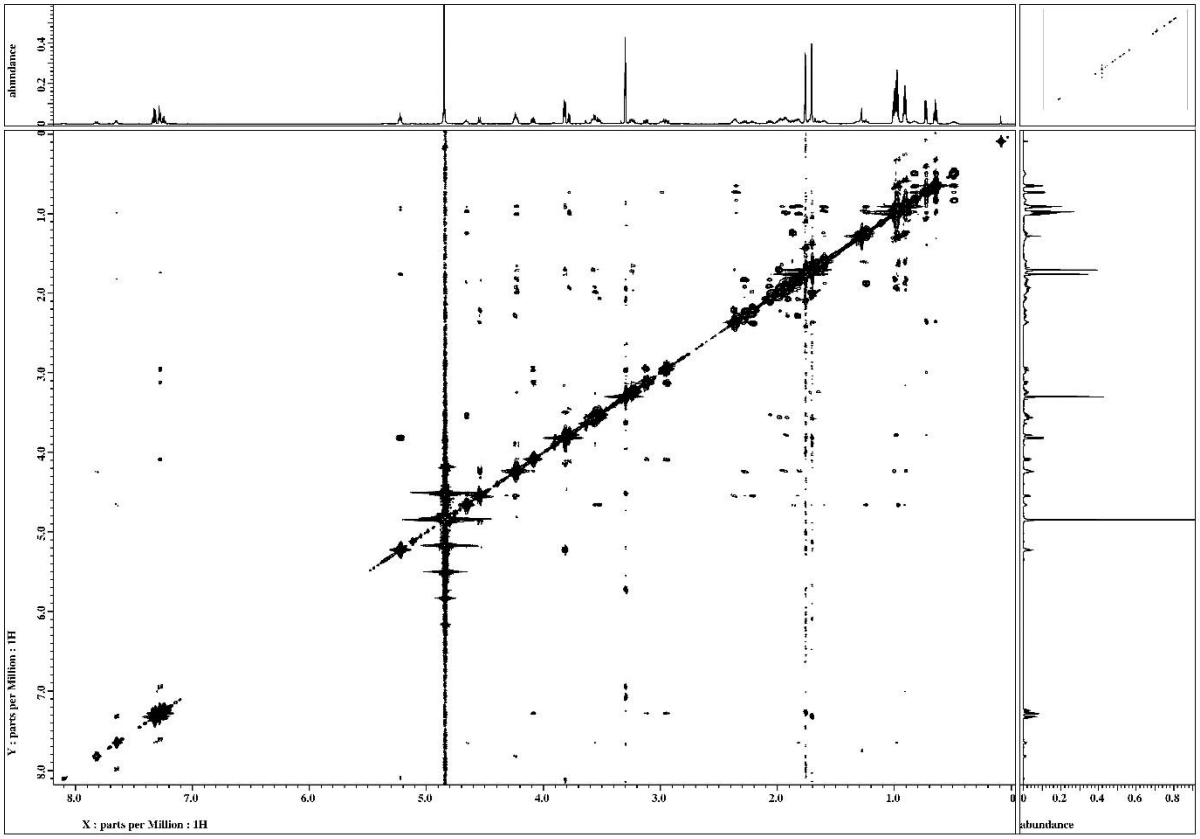

Figure S36. ROESY spectrum of **1** in CD_3OD

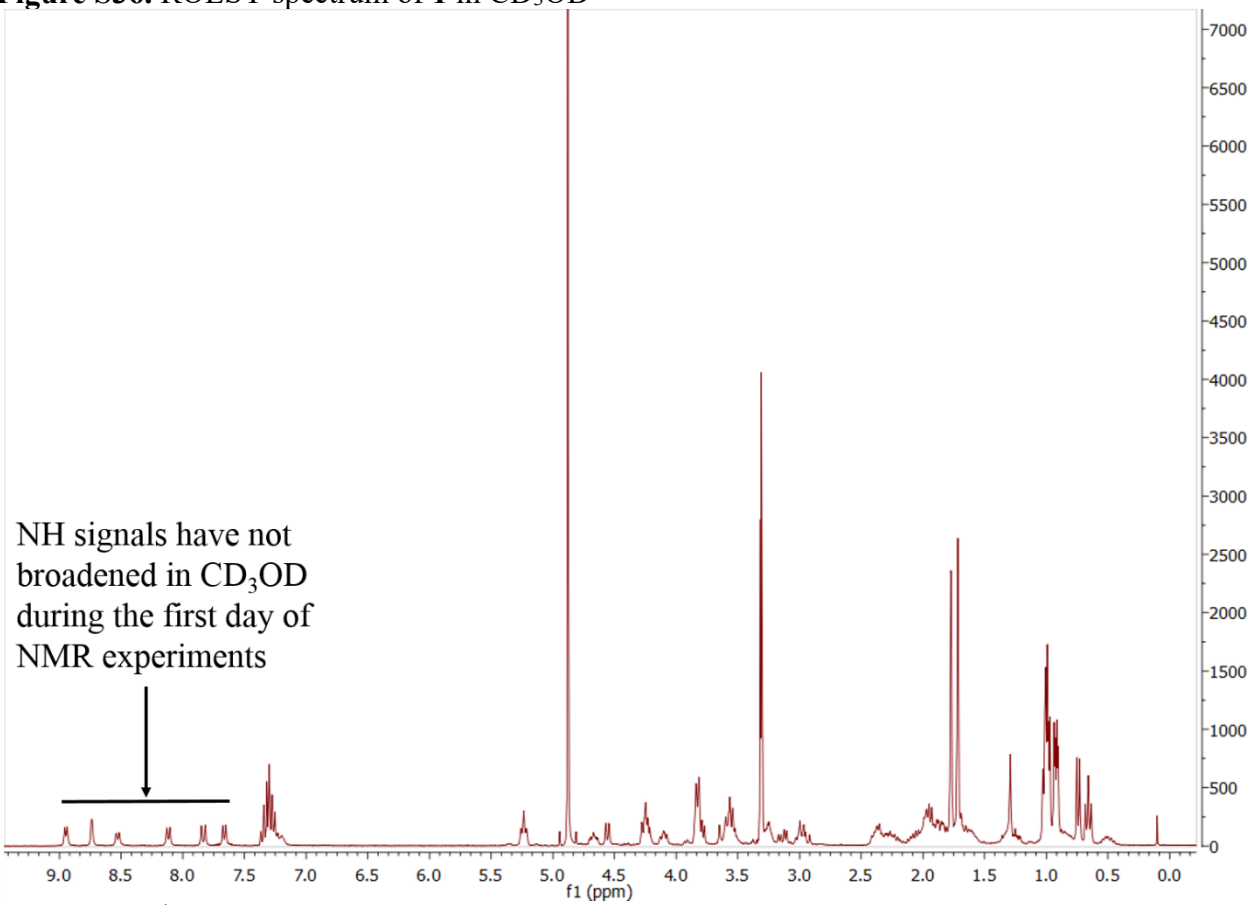

Figure S37. ^1H NMR (300 MHz) spectrum of **1** in CD_3OD

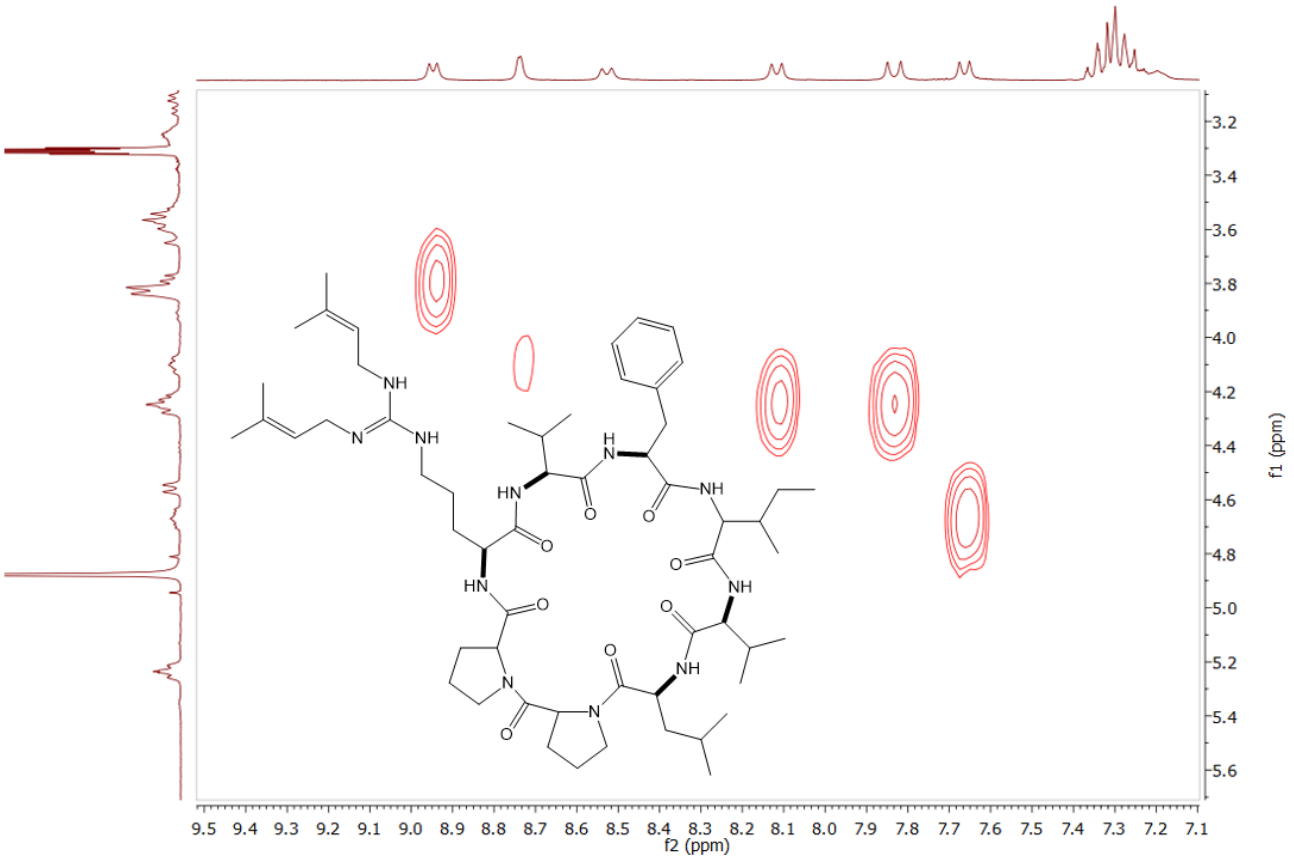

Figure S38. ^{1}H-^{1}H DQF COSY (300 MHz) spectrum of **1** in CD_3OD

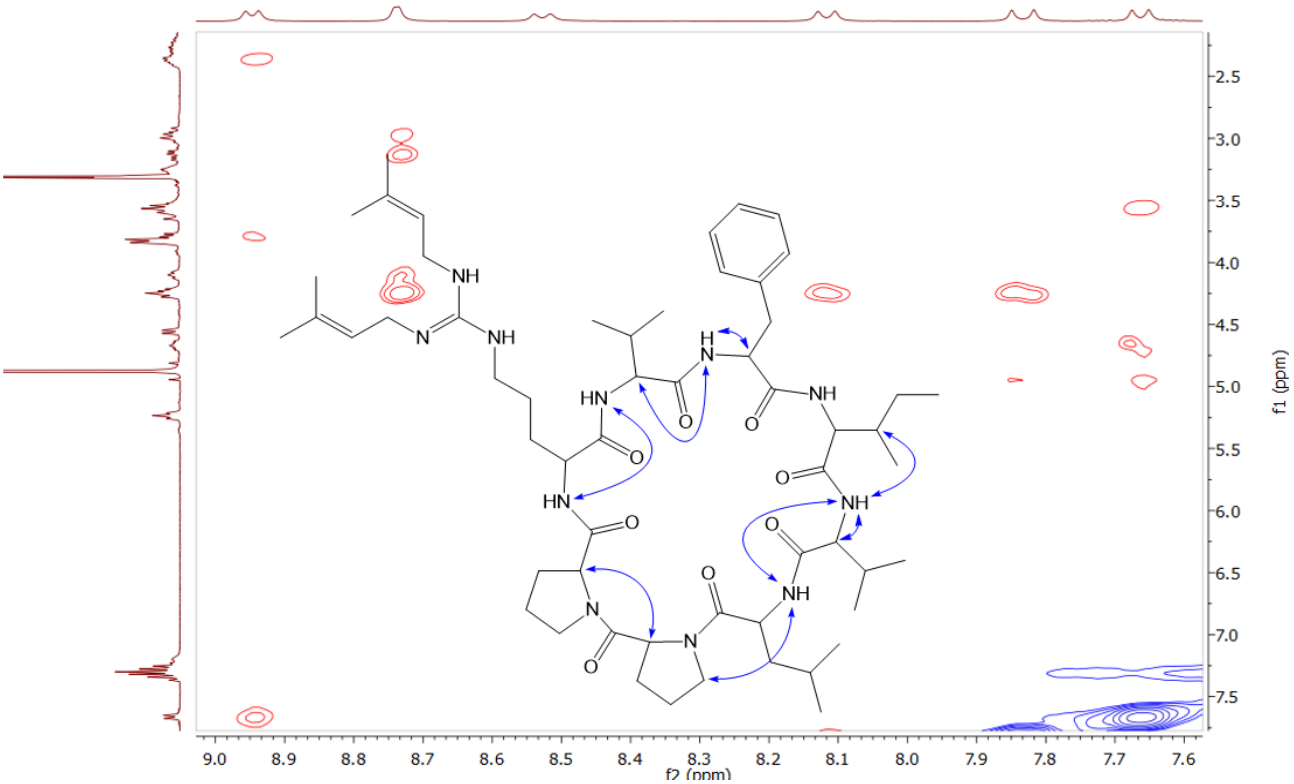

Figure S39. ROESY (300 MHz) spectrum of **1** in CD_3OD

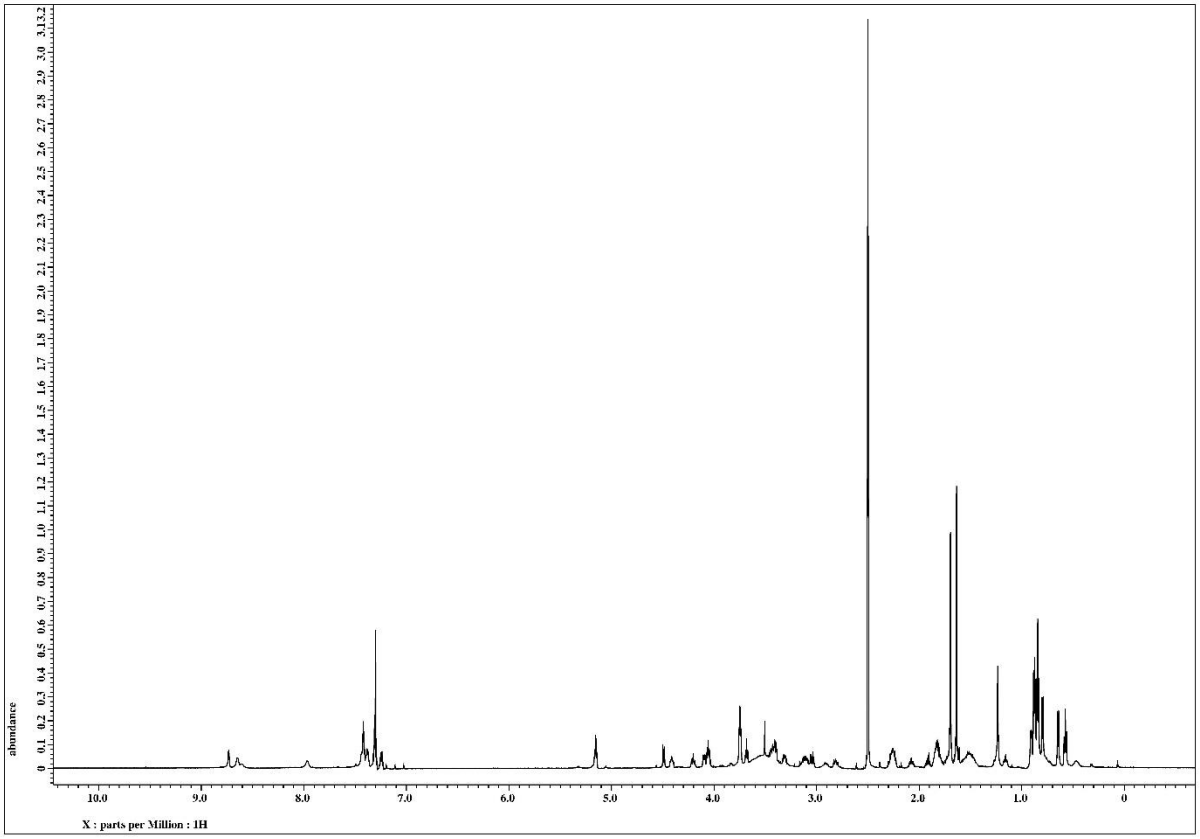

Figure S40. ^{1}H NMR (600 MHz) spectrum of **1** in DMSO-d_6

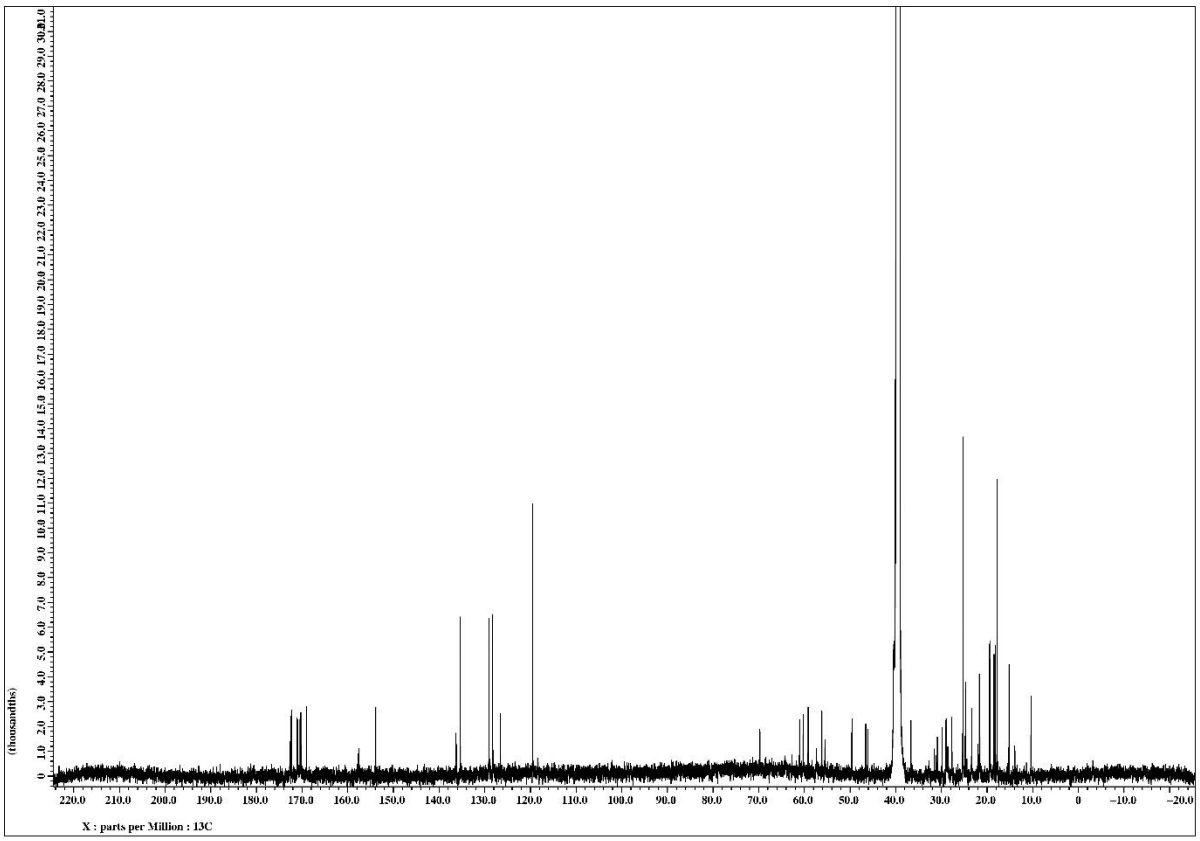

Figure S41. ^{13}C NMR (150 MHz) spectrum of **1** in DMSO-d_6

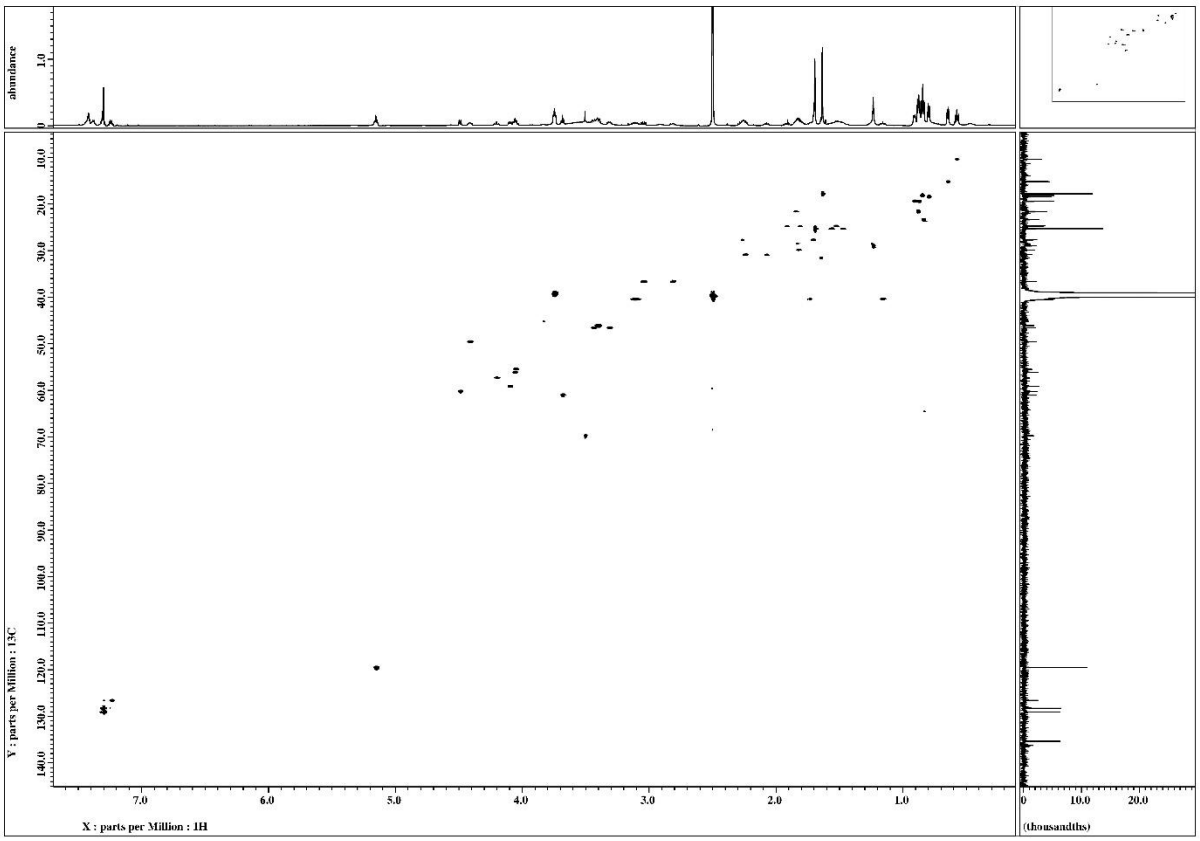

Figure S42. HSQC spectrum of **1** in DMSO-d_6

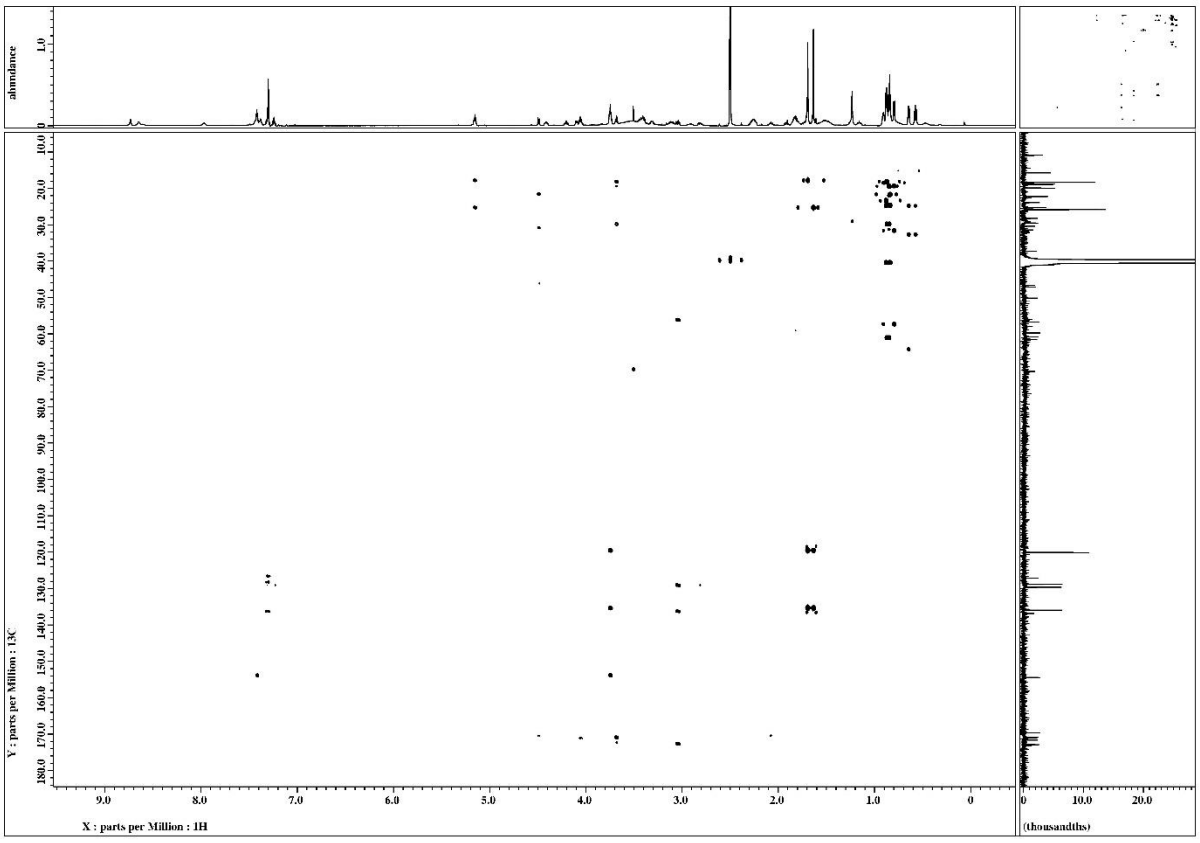

Figure S43. HMBC spectrum of **1** in DMSO-d_6

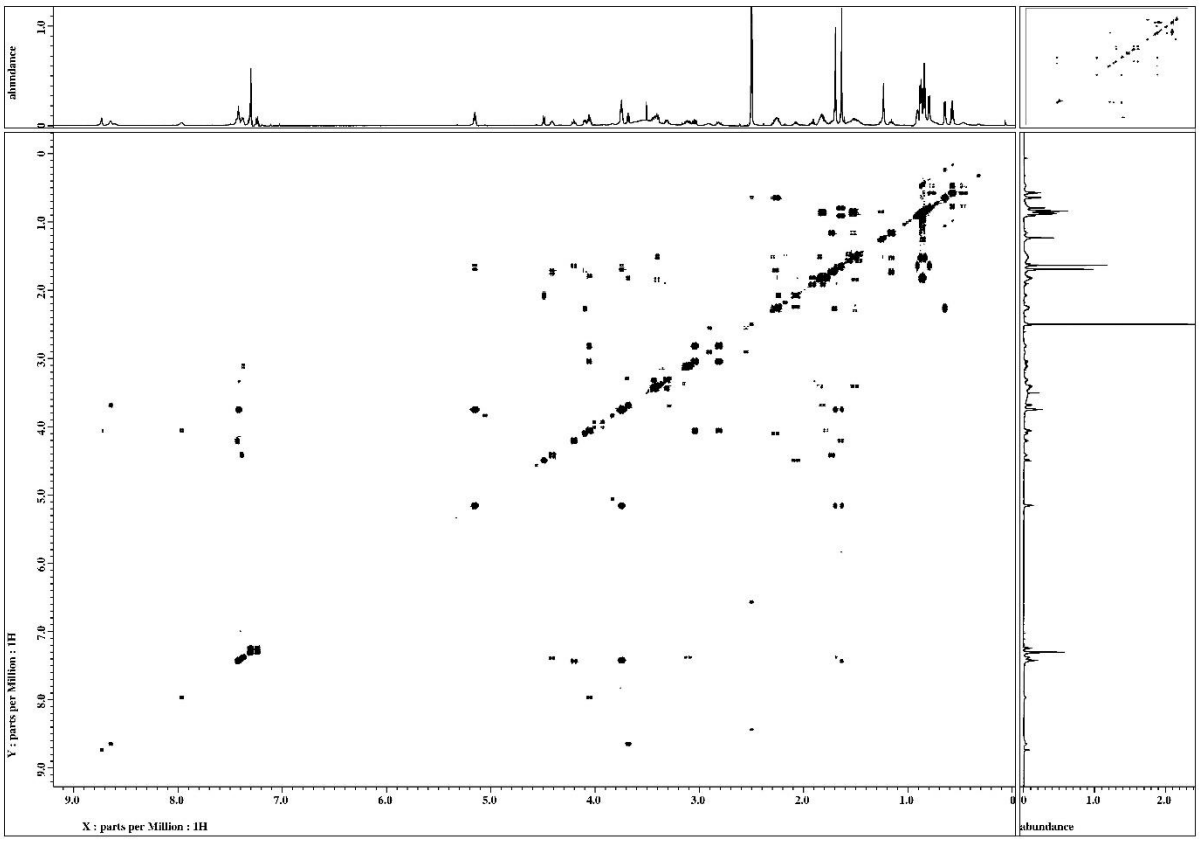

Figure S44. ^{1}H-^{1}H DQF COSY spectrum of **1** in DMSO-d_6

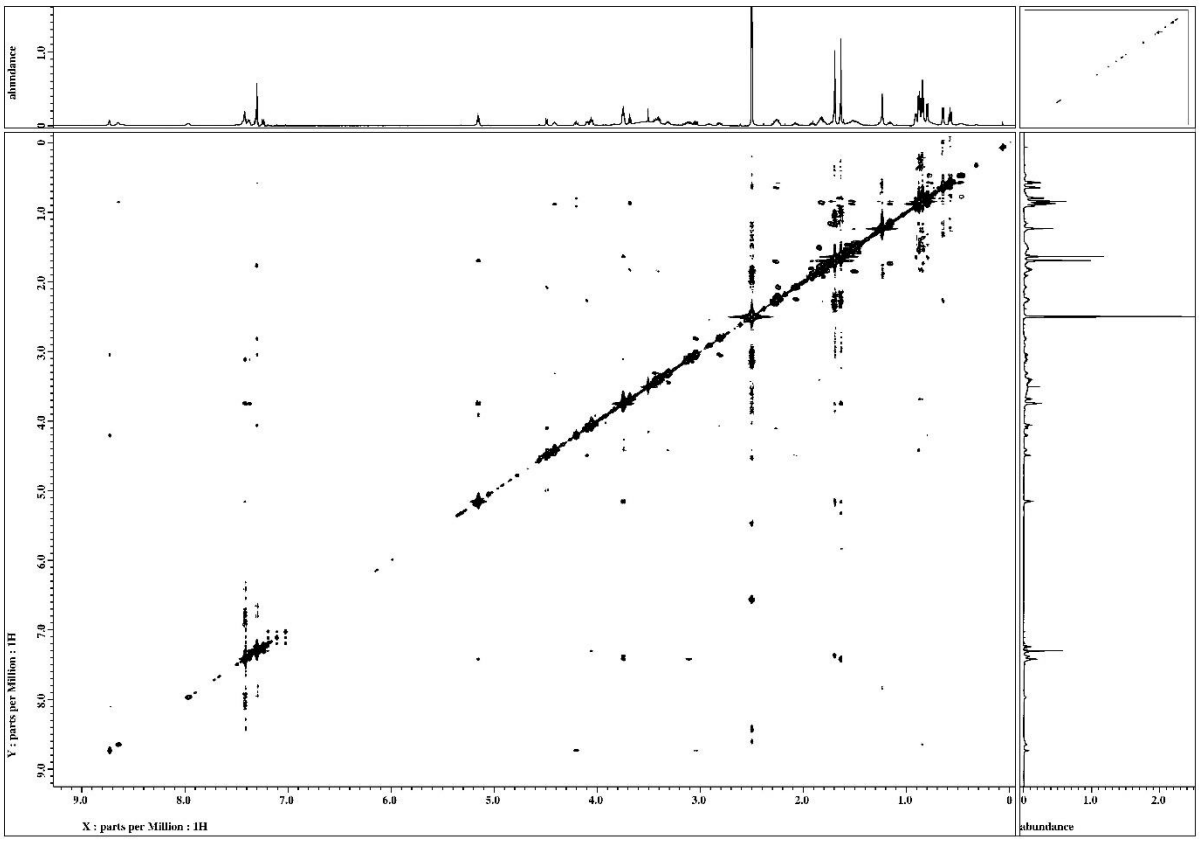

Figure S45. ROESY spectrum of **1** in DMSO-d_6

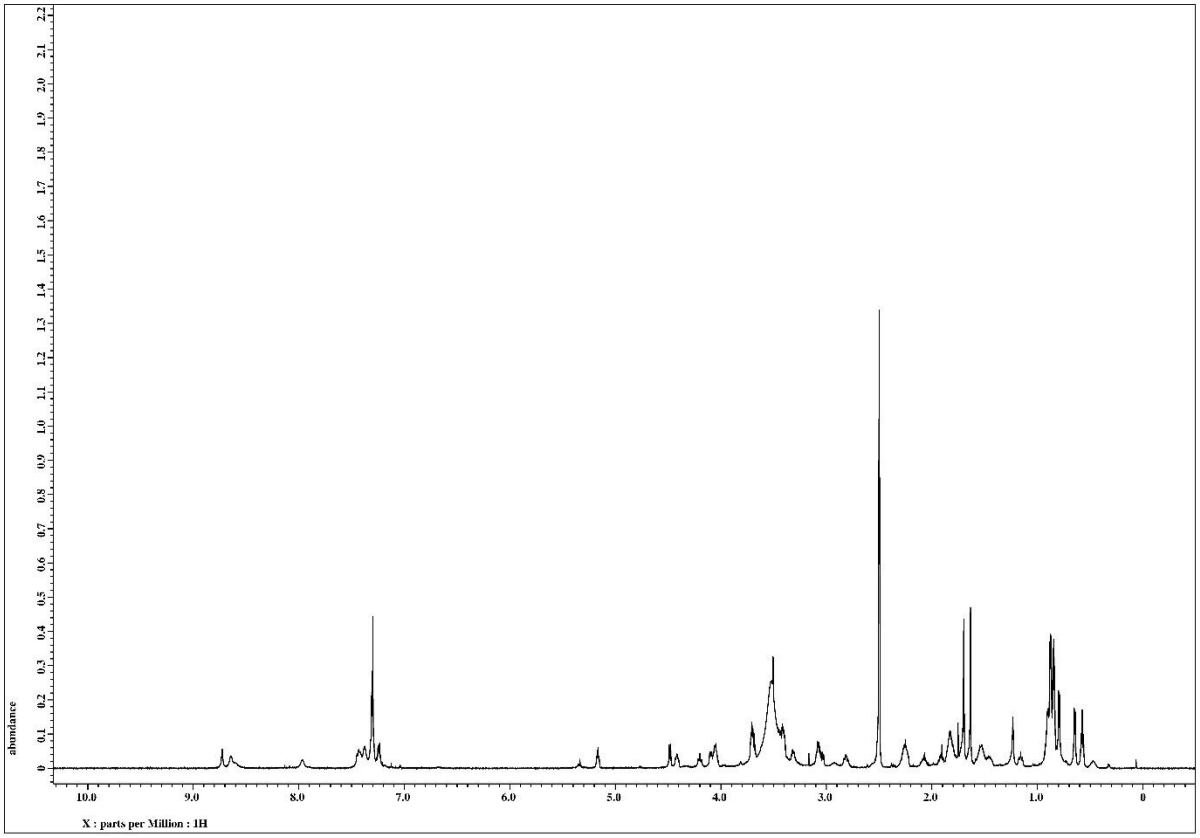

Figure S46. ^{1}H NMR (600 MHz) spectrum of **2** in DMSO-d_6

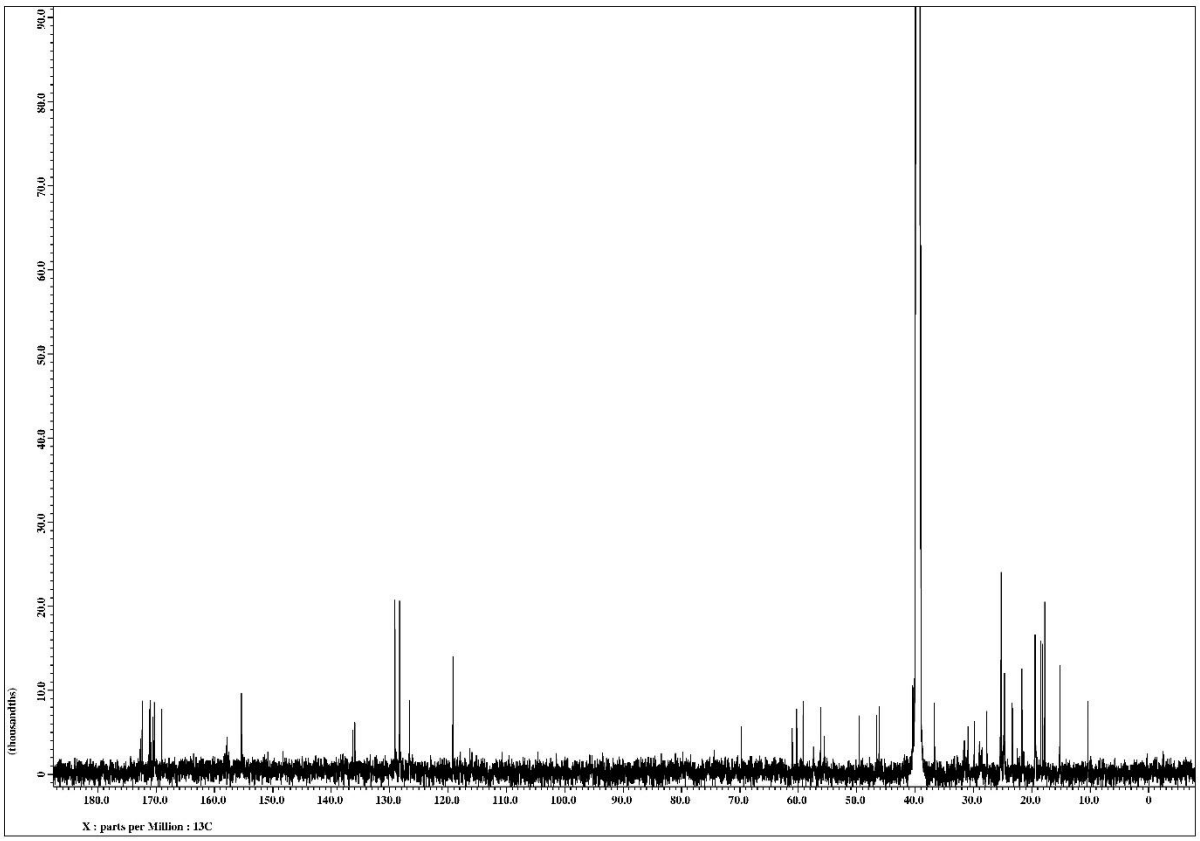

Figure S47. ^{13}C NMR (150 MHz) spectrum of **2** in DMSO-d_6

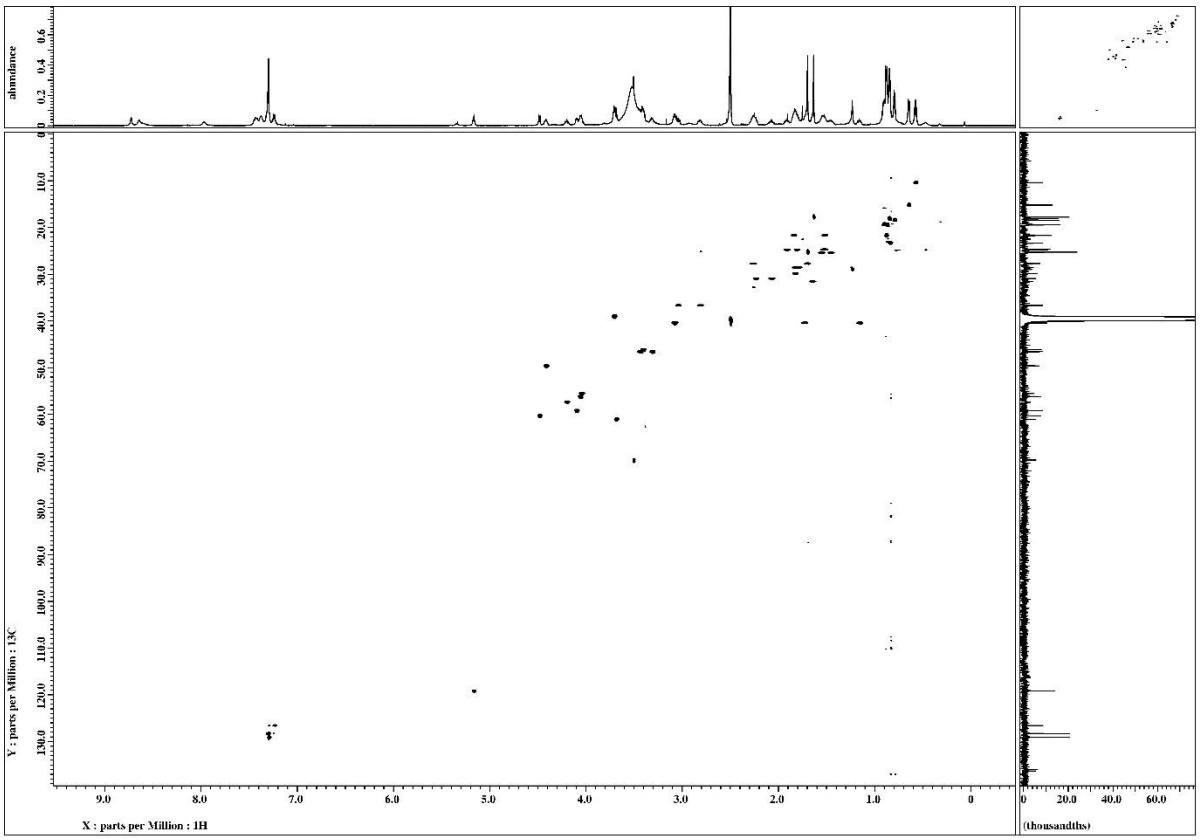

Figure S48. HSQC spectrum of **2** in DMSO-d_6

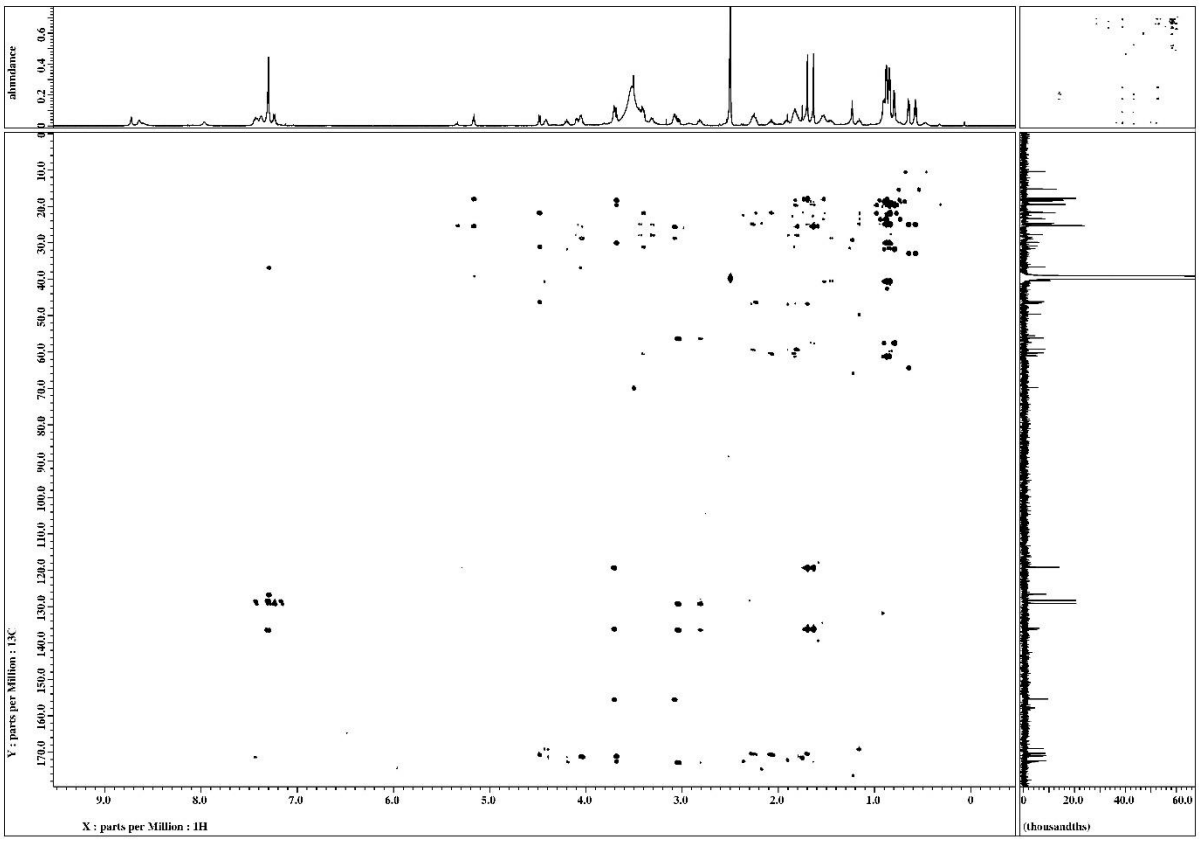

Figure S49. HMBC spectrum of **2** in DMSO-d_6

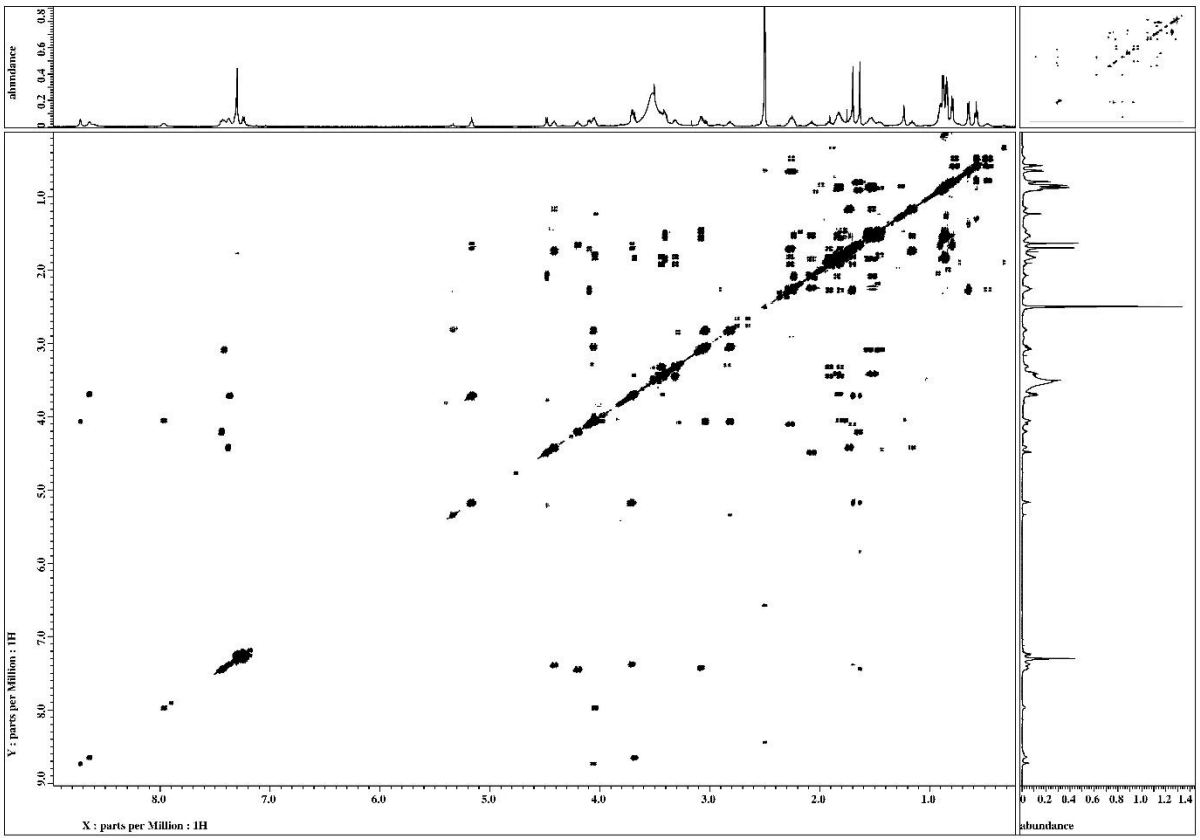

Figure S50. ^{1}H-^{1}H DQF COSY spectrum of **2** in DMSO-d_6

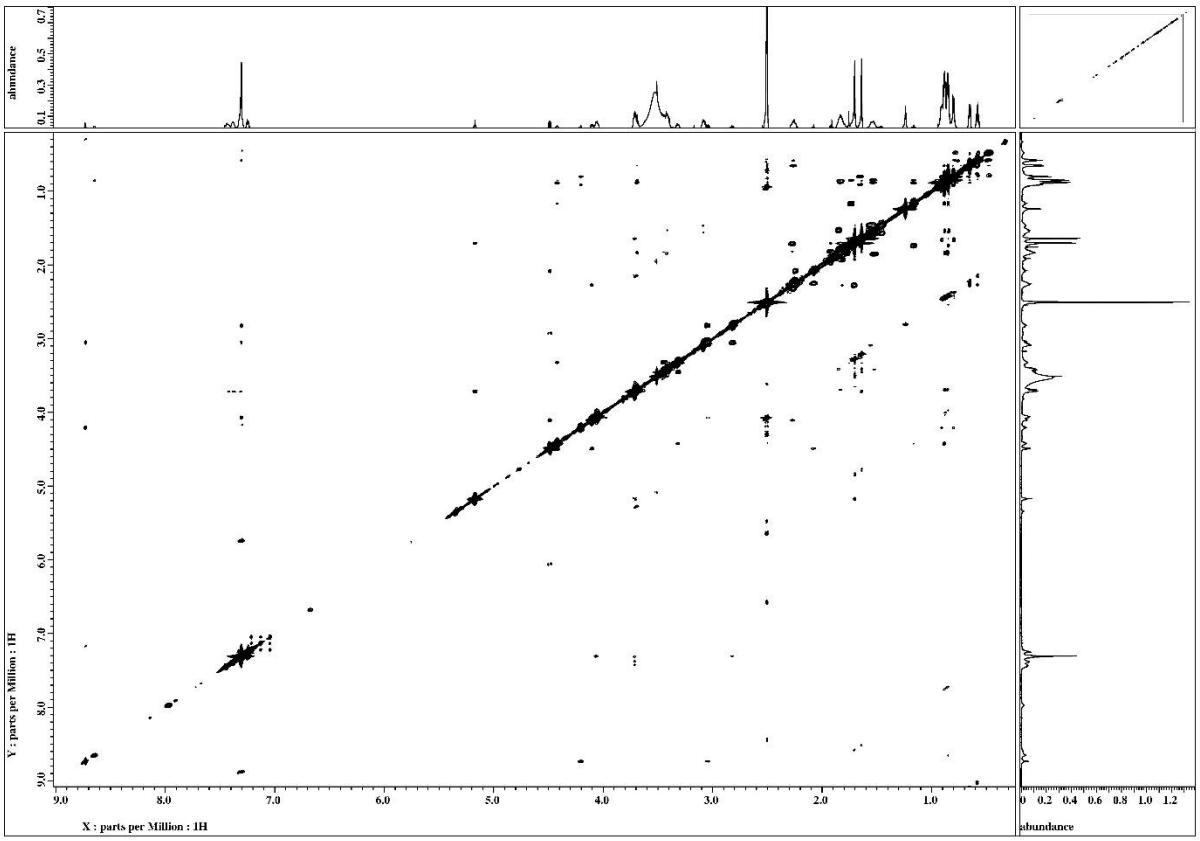

Figure S51. ROESY spectrum of **2** in DMSO-d_6

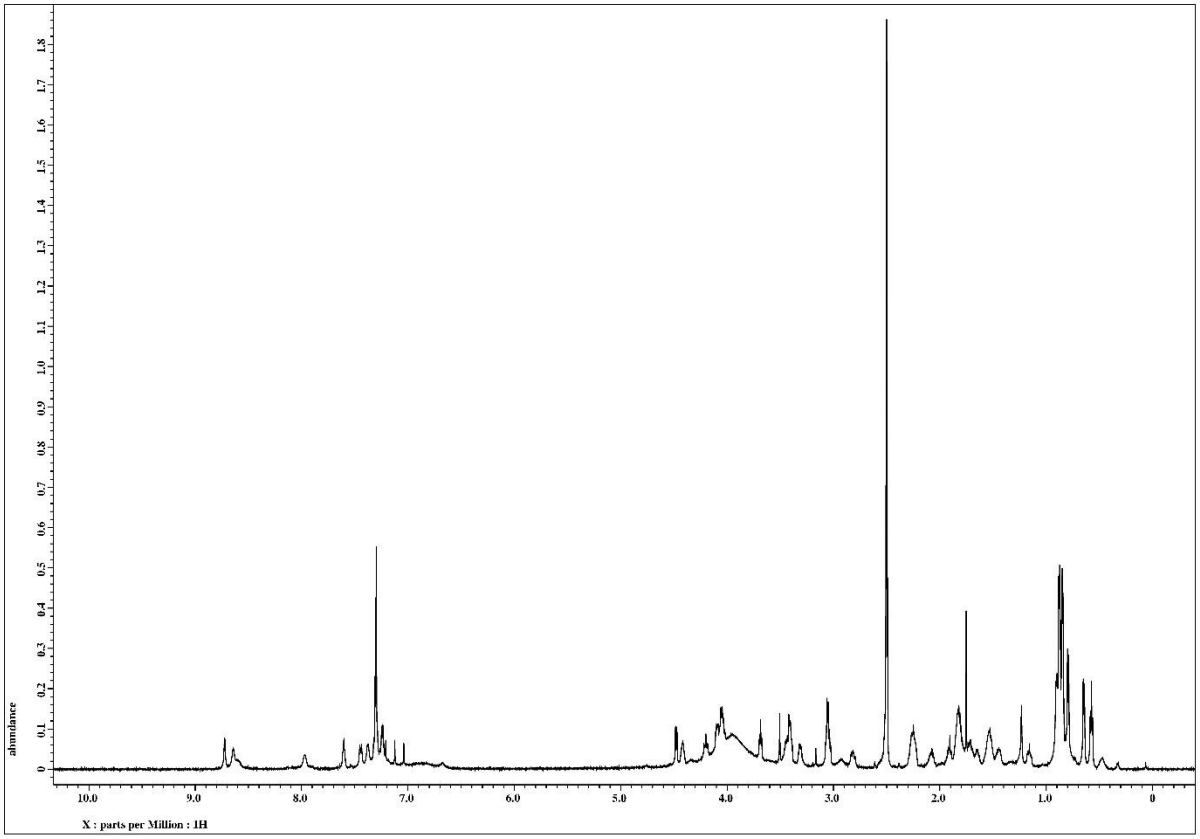

Figure S52. ^{1}H NMR (600 MHz) spectrum of **3** in DMSO-d_6

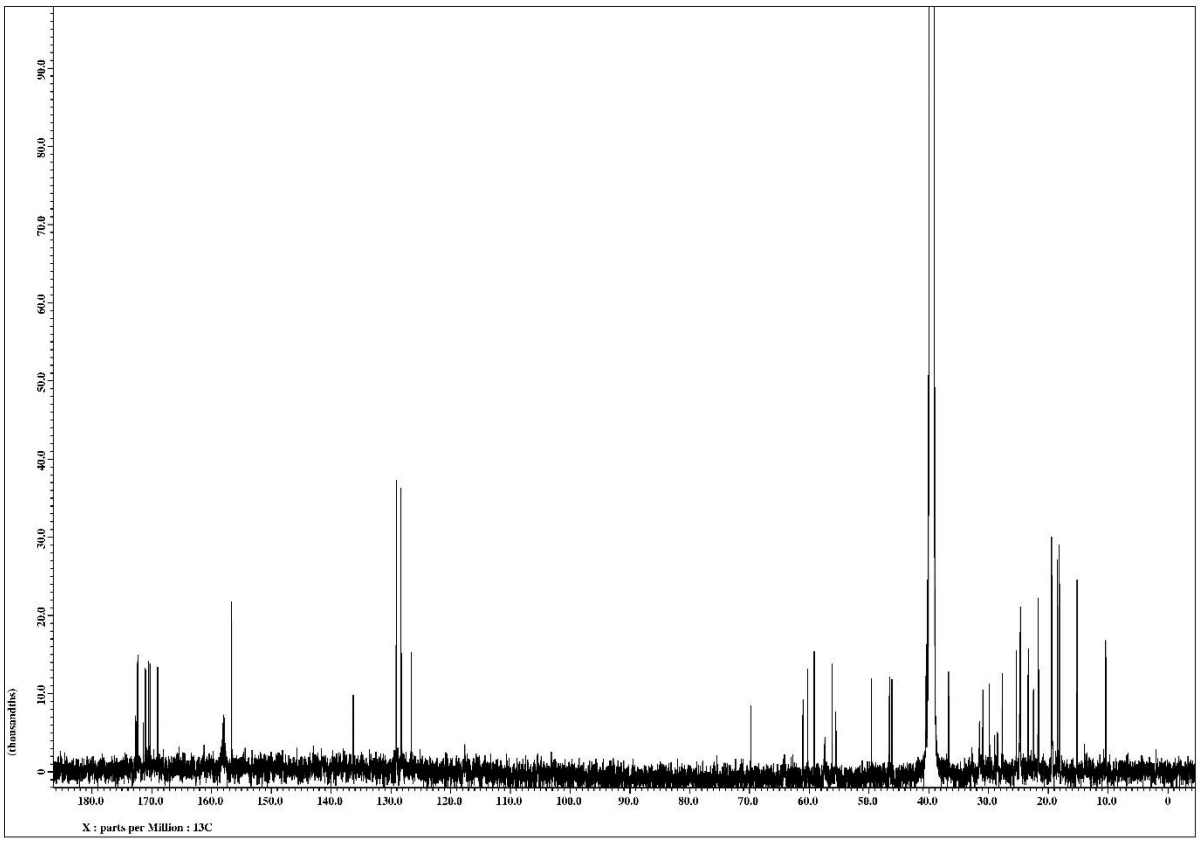

Figure S53. ^{13}C NMR (150 MHz) spectrum of **3** in DMSO-d_6

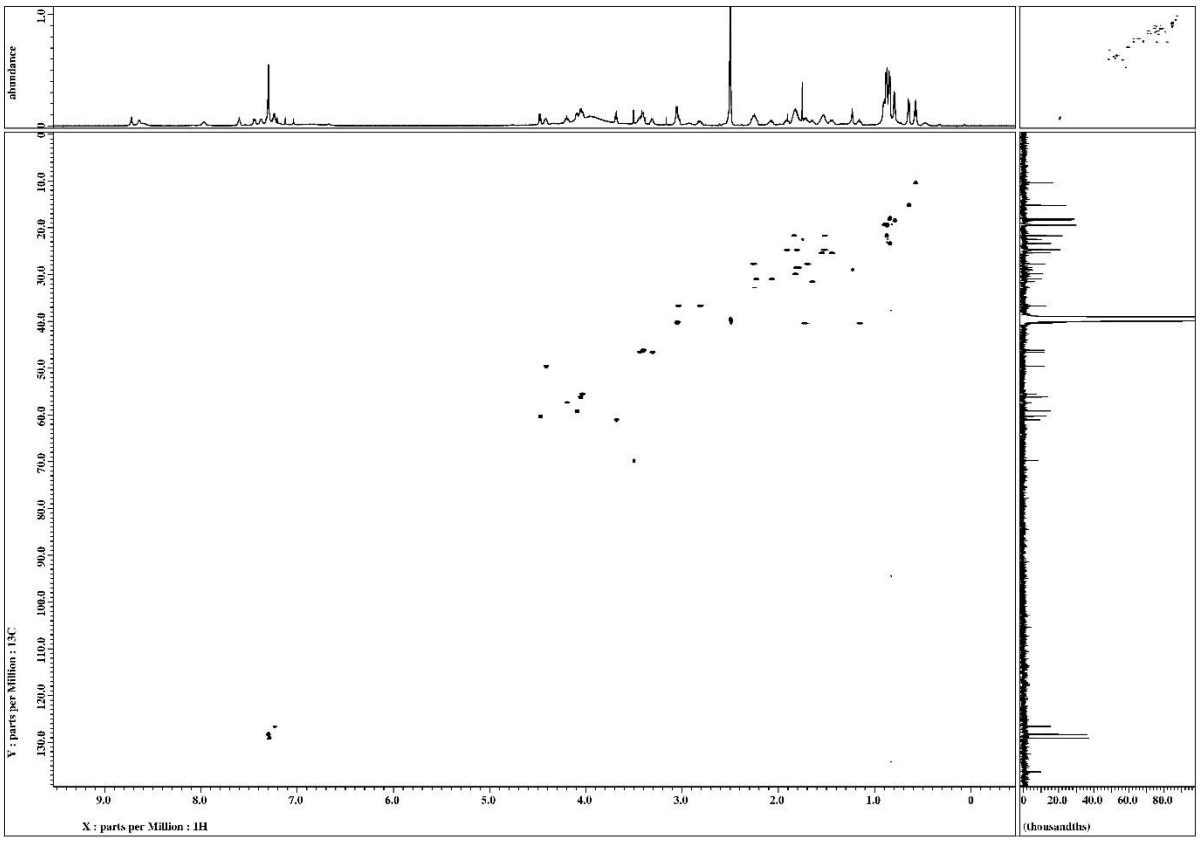

Figure S54. HSQC spectrum of **3** in DMSO-d_6

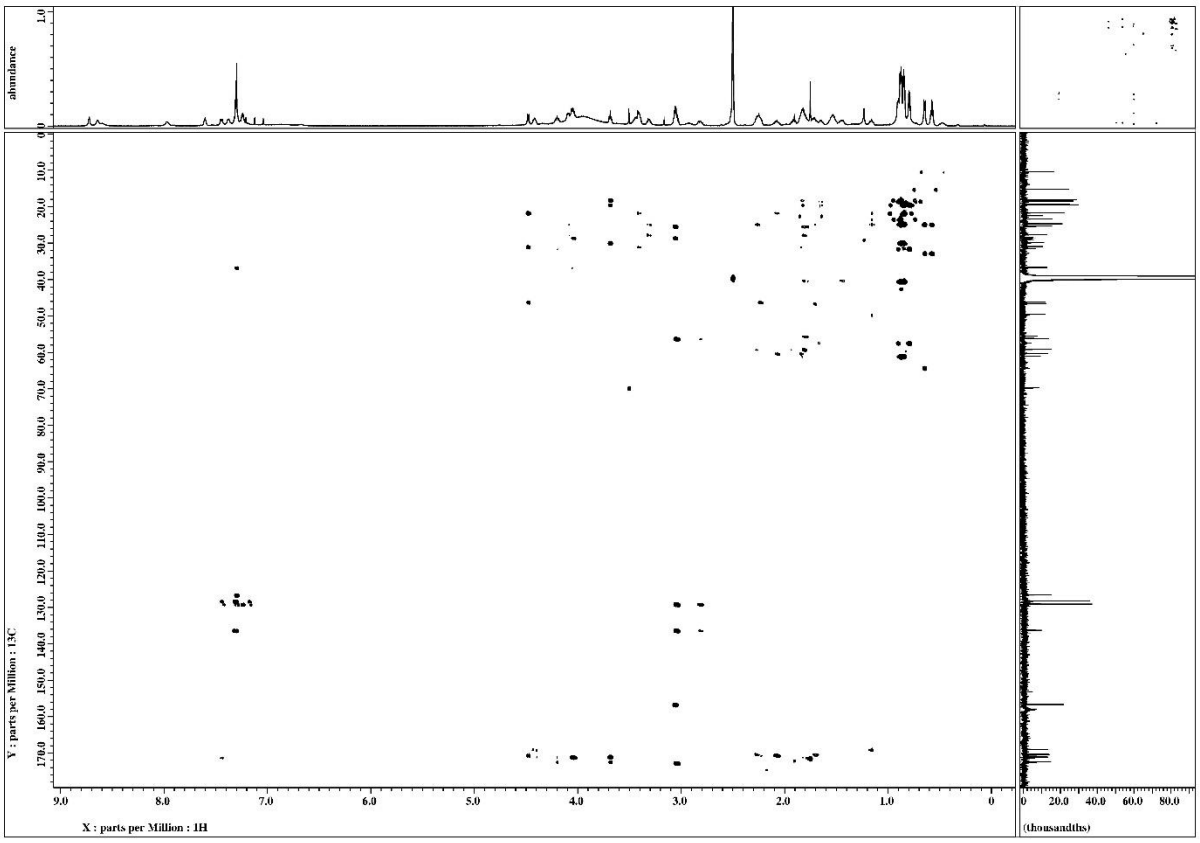

Figure S55. HMBC spectrum of **3** in DMSO-d_6

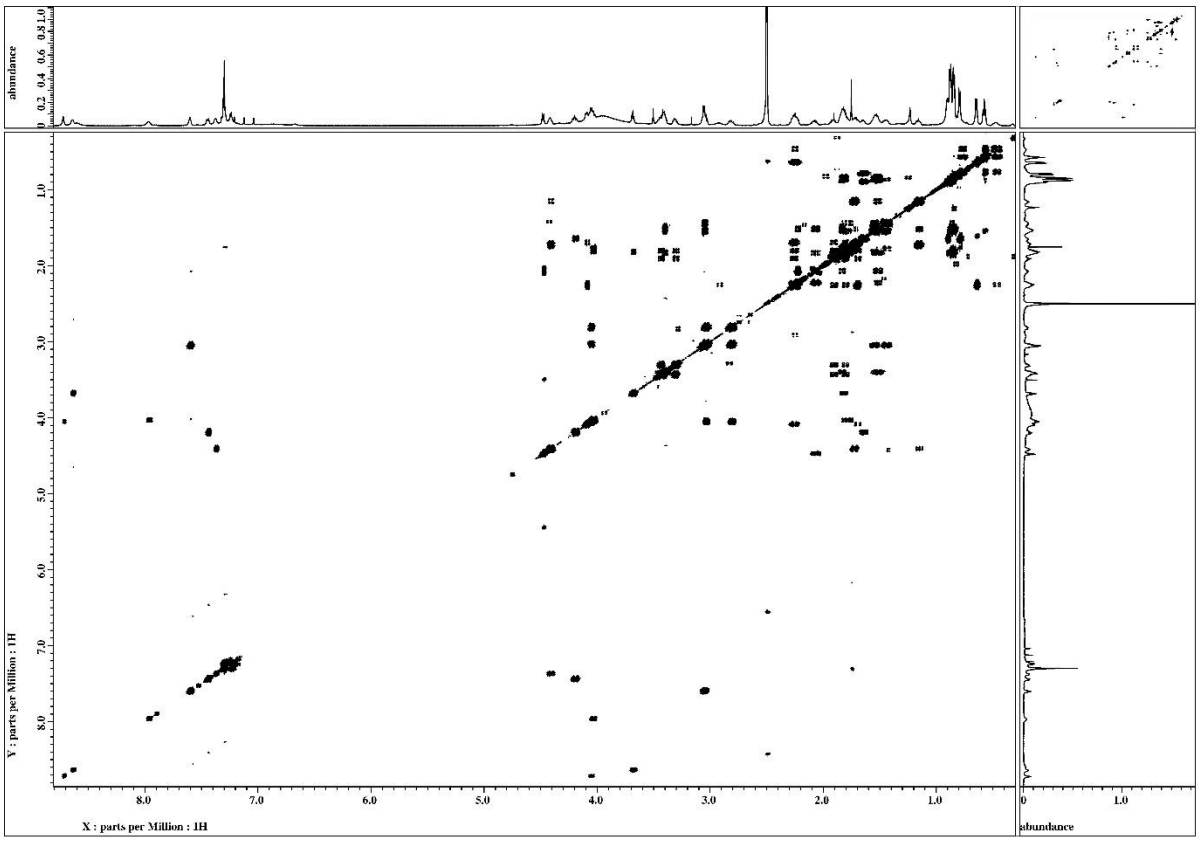

Figure S56. ^{1}H-^{1}H DQF COSY spectrum of **3** in DMSO-d_6

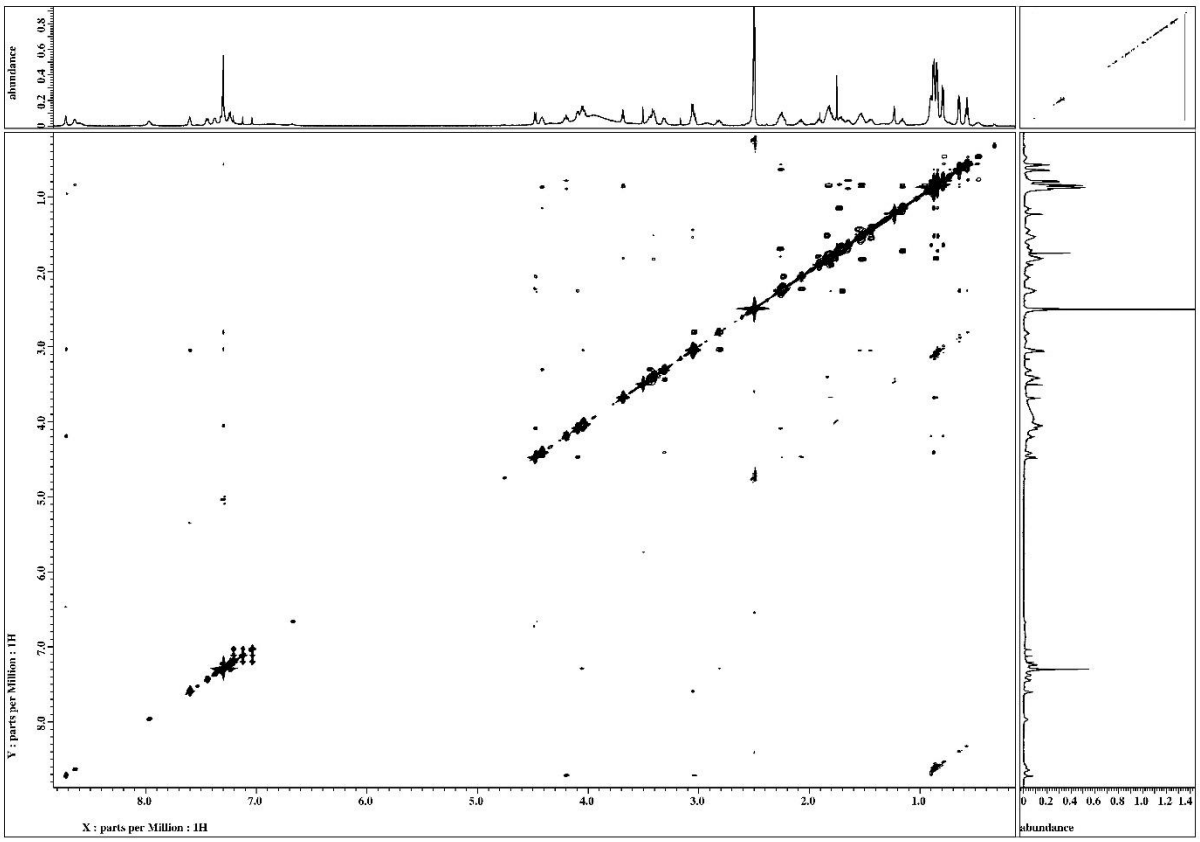

Figure S57. ROESY spectrum of **3** in DMSO-d_6

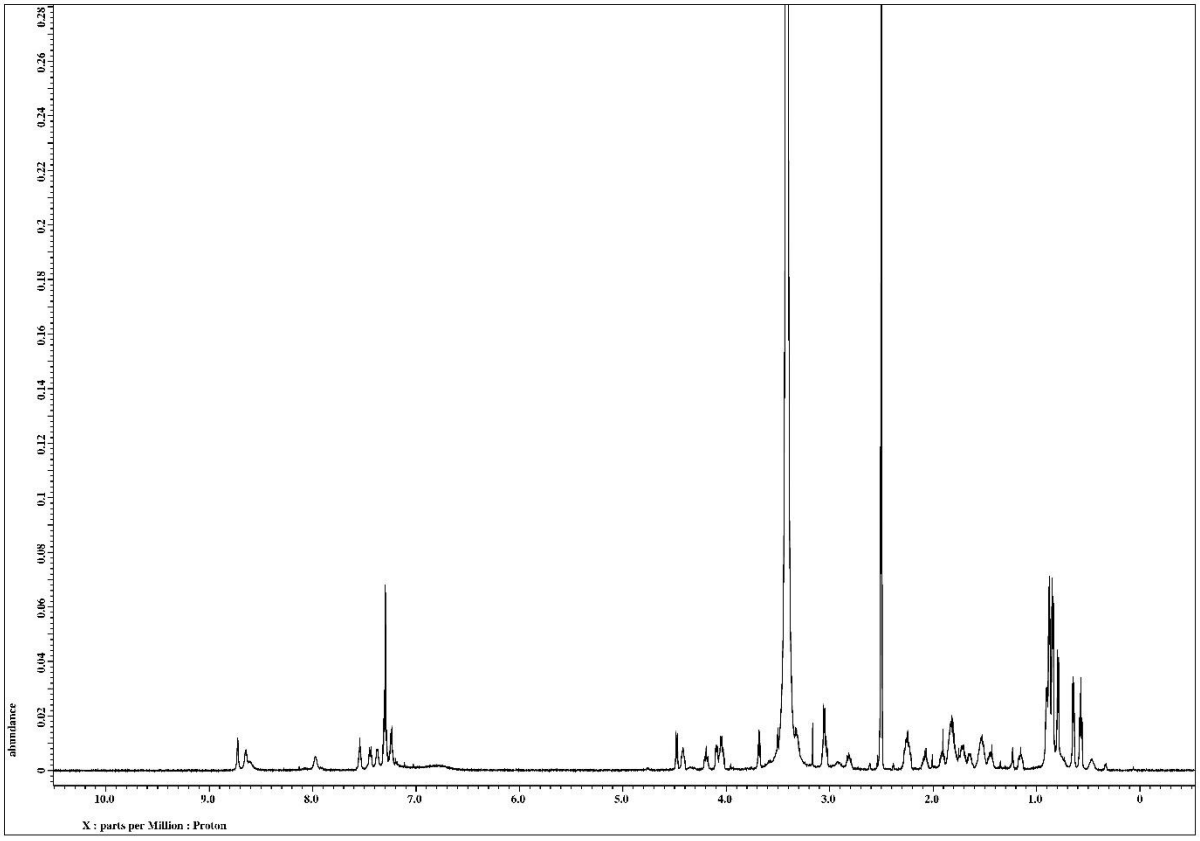

Figure S58. ^{1}H NMR (600 MHz) spectrum of synthetic **3** in DMSO-d_6

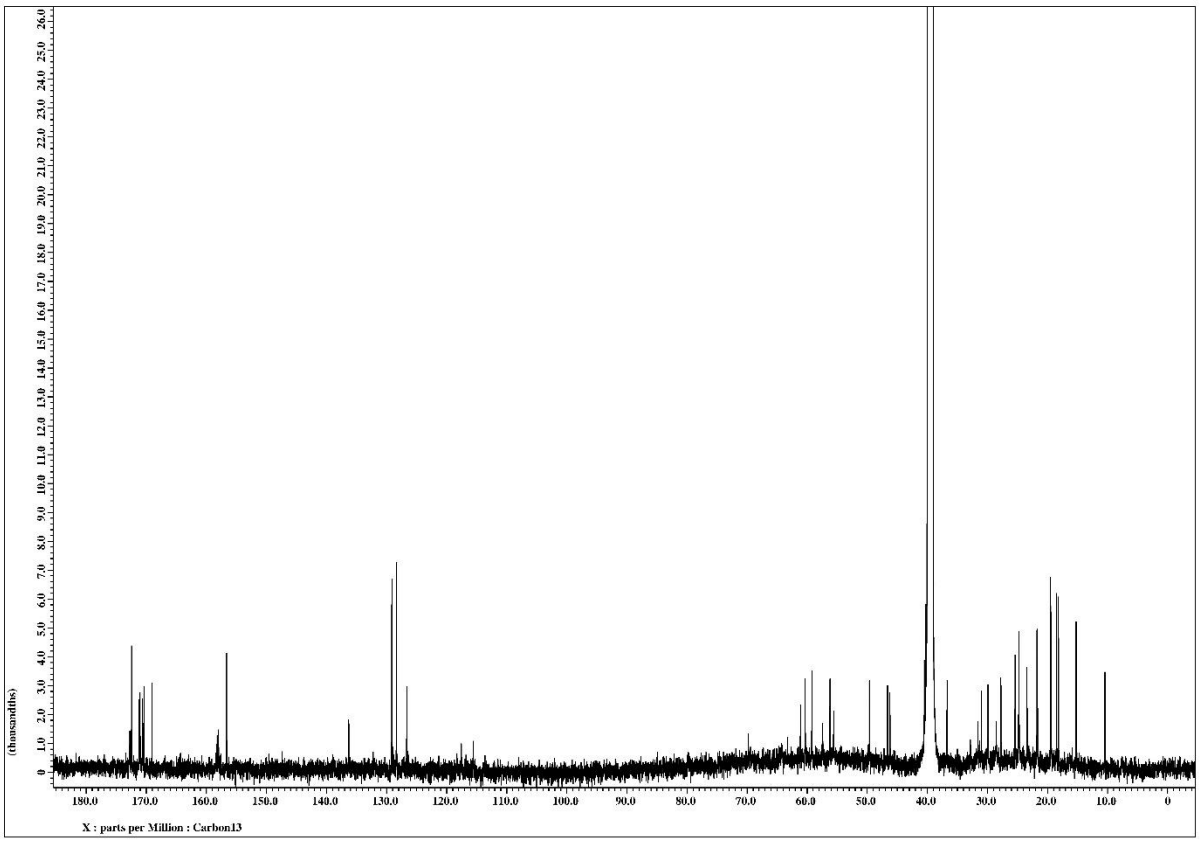

Figure S59. ^{13}C NMR (150 MHz) spectrum of synthetic **3** in DMSO-d_6

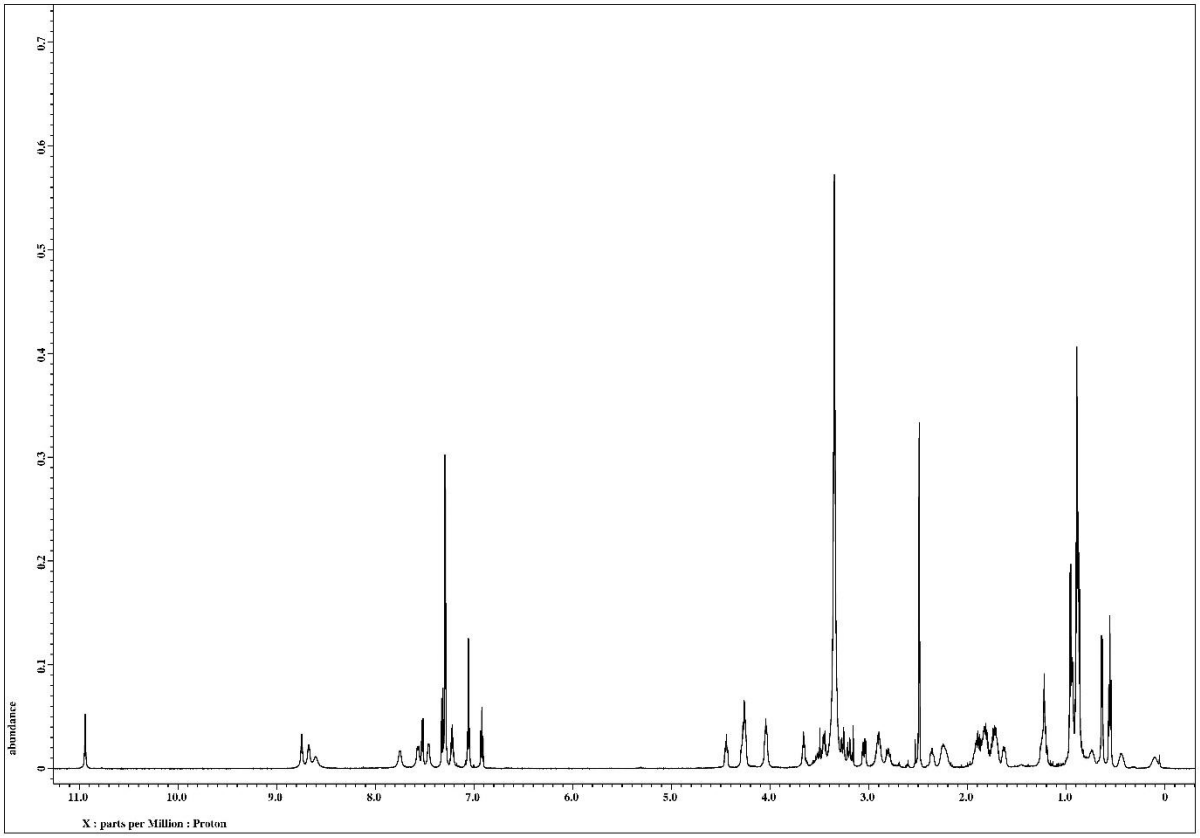

Figure S60. ^{1}H NMR (600 MHz) spectrum of synthesized **6** in DMSO-d_6

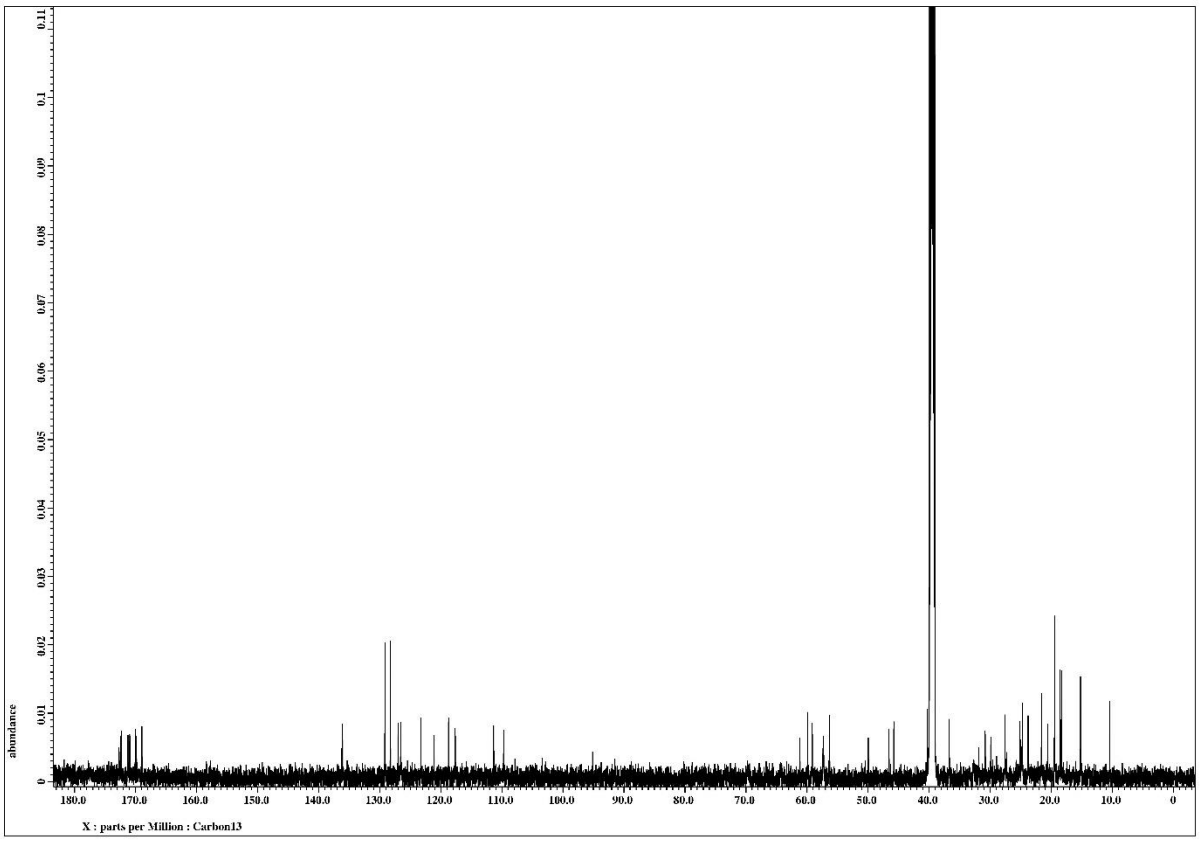

Figure S61. ^{13}C NMR (150 MHz) spectrum of synthesized **6** in DMSO-d_6

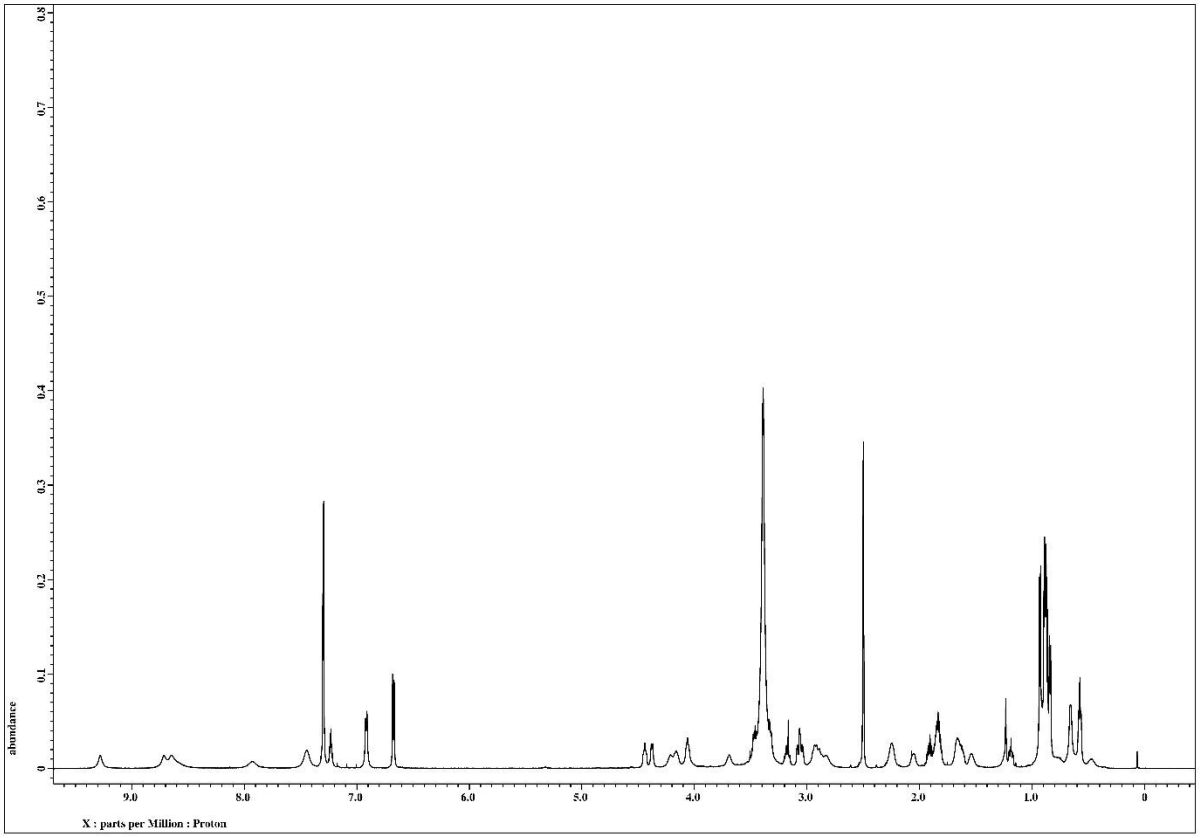

Figure S62. ^{1}H NMR (600 MHz) spectrum of synthesized **7** in DMSO-d_6

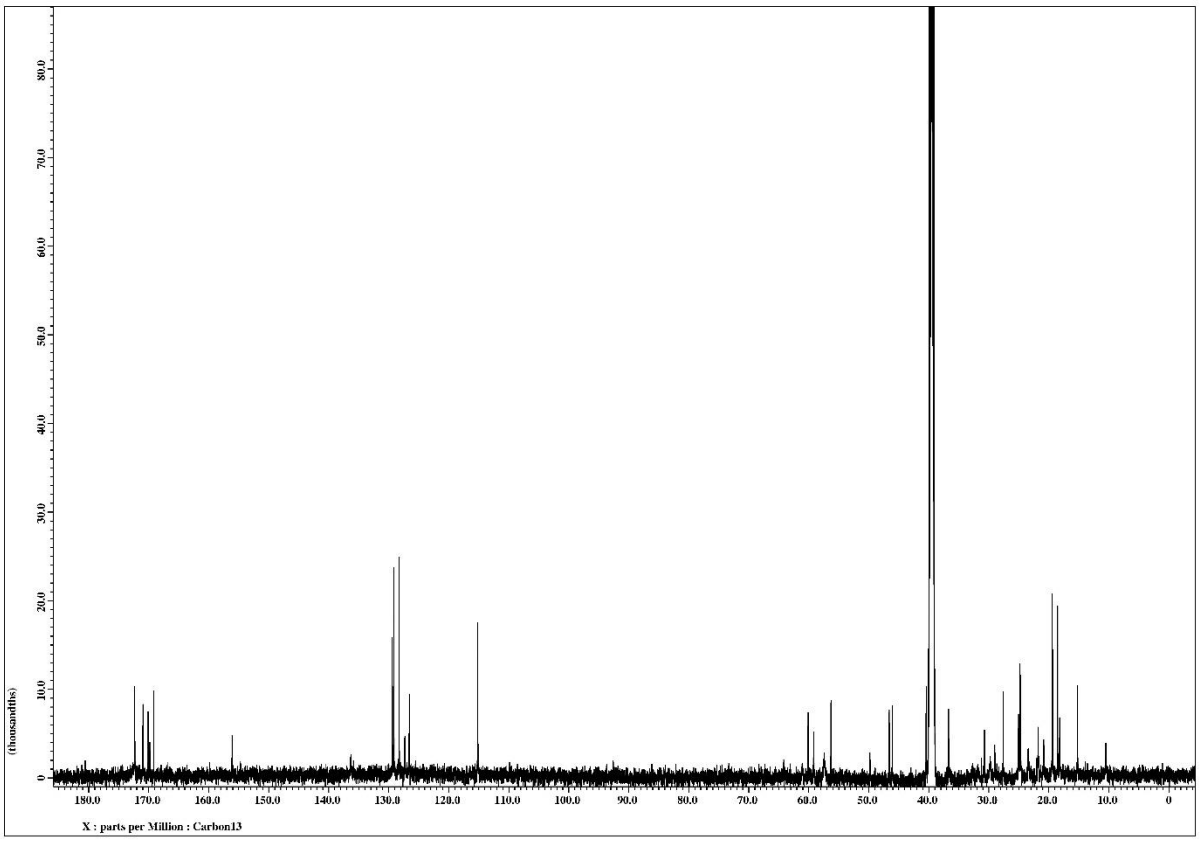

Figure S63. ^{13}C NMR (150 MHz) spectrum of synthesized **7** in DMSO-d_6

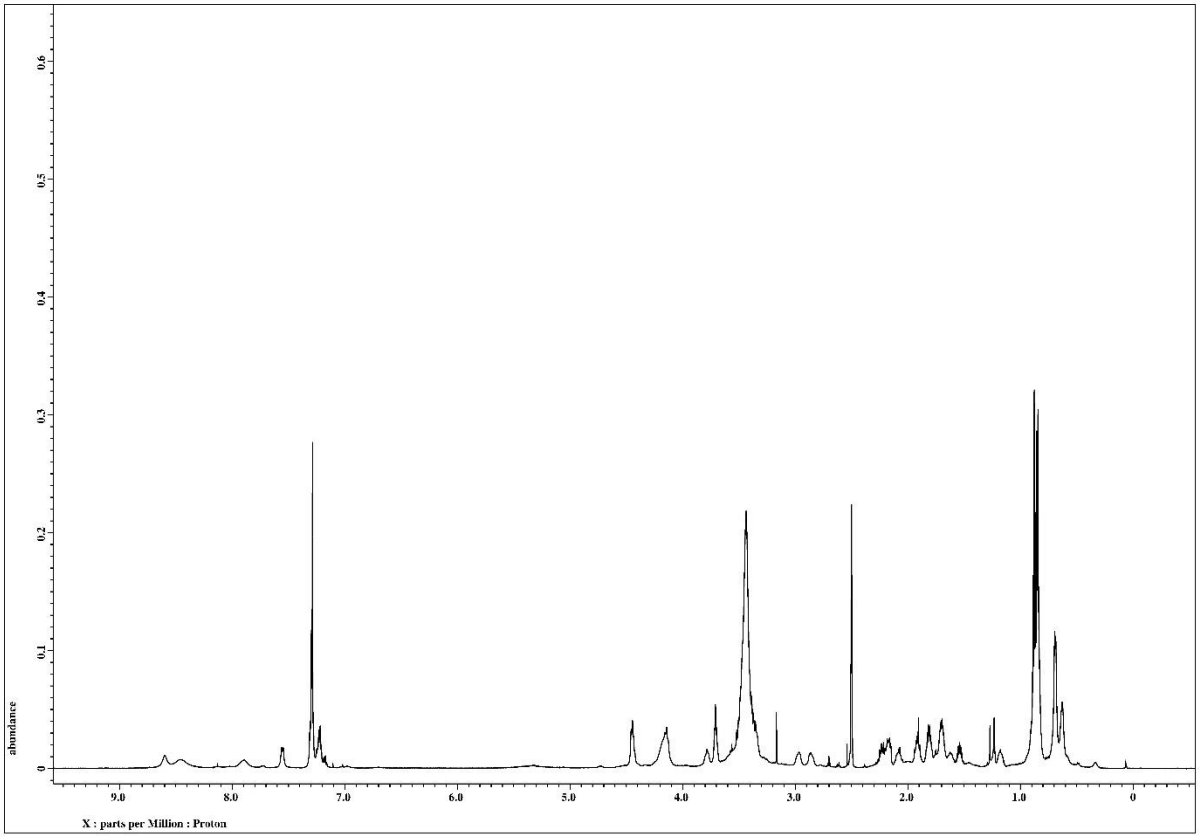

Figure S64. ^{1}H NMR (600 MHz) spectrum of synthesized **8** in DMSO-d_6

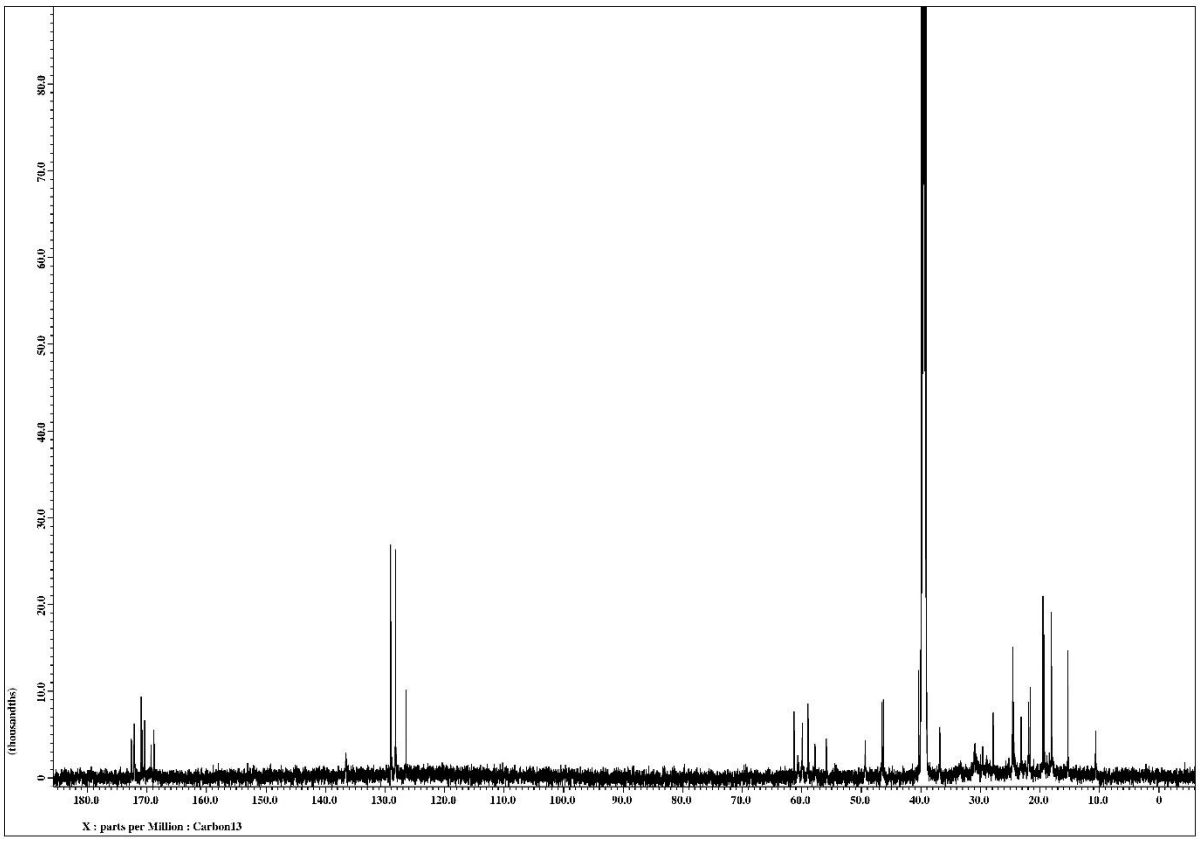

Figure S65. ^{13}C NMR (150 MHz) spectrum of synthesized **8** in DMSO-d_6

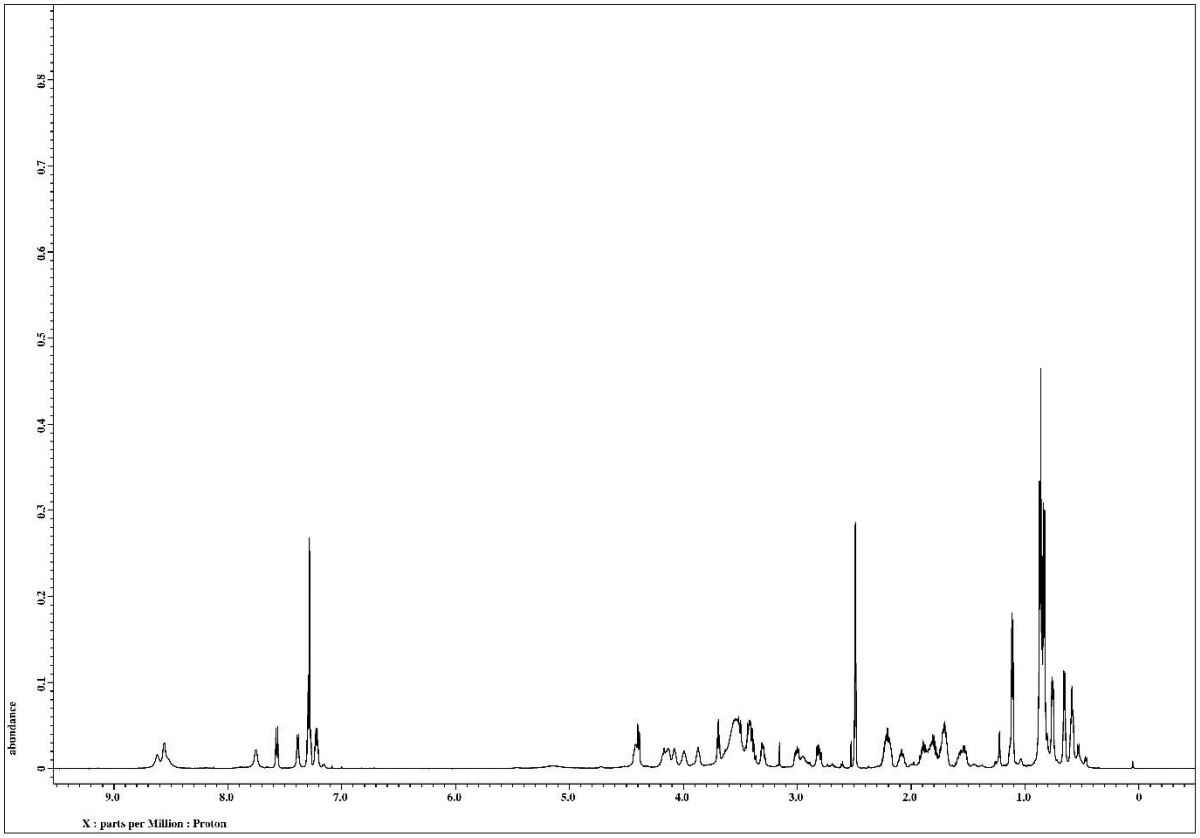

Figure S66. ^{1}H NMR (600 MHz) spectrum of synthesized **9** in DMSO-d_6

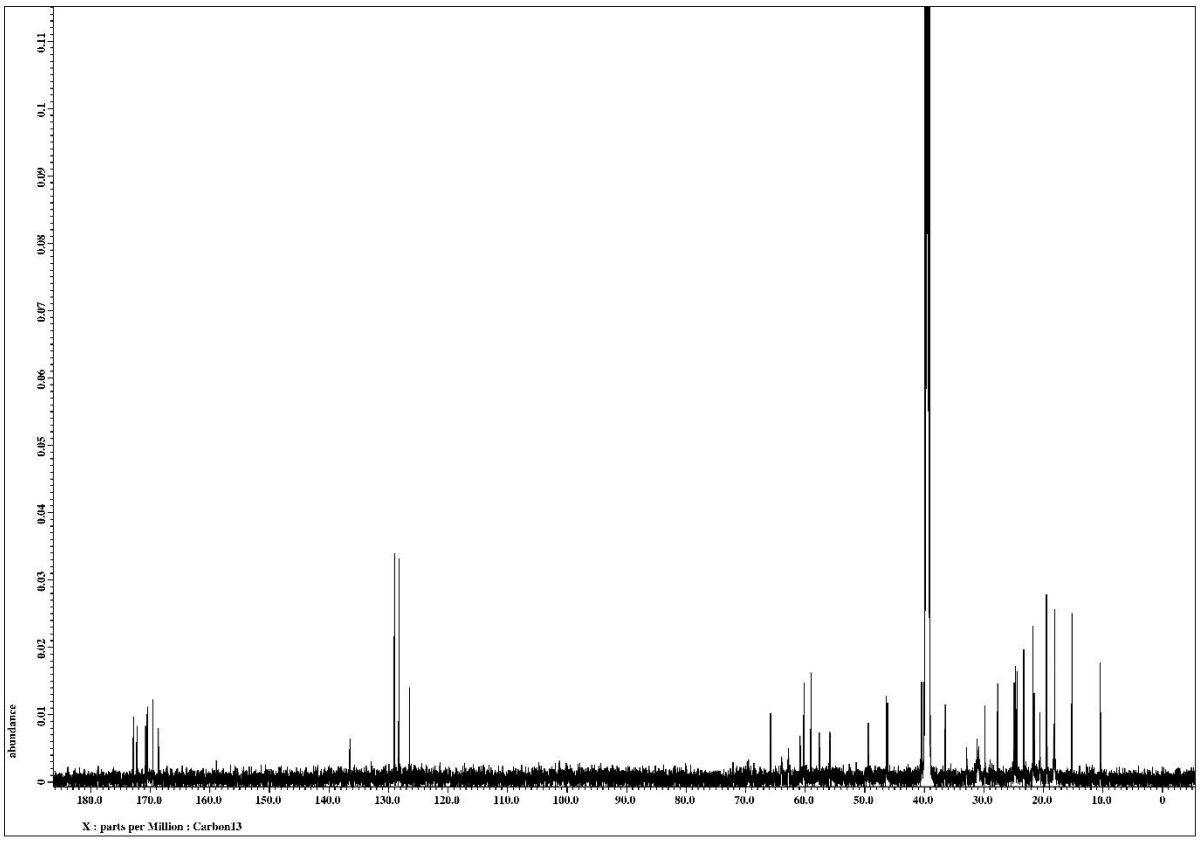

Figure S67. ^{13}C NMR (150 MHz) spectrum of synthesized **9** in DMSO-d_6

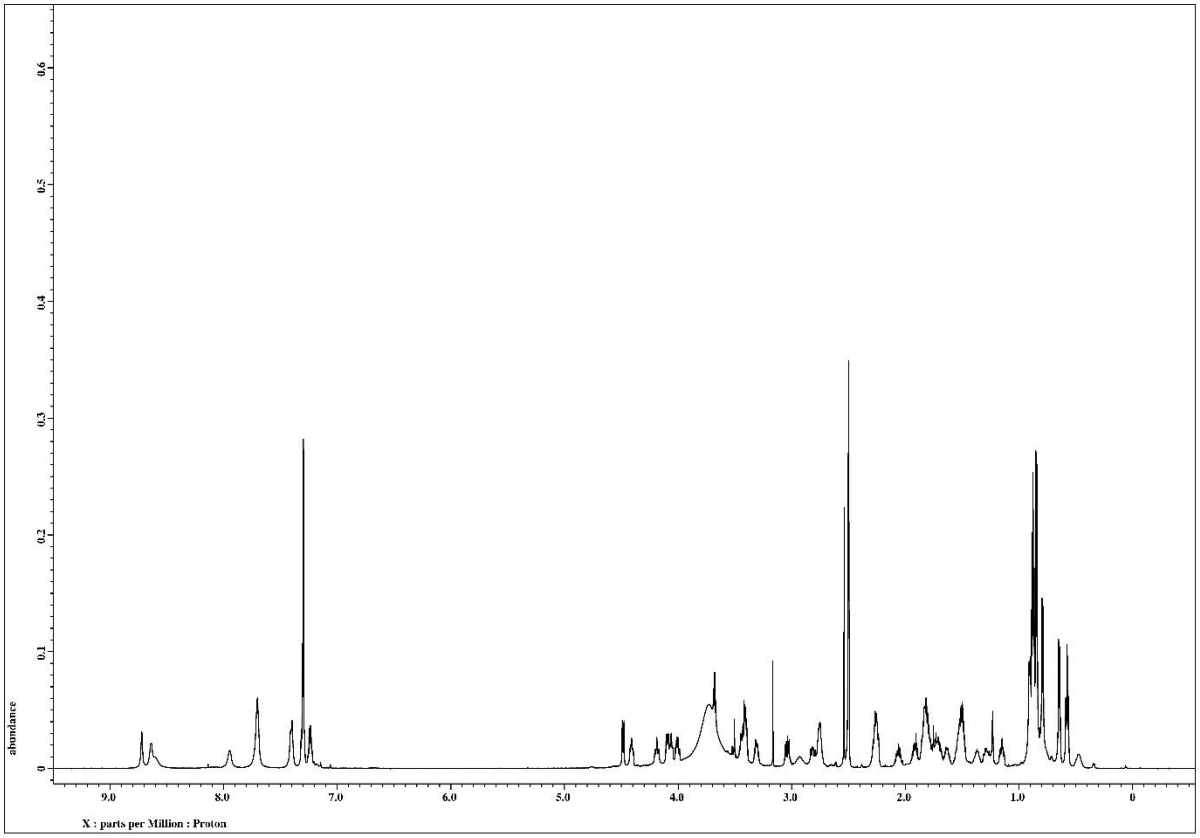

Figure S68. ^{1}H NMR (600 MHz) spectrum of synthesized **10** in DMSO-d_6

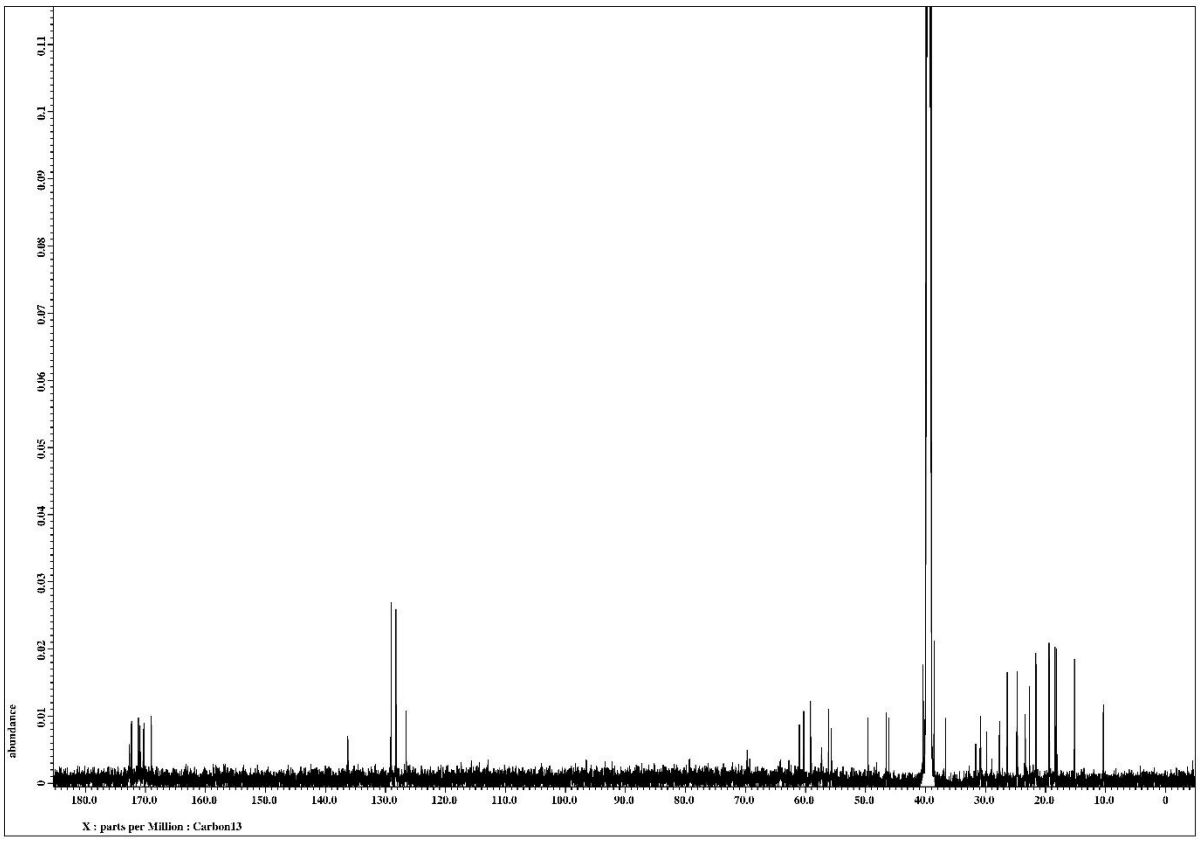

Figure S69. ^{13}C NMR (150 MHz) spectrum of synthesized **10** in DMSO-d_6

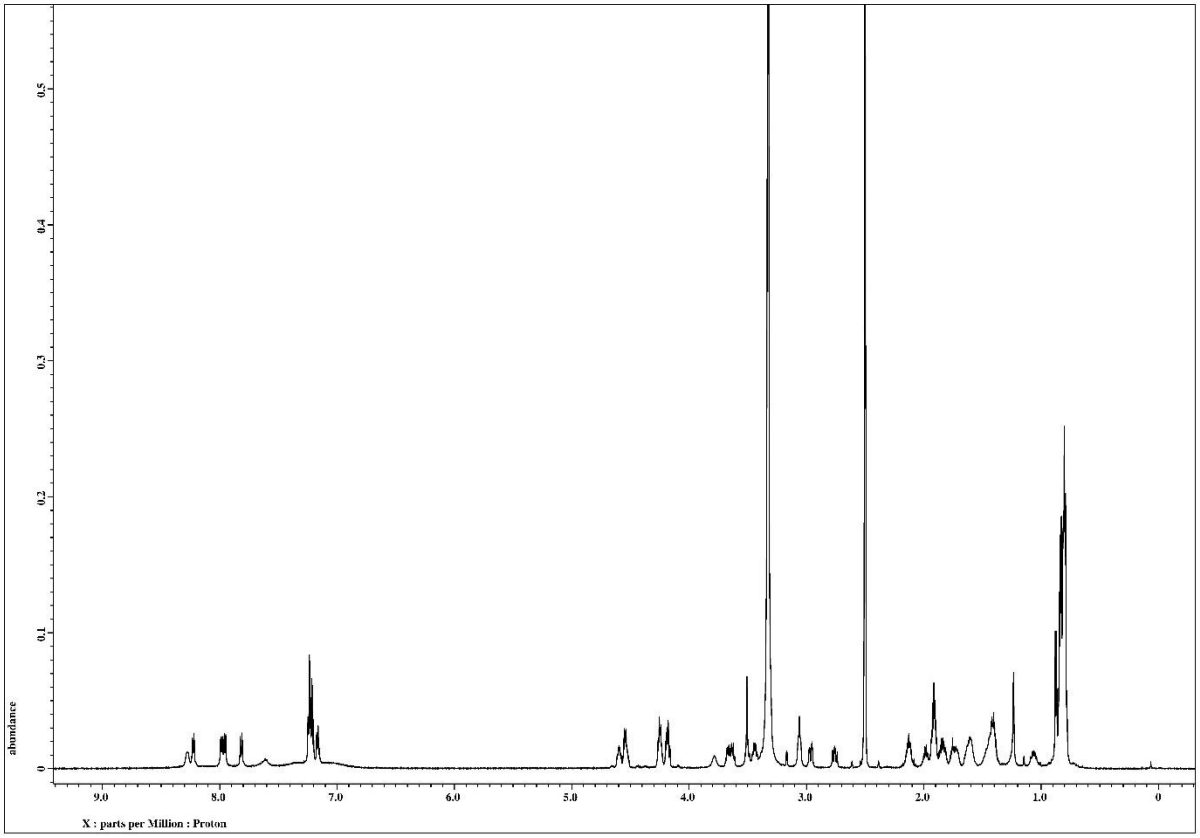

Figure S70. ^{1}H NMR (600 MHz) spectrum of synthesized **11** in DMSO-d_6

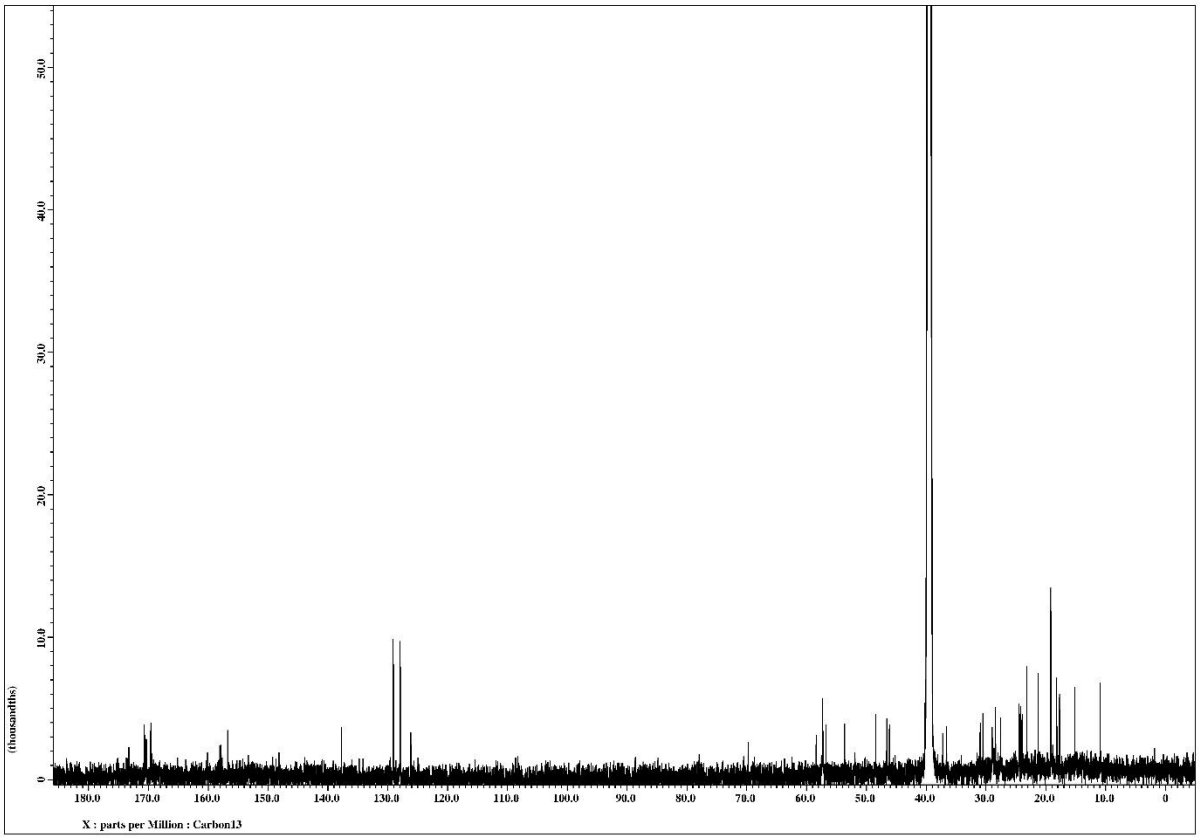

Figure S71. ^{13}C NMR (150 MHz) spectrum of synthesized **11** in DMSO-d_6

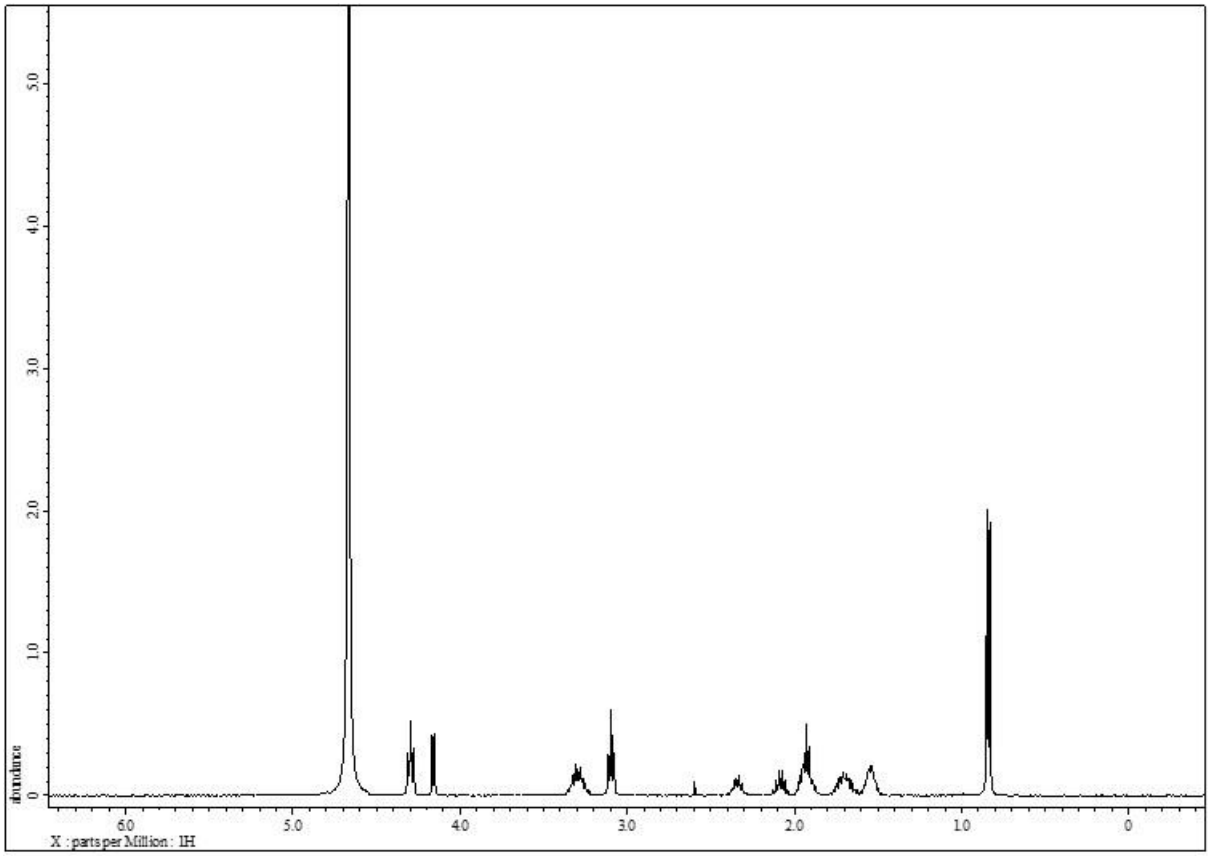

Figure S72. ^{1}H NMR (500 MHz) spectrum of synthesized **12** in D_2O

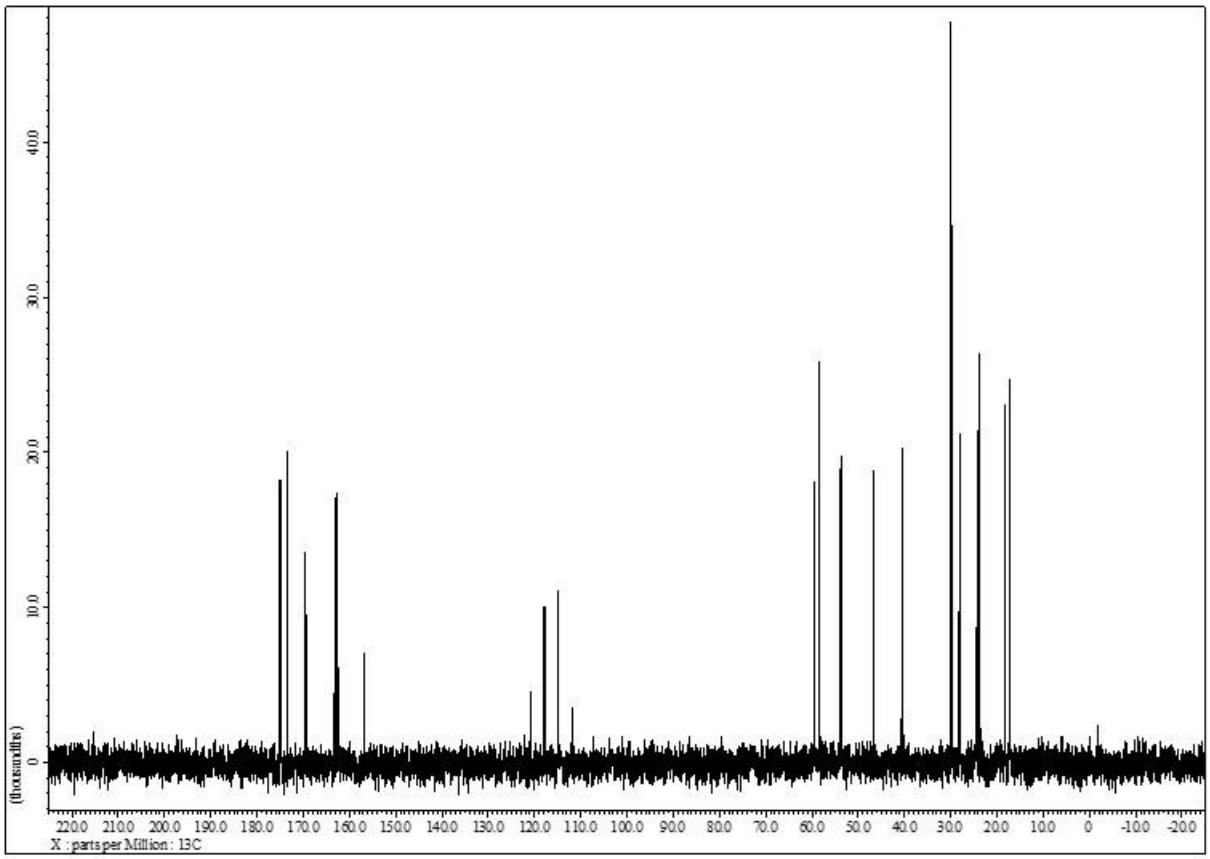

Figure S73. ^{13}C NMR (125 MHz) spectrum of synthesized **12** in D_2O

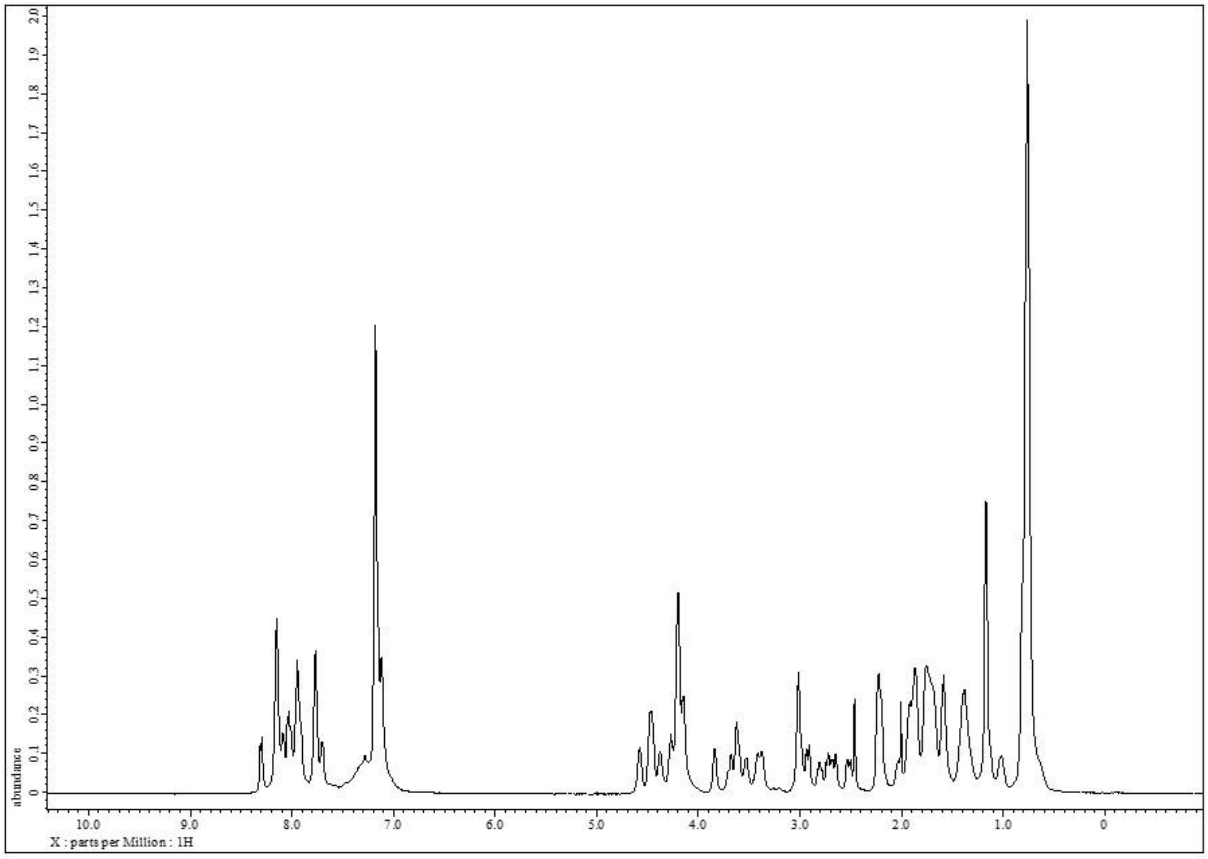

Figure S74. ^{1}H NMR (500 MHz) spectrum of synthesized **13** in DMSO-d_6

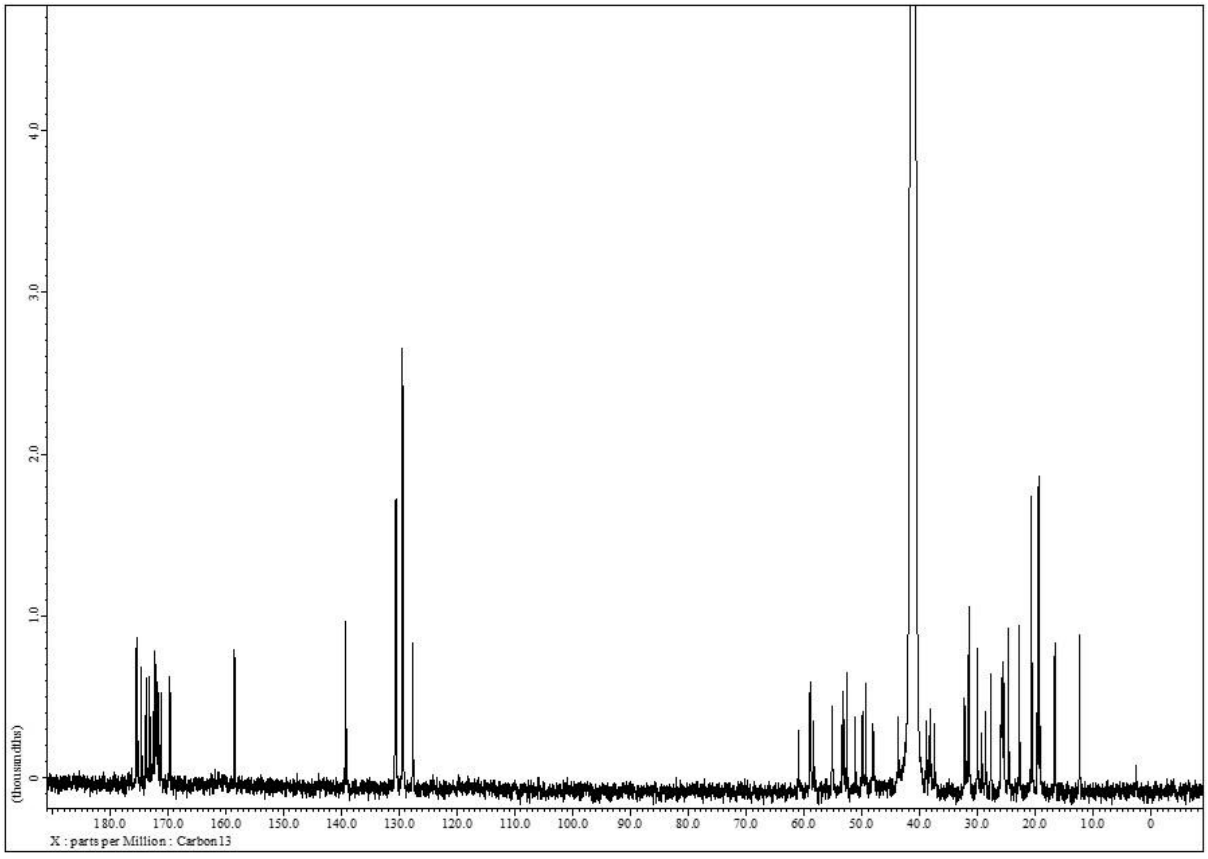

Figure S75. ^{13}C NMR (125 MHz) spectrum of synthesized **13** in DMSO-d_6

References

1. Ishida, K.; Matsuda, H.; Murakami, M.; Yamaguchi, K. Kawaguchipeptin A, a novel cyclic undecapeptide from cyanobacterium *Microcystis aeruginosa* (NIES-88). *Tetrahedron* **1996**, *52*, 9025–9030.

2. Marfey, P. Determination of D-amino acids. II, use of a bifunctional reagent, 1,5-difluoro-2,4-dinitrobenzene. *Carlsberg Res. Commun*. **1984**, *49*, 591–596.

3. Jomori, T.; Shiroyama, S.; Ise, Y.; Kohtsuka, H.; Matsuda, K.; Kuranaga, T.; Wakimoto, T. Scrobiculosides A and B from the deep-sea sponge *Pachastrella scrobiculosa*. *J. Nat. Med*. **2019**, *73*, 814–819.

4. Mosmann, T. Rapid colorimetric assay for cellular growth and survival: application to proliferation and cytotoxicity assays. *J. Immunol. Methods* **1983**, *65*, 55–63.

5. Banfi, E.; Scialino, G.; Monti-Bragadin, C. Development of a microdilution method to evaluate *Mycobacterium tuberculosis* drug susceptibility. *J. Antimicrob. Chemother*. **2003**, *52*, 796–800.

6. Wick, R. R.; Judd, L. M.; Holt, K. E. Performance of neural network basecalling tools for Oxford Nanopore sequencing. *Genome Biol*. **2019**, *20*, 129.

7. Wick, R. R.; Judd, L. M.; Gorrie, C. L.; Holt, K. E. Unicycler: Resolving bacterial genome assemblies from short and long sequencing reads. *PLoS Comput. Biol.* **2017**, *13*, e1005595.

8. Uesaka, K.; Kouno, H.; Terauchi, K.; Fujita, Y.; Omata, T.; Ihara, K. SV Quest: Sensitive structure variation detection tool. https://github.com/kazumaxneo/SV-Quest

9. Walker, B. J.; Abeel, T.; Shea, T.; Priest, M.; Abouelliel, A.; Sakthikumar, S.; Cuomo, C. A.; Zeng, Q.; Wortman, J.; Young, S. K.; Earl, A. M. Pilon: an integrated tool for comprehensive microbial variant detection and genome assembly improvement. *PLoS One.* **2014**, *9*, e112963.

10. A) Tanizawa, Y.; Fujisawa, T.; Kaminuma, E.; Nakamura, Y.; Arita, M. DFAST and DAGA: web-based integrated genome annotation tools and resources. Biosci. Microbiota. Food Health. **2016**, *35*, 173–184. B) Tanizawa, Y.; Fujisawa, T.; Nakamura, Y. DFAST: a flexible prokaryotic genome annotation pipeline for faster genome publication. *Bioinformatics.* **2018**, *34*, 1037–1039.

11. Hyatt, D.; Chen, G. L.; Locascio, P. F.; Land, M. L.; Larimer, F. W.; Hauser, L. J. Prodigal: prokaryotic gene recognition and translation initiation site identification. *BMC Bioinformatics.* **2010**, *11*, 119.

12. Parajuli, A.; Kwak, D. H.; Dalponte, L.; Leikoski, N.; Galica, T.; Umeobika, U.; Trembleau, L.; Bent, A.; Sivonen, K.; Wahlsten, M.; Wang, H.; Rizzi, E.; De Bellis, G.; Naismith, J.; Jaspars, M.; Liu, X.; Houssen, W.; Fewer, D. P. A Unique tryptophan C-prenyltransferase from the kawaguchipeptin biosynthetic pathway. *Angew. Chem., Int. Ed. Engl.* **2016**, 55, 3596–3599.

13. Agarwal, V.; Pierce, E.; McIntosh, J.; Schmidt, E. W.; Nair, S. K. Structures of cyanobactin maturation enzymes define a family of transamidating proteases. *Chem Biol*. **2012**, *19*, 1411–1422.

14. Gu, W.; Dong, S. H.; Sarkar, S.; Nair, S. K.; Schmidt, E. W. The Biochemistry and structural biology of cyanobactin pathways: enabling combinatorial biosynthesis. *Methods Enzymol.* **2018**, *604*, 113–163.

15. Eddy, S. R. Accelerated profile HMM searches. *PLoS Comput. Biol.* **2011**, *7*, e1002195.

16. Zdobnov E. M.; and Apweiler R. InterProScan—an integration platform for the signature-recognition methods in InterPro. *Bioinformatics*. **2001**, *17*, 847–848.

17. Waterhouse, A. *et al.* SWISS-MODEL: homology modelling of protein structures and complexes. *Nucleic Acids Res.* **2018**, *46*, W296–W303.

18. Gilchrist, C. L. M.; Chooi, Y. H. Clinker & clustermap.js: Automatic generation of gene cluster comparison figures. *Bioinformatics.* **2021**, btab007. doi: 10.1093/bioinformatics/btab007.

19. Chen, I. A. *et al.* IMG/M: integrated genome and metagenome comparative data analysis system. *Nucleic Acids Res.* **2017**, *45*, D507−D516.

20. Kumar, S.; Stecher, G.; Li, M.; Knyaz, C.; Tamura, K. MEGA X: molecular evolutionary genetics analysis across computing platforms. *Mol. Biol. Evol.* **2018**, *35*, 1547–1549.

21. Purushothaman, M.; Sarkar, S.; Morita, M.; Gugger, M.; Schmidt, E. W.; Morinaka, B. I. Genome-Mining-Based Discovery of the Cyclic Peptide Tolypamide and TolF, a Ser/Thr Forward *O*-Prenyltransferase. *Angew. Chem., Int. Ed.* **2021**, *60*, 8460–8465.